

# **Identification of novel cytosolic binding partners of the cell recognition molecule CHL1 and study of their functional interactions**

Dissertation zur Erlangung des Doktorgrades an der Fakultät für Mathematik,  
Informatik und Naturwissenschaften  
Fachbereich Biologie  
der Universität Hamburg

Dissertation with the aim of achieving a doctoral degree at the Faculty of  
Mathematics, Informatics and Natural Sciences  
Department of Biology  
University of Hamburg

Submitted by **Mehrnaz Azami Movahed**  
2016 in Hamburg

Day of oral defense: March 31<sup>th</sup>, 2017

The following evaluators recommended the admission of the dissertation:

Prof. Dr. Melitta Schachner

Prof. Dr. Thorsten Burmester



Universitätsklinikum  
Hamburg-Eppendorf

Center for Molecular  
Neurobiology Hamburg

Research Group:  
Neuronal Translational  
Control

Martinstraße 52  
20246 Hamburg

Kent Duncan, PhD

Phone: +49(0)40 7410-56274  
Fax: +49(0)40 7410-53436  
Kent.Duncan@zmnh.uni-hamburg.de  
www.zmnh.uni-hamburg.de

Delivery address:  
Falkenried 94  
20251 Hamburg

Universitätsklinikum Hamburg-Eppendorf Martinstraße 52 20246 Hamburg  
Zentrum für Molekulare Neurobiologie - Forschergruppen

October 12, 2016

**English language Thesis Certification: Mehrnaz Azami Movahed**

To whom it may concern:

**Mehrnaz Azami Movahed**, who was born on 11.05.1979 in Tehran, Iran, is submitting her doctoral dissertation in English. The title of her thesis is: 'Identification of novel cytosolic binding partners of the cell recognition molecule CHL1 and study their functional interactions'.

I hereby certify as a native speaker and molecular biologist that the English language used in this thesis is sufficiently correct for submission.

Yours truly,

Universität Hamburg  
Universitätsklinikum Hamburg-Eppendorf  
Zentrum für Molekulare Neurobiologie  
AG Duncan  
Falkenried 94 · D-20251 Hamburg

**Kent Duncan, Ph.D.**

**Hamburg, October 12, 2016**

Zertifikat Nr. QS-6568HH  
und EM-8126HH



Universitätsklinikum Hamburg-Eppendorf  
Körperschaft des öffentlichen Rechts  
Gerichtsstand: Hamburg  
USt-ID-Nr.: DE21 8618 948

Vorstandsmitglieder:  
Prof. Dr. Burkhard Göke (Vorsitzender)  
Prof. Dr. Uwe Koch-Gromus  
Joachim Pröbß  
Rainer Schoppik

Bankverbindung:  
HSH Nordbank  
Kto.-Nr.: 104364000; BLZ: 21050000  
IBAN-Nr.: DE9721050000104364000  
BIC: HSHNDEHH

### **Eidesstattliche Versicherung**

Hiermit erkläre ich an Eides statt, dass ich die vorliegende Dissertationsschrift selbst verfasst und keine anderen als die angegebenen Quellen und Hilfsmittel benutzt habe.

Hamburg, den 12.October 2016

Unterscrit ..... *M.A.M* .....

### **Declaration on oath**

I hereby declare, on oath, that I have written the present dissertation by my own and have not used other than the acknowledged resources and aids.

Hamburg, 12.October 2016

Signature..... *M.A.M* .....

## Table of contents

Abstract.....	13
Zusammenfassung .....	15
I. Introduction .....	17
1. Cell adhesion molecules .....	17
1.1. Structural features of IgSF CAMs .....	17
1.2. The L1 family.....	18
1.3. Structure, modifications and interactions of L1 .....	19
1.4. Functions of the cell adhesion molecule L1.....	20
1.5. Close homologue of L1 (CHL1) .....	21
1.6. The close homologue of L1 (CHL1): expression pattern and functions.....	22
1.7. Interactions of the close homologue of L1 (CHL1).....	24
2. Novel binding partners of CHL1 .....	25
2.1. ALG-2 (apoptosis-linked gene 2): Structure and functions .....	25
2.2. Synaptogyrin family members .....	26
2.3. Dopamine transporter (DAT) as a novel binding partner of CHL1 .....	27
2.3.1. Dopamine transporter: structure and interactions .....	27
2.3.2. Dopamine transporter function.....	28
II. Aims of the study .....	30
III. Materials .....	31
1. Antibodies .....	31
1.1. Primary antibodies .....	31
1.2. Secondary antibodies .....	32
2. Chemicals.....	32

3. Buffers and solutions .....	32
4. Molecular weight ladder .....	36
4.1. DNA ladder .....	36
4.2. Protein ladder .....	37
5. Animals .....	37
6. Bacterial strains.....	37
7. Plasmids .....	37
8. Primers .....	39
9. Kits.....	40
IV. Methods .....	40
1. Molecular biology methods .....	40
1.1. Molecular cloning and PCR.....	40
1.1.1. Sub-cloning of CHL1 from pcDNA-CHL1 construct in to GFP vector	41
1.1.2. Cloning of CHL1 and Dopamine transporter (DAT) in bicistronic IRES Vector .....	42
1.2. Horizontal agarose gel electrophoresis of DNA .....	44
1.3. Determination of DNA concentration.....	44
1.4. Transformation of bacteria.....	44
1.5. Plasmid isolation from <i>Escherichia coli</i> culture .....	44
1.6. DNA sequencing .....	45
2. Protein biochemistry methods .....	45
2.1. Production of recombinant proteins.....	45
2.1.1 Expression of recombinant proteins in <i>E. coli</i> . .....	45
2.1.2. Purification of recombinant proteins .....	45
2.2. Determination of protein concentration .....	46

2.3. SDS -PAGE.....	46
2.4. Coomassie staining of polyacrylamide gels.....	46
2.5. Western blot .....	46
2.6. Brain homogenization .....	47
2.7. Isolation of subcellular fractions.....	47
2.8. Affinity chromatography.....	48
2.8.1. Preparation of cyanogen bromide-activated-Sepharose and ligand immobilization.....	48
2.8.2. Affinity chromatography .....	49
2.9. Binding protein assays .....	49
2.9.1. Co-Immunoprecipitation (Co-IP) .....	49
2.9.2. Pull-down assay.....	49
3. Cell biology.....	50
3.1. Cell line culture .....	50
3.2. Transfection of cell-lines with TurboFect.....	50
3.3. Primary culture.....	50
3.3.1. Cell culture of primary hippocampal neurons .....	50
3.3.2. Primary culture of cerebellar granule neurons .....	51
3.3.3. Coating of glass cover slips with poly-L-lysine .....	51
3.4. Immunocytochemistry.....	51
3.5. Live cell staining .....	52
3.6. Immunohistochemistry.....	52
3.7. Tyrosine hydroxylase (TH) immunostaining .....	53
3.8. Proximity ligation assay.....	53
3.9. MTT assay.....	54

3.10. Staining of live cells with calcein .....	55
3.11. Calcium imaging .....	55
3.12. Fluorescence resonance energy transfer (FRET) .....	55
V. Results.....	57
1. Identification of potential binding partners of CHL1 and NCAM180 by affinity chromatography .....	57
1.1. Expression and purification of recombinant CHL1-ICD and NCAM180-ICD .....	57
1.2. Affinity chromatography of brain homogenates using immobilized CHL1-ICD and NCAM180-ICD .....	58
1.3. Detection and identification of the CHL1 and NCAM180 binding proteins	59
1.3.1. Isolation of CHL1 binding partners from crude brain homogenate ....	59
1.3.2. List of potential interaction partners of CHL1 identified in Mass spectroscopy analysis .....	60
1.3.3. Isolation of CHL1 and NCAM180 binding partners from subcellular fractions .....	61
1.3.4. Mass spectroscopy analysis of the potential interaction partners of CHL1 and NCAM180 corresponds to subcellular fractions of the brain.....	62
2. Study the interaction of CHL1 with ALG-2 .....	64
2.1. Verification of the CHL1- ALG-2 interaction by Co-IP .....	64
2.2. Investigation of CHL1- ALG-2 interaction by pull down assay.....	64
2.3. Immunostaining of ALG-2 and CHL1 in cerebellar neurons (Fixed cells)	65
2.4. Prominent co-localization of CHL1 and ALG-2 in primary cerebellar neurons (Live cells).....	66
2.5. Partial co-localization of CHL1 and ALG-2 in primary cerebellar neurons stimulated with CHL-Fc.....	68
2.6. CHL1 interacts with ALG-2 <i>in situ</i> (cerebellar and hippocampal tissues).	69

2.7. CHL1 co-localizes with ALG-2 in transfected NIH- 3T3 cells .....	70
2.8. Treatment of NIH-3T3 cells with thapsigargin induces nuclear import of ALG-2, but not CHL1 .....	71
2.9. CHL1 protects NIH-3T3 cells from TG-induced apoptosis .....	72
3. Study the interaction of CHL1 with synaptogyrin.....	74
3.1. Co-IP of CHL1 and synaptogyrin-3 from mouse brain lysate .....	75
3.2. Synaptogyrin-3 is pulled down with the CHL1-ICD .....	76
3.3. CHL1 prominently co-localizes with synaptogyrin-3 in cultured cerebellar and hippocampal neurons only after stimulation with CHL1-Fc.....	76
3.4. Treatment of hippocampal neurons with the extracellular domain of CHL1 triggers a calcium response .....	78
3.5. Co-localization of CHL1 and synaptogyrin-3 in striatal tissue .....	79
3.6. Close interaction between CHL1 and synaptogyrin-3 <i>in situ</i> .....	79
3.7. Verification of CHL1 and synaptogyrin-3 interaction by FRET .....	80
4. Study the interaction of CHL1 with dopamine transporter (DAT) .....	81
4.1 Analysis of CHL1-DAT interaction <i>in situ</i> .....	82
4.2. Verification of ‘CHL1-DAT-Synaptogyrin-3’ association by Co-IP .....	82
4.3. Co-localization of ‘CHL1-DAT-Synaptogyrin-3’ complex in striatum .....	84
5. Functional analysis of the interaction between CHL1 and dopamine transporter	85
5.1. Internalization of CHL1 with DAT after stimulation by PMA in transfected HEK cells .....	85
5.2. Immunohistochemical staining of the midbrain dopaminergic system in wildtype and CHL1-deficient mice .....	87
VI. Discussion .....	88
6.1. Identification of potential binding partners of CHL1 and NCAM180 .....	88
6.2. Investigation of CHL1-ALG-2 physical and functional interaction.....	88

6.3. Investigation of the interaction of CHL1 and synaptogyrin-3.....	92
6.4. Investigation of the interaction of CHL1 and the dopamine transporter (DAT) .....	95
6.5. Functional interplay between CHL1 and DAT.....	96
6.5.1. CHL1 internalizes with DAT after stimulation by PMA.....	96
6.5.2. CHL1 role in maintenance and/or survival of dopaminergic neurons.....	97
Conclusion.....	98
VII. References.....	99
VIII. List of abbreviations.....	110
Acknowledgements.....	113

## List of figures

Figure 1. Schematic representation of immunoglobulin superfamily members. ....	18
Figure 2. Structural features of CHL1.....	22
Figure 3. Schematic structure of human ALG-2 protein.....	26
Figure 4. Schematic illustration of the synaptic vesicle protein: synaptogyrin-3. ....	27
Figure 5. Interaction of dopamine transporter with binding partners.....	28
Figure 6 . GeneRuler™ 1kb DNA Ladder Plus (Fermentas, SM1331). ....	36
Figure 7. SDS-PAGE band profile of the PageRuler protein Ladder, (Thermofisher, 26619).....	37
Figure 8. Protocol overview of cloning with InFusion Cloning Kit (Clontech) .....	40
Figure 9. Schematic illustration of proximity ligation assay.....	54
Figure 10. Production of recombinant intracellular domains of CHL1 and NCAM180. ....	58
Figure 11. Isolation of CHL1 binding partners. ....	59
Figure 12. Isolation of interacting partners of CHL1 and NCAM180. ....	61
Figure 13. Co-immunoprecipitation of CHL1 with the ALG-2 antibody from mouse brain lysate.....	64
Figure 14. ALG-2 is pulled down with the intracellular domain of CHL1.....	65
Figure 15. Immunostaining of CHL1 and ALG-2 in primary cerebellar neurons after fixation.....	66
Figure 16. CHL1 co-localizes with ALG-2 in primary cerebellar neurons (Live cells) .....	67
Figure 17. CHL1 partially co-localizes with ALG-2 after treatment of cerebellar neurons with CHL1-Fc .....	68
Figure 18. Close interaction between CHL1 and ALG-2 in the cerebellum and the hippocampus. ....	69
Figure 19. Interaction of CHL1 and ALG-2 in transfected NIH- 3T3 cells.....	70
Figure 20. Thapsigargin triggers nuclear import of ALG-2, but not CHL1.....	71
Figure 21. CHL1 enhances NIH-3T3 cell survival under TG treatment.....	74
Figure 22. Interaction of CHL1 and synaptogyrin-3 is calcium dependent. ....	75

Figure 23. Synaptogyrin-3 is pulled down with the ICD of CHL1.....	76
Figure 24. Co-localization of CHL1 and synaptogyrin-3 in cerebellar and hippocampal neurons treated with CHL1-Fc .....	77
Figure 25. Application of CHL1-Fc enhances intracellular calcium levels in cultured hippocampal neurons.....	79
Figure 26. Immunostaining of CHL1 and synaptogyrin-3 in the striatum.....	79
Figure 27. Close interaction between CHL1 and synaptogyrin-3 <i>in situ</i> .....	80
Figure 28. Verification of CHL1 and synaptogyrin-3 interaction by FRET using sensitized emission method .....	81
Figure 29. Close interaction of CHL1 and DAT <i>in situ</i> .....	82
Figure 30. Verification of ‘CHL1-DAT-Synaptogyrin-3’ complex by Co-IP.....	83
Figure 31. CHL1 co-localizes with both synaptogyrin-3 and DAT in striatal tissue...	84
Figure 32. Visualization of CHL1 internalization with DAT in transfected HEK 293 cells.....	86
Figure 33. Tyrosine hydroxylase (TH) immunostaining of the midbrain dopamine neurons in wildtype and CHL1-deficient mice. ....	87
Figure 34. Clustering of CHL1 on cell surface, calcium influx and interaction with ALG-2.....	90
Figure 35. Schematic model of exocytosis.....	93

## **List of tables**

Table 1. Primary antibodies are listed in alphabetical order. ....	31
Table 2. Buffers and solutions in alphabetical order.....	36
Table 3. Expression vectors used for mammalian and bacterial systems. ....	38
Table 4. List of the primers that used for cloning. ....	39
Table 5. List of potential interaction partners of CHL1 identified by mass spectrometry. ....	60
Table 6. List of potential binding partners of CHL1-ICD and NCAM180-ICD.....	63

## Abstract

The close homologue of L1 (CHL1) is a member of the immunoglobulin superfamily and belongs to the L1 family of recognition molecules that are mainly expressed during development of the nervous system. Ablation of CHL1 in mice leads to impairments in synaptic transmission, long term potentiation, working memory, gating of sensorimotor information and stress response, as well as alterations in social and exploratory behavior. Being interested in molecules interacting with the intracellular domain of CHL1 and with the hope to find bi-directionally acting modifiers of individual CHL1 functions, I searched for novel CHL1 interaction partners using homogenates from adult brains and an immobilized recombinant intracellular CHL1 domain for affinity chromatography. Bound proteins were subjected to mass spectrometry. Among the putative binding partners, the following could be listed: Synaptosomal-associated protein-25 (SNAP-25), vesicle-associated membrane protein 2 (Vamp2), programmed cell death protein 6 (PDCD6) also called apoptosis-linked gene-2 protein (ALG-2), peflin1 (PEF-1), sorcin, synaptogyrin-1, synaptogyrin-3, the Ras-related proteins Rab 1A and Rab 14, also cofilin and doublecortin (DCX). The listed proteins are the most interesting ones and some of these were further analyzed in my Ph.D. study.

As a first novel binding partner, I was interested in the apoptosis-linked gene-2 protein (ALG-2) also called programmed cell death protein 6 (PDCD6). ALG-2 has a regulatory role in late apoptosis. Also, overexpression of ALG-2 is observed in different human cancer types. The interaction of CHL1 and ALG-2 was further verified by Co-IP and pull down assays. Notably, live staining of cultured cerebellar neurons treated with antibody against the extracellular domain of CHL1 revealed significant co-localization of CHL1 with ALG-2 along neurites. This can possibly be explained by clustering of CHL1 followed by calcium influx *via* VDCC, which could trigger association between CHL1 and ALG-2. Duolink assay indicated that endogenous CHL1 and ALG-2 are in close proximity in parallel fibers in the cerebellum. The MTT assay has shown that CHL1 enhances cell survival exposed to calcium toxicity and thapsigargin-induced apoptosis, suggesting CHL1 may play role as a 'neuroprotective' molecule during calcium overload and excitotoxicity in parallel fibers.

Secondly, I identified synaptogyrin-1 and synaptogyrin-3 as novel CHL1 binding partners. Synaptogyrin-3 as a synaptic vesicle protein is involved in neurotransmitter release and also

interacts with the dopamine transporter (DAT) to positively regulate DAT activity. The present work demonstrates a novel binding of CHL1 to synaptogyrin-3 in a calcium dependent manner, which may further correlated with neurotransmitter release through exocytosis and synaptic plasticity.

DAT is a presynaptic plasma membrane protein that regulates the re-uptake of dopamine back into nerve terminals, and thus is essential for homeostasis of dopamine at the synapse. DAT function and dopamine signaling contribute to neurological and psychiatric diseases including Parkinson's diseases, depression, schizophrenia, attention deficit hyperactivity disorder (ADHD), Tourette syndrome and bipolar disorder. In addition, DAT plays an important role in addiction and is the principle target for psychostimulants, such as cocaine and amphetamine. Since synaptogyrin-3 interacts with DAT and CHL1, I investigated whether CHL1 also interacts directly with DAT. The interaction of CHL1 with synaptogyrin-3 and DAT was confirmed through Co-IP and immunostaining of striatal tissues, suggesting these three proteins could form a complex. The association of CHL1-DAT could possibly be important in maintaining the dopaminergic tone at the synapse. In this context, DAT trafficking was studied in the presence of CHL1. An internalization assay revealed that CHL1 internalizes with DAT upon PKC-stimulation by PMA. This may further influences on the DAT activity due to DAT surface loss caused by CHL1-mediated endocytosis. Finally, immunohistochemical stains for TH in CHL1-deficient mice revealed obvious loss of midbrain dopamine neurons based on the lower density of TH-positive cells in substantia nigra (SN) as compared to the wild-type tissue, suggesting that CHL1 plays an important role in the maintenance and/or survival of dopaminergic neurons.

While CHL1 is linked to mental retardation, schizophrenia, major depression, epilepsy, and autism spectrum disorders in humans, investigations of these interactions may help to understand the mechanisms underlying CHL1 functions in the brain.

# Zusammenfassung

CHL1, das Homolog von L1, ist ein Mitglied der Immunglobulin-Superfamilie und gehört zur Familie der L1 Erkennungsmoleküle, die hauptsächlich während der Entwicklung des Nervensystems exprimiert werden. Ablation von CHL1 in Mäusen führt zu Beeinträchtigungen in der synaptischen Übertragung, in der Langzeitpotenzierung, sowie im Arbeitsgedächtnis und in der Übertragung von sensomotorischen Informationen. Weiterhin führt dies zu Stressreaktion sowie zu Veränderungen im Sozial- und Erkundungsverhalten. Die vorliegende Arbeit widmete sich der Suche nach Molekülen, die mit der intrazellulären Domäne von CHL1 wechselwirken. Mit der Hoffnung, bidirektional wirkende Modifikatoren zu finden bzw. deren Interaktionen mit einzelnen CHL1 Funktionen verknüpfen zu können, wurde in dieser Arbeit nach potentiellen neuen CHL1 Interaktionspartnern gesucht. Hierzu wurden homogene Gemische von erwachsenen Gehirnen verwendet und außerdem eine rekombinante intrazelluläre immobilisierte Domäne von CHL1, die für die Affinitätschromatographie geeignet ist. Gebundene, immobilisierte Proteine wurden mittels Massenspektrometrie analysiert. Unter den putative Bindungspartnern wurden folgende Proteine identifiziert: Synaptosomal-assoziiertes Protein-25 (SNAP-25), Vesikel-assoziiertes Membranprotein 2 (VAMP2) Programmierter Zelltod Protein 6 (PDCD6), auch als Apoptose-verknüpftes-Gen-2-Protein (ALG-2) bekannt, Peflin1 (PEF-1), Sorcin, Synaptogyrin-1, Synaptogyrin-3, die Ras-verwandten Proteine Rab 1A und Rab 14, sowie Cofilin und Double (DCX). Diese gelisteten Proteine erschienen als die interessantesten und einige von den aufgeführten Proteinen wurden weiterhin in dieser Arbeit analysiert.

Als erster potentieller Bindungspartner, wurde das Apoptose-Linked-Gen-2-Protein (ALG-2), auch als programmierter Zelltod Protein 6 ( PDCD6 ) bekannt, untersucht. ALG-2 spielt eine wesentliche regulatorische Rolle bei der späten Apoptose. Eine Überexpression von ALG-2 wird in verschiedenen humanen Krebsarten beobachtet. Das Zusammenspiel von CHL1 und ALG -2 wurde hier weiter durch Co-IP und weiteren Methoden überprüft. Eine Live- Färbung von kultivierten zerebellären Neuronen, welche mit einem Antikörper gegen die extrazelluläre Domäne von CHL1 behandelt wurden, ergab eine signifikant erkennbare Co-Lokalisation von CHL1 und ALG-2 entlang den Neuriten. Der MTT-Test ergab, dass CHL1 Zellen, welche Thapsigargin-induzierter Apoptose ausgesetzt waren, verbessert überlebten. Dies deutet darauf hin, dass CHL1 eine wesentliche Rolle als "neuroprotektives" Molekül während der Calciumüberladung und Exzitotoxizität in parallelen Fasern spielen könnte.

Weiterhin wurden Synaptogyrin-1 und Synaptogyrin-3 als neue CHL1-Bindungspartner

identifiziert. Die vorliegende Arbeit zeigt die Bindung von CHL1 an das Synaptogyrin-3 synaptisches Vesikel Protein, welches mit Neurotransmitterfreisetzung durch Exozytose und synaptische Plastizität weiter korreliert sein kann. Synaptogyrin-3 ist im synaptischen Vesikel-Haushalt beteiligt, interagiert mit dem Dopamin-Transporter (DAT) und reguliert die positive DAT-Aktivität.

DAT ist ein präsynaptisches Plasmamembranprotein, welches die Wiederaufnahme von Dopamin zurück in Nervenendigungen reguliert und ist somit für die Homöostase von Dopamin an der Synapse verantwortlich. Die DAT-Funktion und die Dopamin-Signalisierung tragen zu neurologischen und psychiatrischen Erkrankungen wie Parkinson-Krankheit, Depression, Schizophrenie, Tourette-Syndrom, Aufmerksamkeitsdefizit Hyperaktivitätsstörung (ADHS) und einer bipolaren Störung bei. Darüber hinaus spielt DAT eine wichtige Rolle in Suchterkrankungen und ist das prinzipielle Ziel für Psychostimulantien wie Kokain und Amphetamin. Da Synaptogyrin-3 mit DAT und CHL1 in Wechselwirkung tritt, wurde in der vorliegenden Arbeit untersucht, ob CHL1 auch direkt mit DAT in Wechselwirkung treten kann. Das Zusammenspiel von CHL1 mit Synaptogyrin-3 und DAT wurde durch Co-IP und Immunfärbung von Striatum-Gewebe bestätigt, was darauf hindeutet, dass diese drei Proteine einen Komplex bilden könnten. Der Verbund von CHL1 und DAT könnte bei der Aufrechterhaltung der dopaminergen Situation an der Synapse wichtig sein. Zur Beantwortung dieser Frage, der funktionellen Aufgabe von DAT, wurden in Anwesenheit von CHL1 weitere Analysen durchgeführt. Es konnte gezeigt werden, dass CHL1 mit DAT internalisiert, nach der Stimulation durch PMA. Die indirekte Wirkung von CHL1 auf die DAT-Aktivität könnte aufgrund einem DAT-Oberflächenverlust durch CHL1-vermittelte Endozytose erklärt werden. Schließlich konnte durch eine TH-immunhistochemische Färbung des dopaminergen Systems des Mittelhirns in Wildtyp- und CHL1-defizienten Mäusen gezeigt werden, dass die Dichte von TH-positiven Neuronen in der Substantia nigra (SN) vornehmlich in adulten CHL1-defizienten Mäusen vermindert ist, im Vergleich zum Gehirn von Wildtyp-Mäusen. Dies deutet darauf hin, dass CHL1 eine wichtige Rolle spielt bei der Aufrechterhaltung und/oder für das Überleben von dopaminergen Neuronen.

Da CHL1 mit geistiger Behinderung bei Menschen in Zusammenhang steht, oder auch mit Schizophrenie, Depression, Epilepsie und Autismus-Spektrum-Störungen, können Untersuchungen seiner Wechselwirkungen und zugehörige liegende Mechanismen von CHL1-Funktionen im Gehirn dazu verhelfen, die Zusammenhänge mit diesen Erkrankungen besser zu verstehen.

# **I. Introduction**

## **1. Cell adhesion molecules**

Cell adhesion molecules (CAMs) are a group of transmembrane proteins that involve in cell-cell or cell-extracellular matrix (ECM) adhesion. They are involved in signal transduction pathways (Panicker *et al.*, 2003), cell migration, proliferation and differentiation (Walsh and Doherty, 1997, Kiryushko *et al.*, 2004). CAMs are mostly divided into four main families: Immunoglobulin superfamily (IgSF) (Williams and Barclay, 1988, Brummendorf *et al.*, 1998), integrins (Hynes, 1992, Reichardt and Tomaselli, 1991), cadherins (Kemler and Ozawa, 1989, Takeichi, 1991), and selectins. The CAMs of the immunoglobulin superfamily play an essential role in morphogenesis (Krog and Bock, 1992, Williams and Barclay, 1988), development and function of nervous system. IgSF CAMs are involved in neurite outgrowth, axonal path-finding, neurite fasciculation at early developmental stages (Brummendorf *et al.*, 1998) along with learning, memory, and regeneration after injury in adults.

### **1.1. Structural features of IgSF CAMs**

The Ig superfamily CAMs are consist of several subfamilies, such as NCAM family, L1 family, Nectin family, TAG-1 and MAG (Crossin and Krushel, 2000). IgSF CAMs are composed of at least one immunoglobulin (Ig) domain at the extracellular region in the MAG family, and up to six Ig-like domains in the L1 and CHL1 molecules. In NCAM, L1 and CHL1 subfamilies, Ig- like domains are followed by fibronectin subtype III repeats (FN-III). Neural IgSF molecules are attached to the cell membrane through either a transmembrane region or a glycosyl phosphatidyl inositol (GPI) anchor such as NCAM120. There are many glycosylation sites at the extracellular portion of these molecules. Although the sulfated glucuronic acid is observed in most IgSF CAMs as a HNK-1 (human killer cell glycan) carbohydrate epitope, polysialic acid (PSA) is detected only in NCAM. The abundance and distribution of attached PSA to NCAM are influencing NCAM biological functions (Schachner and Martini, 1995).

Intensive studies have shown that immune recognition molecules such as antibodies and T-cell receptors have evolutionary origins with cell adhesion molecules (CAMs). NCAM was the first adhesion molecule that was identified and an evolutionary development between NCAM and immunoglobulins was reported (Hemperly *et al.*, 1986). The sequencing of the

human genome has revealed that the immunoglobulin superfamily is one of the major protein families in the human genome (Lander *et al.*, 2001), playing critical roles in the immune system, nervous system and other tissues. Here, the typical members of the neuronal Ig SF are depicted (Fig.1).

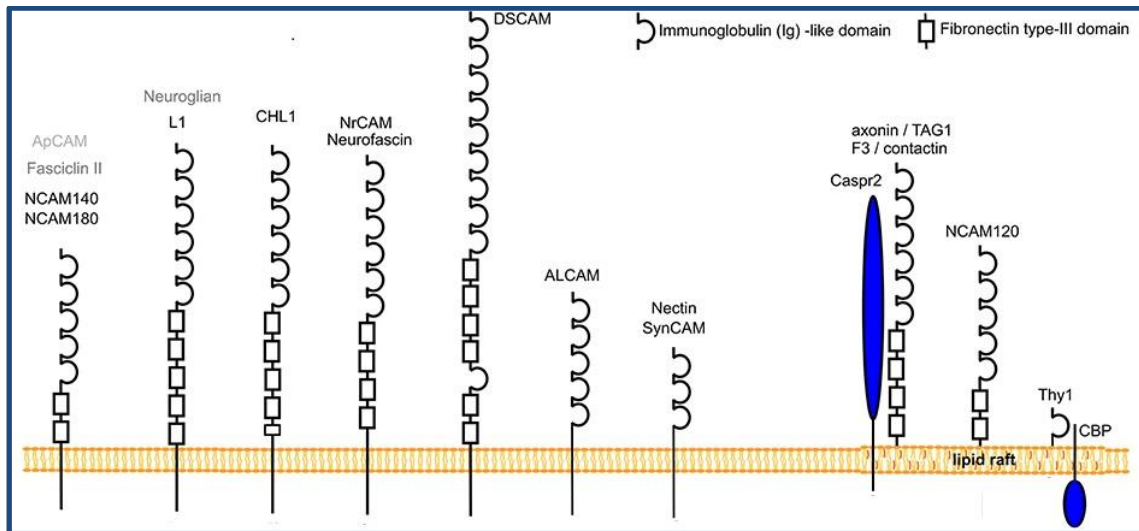


**Figure 1. Schematic representation of immunoglobulin superfamily members.**

Ig SFs are shown as either transmembrane or GPI-linked molecules. Ig-like domains are shared by all family members, while FN-III domains are found only for distinct members. **Presentation was taken from (Leshchyns'ka and Sytnyk, 2016).**

## 1.2. The L1 family

L1 is a family of neural immunoglobulin superfamily proteins (Brummendorf and Rathjen, 1996, Hortsch, 1996) that are sub-grouped into four members in mammals: L1 (Moos *et al.*, 1988), the close homologue of L1 (CHL1) (Holm *et al.*, 1996), the neuron-glia cell adhesion molecule (NgCAM), NgCAM-related cell adhesion molecule (NrCAM) (Grumet *et al.*, 1991) and neurofascin (Volkmer *et al.*, 1992). Alternative splicing of neurofascin (Hassel *et al.*, 1997) and NrCAM (Lane *et al.*, 1996) produces various isoforms of these molecules, while few isomers of human L1 was reported (Jouet *et al.*, 1995). The neural cell adhesion molecule L1 is a prototype member of this family. It is a neural transmembrane protein which is both glycosylated and phosphorylated, having various molecular weights of 200, 180, 140, and 80 kDa (Sadoul *et al.*, 1988) identified in mice (Rathjen and Schachner, 1984). L1 has been observed not only on post-mitotic neurons, but also on unmyelinated axons in the CNS.

Additionally, in the peripheral nervous system, neurons and non-myelinating schwann cells can express L1 (Miura *et al.*, 1992, Martini and Schachner, 1986).

Further studies have detected L1 expression by the kidney (Debiec *et al.*, 1998), specific endothelial and epithelial cells, and also tumor cell lines (Linnemann *et al.*, 1989, Patel *et al.*, 1991, Reid and Hemperly, 1992, Katayama *et al.*, 1997), indicating L1 also plays a role in migration and adhesion of non-neural tissue. Moreover, overexpression of L1 has been reported in many human cancers such as ovarian and endometrial carcinoma, pancreatic ductal adenocarcinoma, melanoma, glioblastoma (Kiefel *et al.*, 2012).

### **1.3. Structure, modifications and interactions of L1**

L1 is a transmembrane protein composed of six immunoglobulin-like (Ig) domains followed by five fibronectin-type III repeats (FNIII) at the extracellular domain, a transmembrane region, and a conserved intracellular tail in the cytoplasmic space (Moos *et al.*, 1988). L1 mediates different functions through L1 - L1 homophilic interactions (Su *et al.*, 1998, Freigang *et al.*, 2000, Meijers *et al.*, 2007, Mortl *et al.*, 2007, Sawaya *et al.*, 2008) or through variety of heterophilic interactions with L1 binding partners such as integrins, CD24, neurocan and neuropilin 1 (Schachner, 1997, Brummendorf *et al.*, 1998, Loers and Schachner, 2007, Herron *et al.*, 2009, Schafer and Altevogt, 2010). Interaction studies demonstrated that the highly conserved intracellular domain of L1 interacts with cytoskeletal proteins ankyrin, actin, spectrin and ERM (ezrin-radixin-moesin) proteins (Bennett and Baines, 2001, McCrea *et al.*, 2009).

Several studies have shown that L1 undergoes different post-translational modifications that modulate the functions of L1. The high number of glycosylation sites at the extracellular region of L1 promote homophilic interactions (Wei and Ryu, 2012). Furthermore, ubiquitination of the cytoplasmic tail of L1 molecule was reported (Schafer *et al.*, 2010). Ectodomain shedding has a crucial role in regulating the function of L1 molecule (Arribas and Borroto, 2002). Full-length L1 as an insoluble transmembrane protein could be proteolytically cleaved by serine proteases and ADAM10 (a disintegrin and metalloproteinase), consequently leading to soluble fragments released into the intracellular spaces. Several studies have reported that L1 soluble fragments contribute to cell migration (Mechtersheimer *et al.*, 2001, Yang *et al.*, 2009), cell protection against apoptosis and

promote cell survival (Stoeck *et al.*, 2007, Sebens Muerkoster *et al.*, 2007, Voura *et al.*, 2001, Nishimune *et al.*, 2005) and play a role as proangiogenic factors (Hall and Hubbell, 2004, Friedli *et al.*, 2009).

Recombinant L1-Fc was prepared by fusing the extracellular domain of L1 to the Fc region of human immunoglobulin. Studies have shown that application of L1-Fc resulted in neuron survival and neurite outgrowth through the mimicking of homophilic interactions and L1-mediated cellular responses (Appel *et al.*, 1995, Chen *et al.*, 1999, Mechtersheimer *et al.*, 2001, Kiefel *et al.*, 2012).

#### **1.4. Functions of the cell adhesion molecule L1**

L1 is implicated in brain development and morphogenesis, such as synapse formation and synaptic plasticity, glial formation, neuritogenesis, fasciculation of axons, axonal guidance and pathfinding, neuronal migration (Keilhauer *et al.*, 1985, Fischer *et al.*, 1986, Chang *et al.*, 1987, Hortsch, 1996, Kamiguchi and Lemmon, 1997, Lee *et al.*, 2008), as well as learning and memory (Law *et al.*, 2003), regeneration after injury (Maness and Schachner, 2007) and myelination processes (Lindner *et al.*, 1983, Wood *et al.*, 1990, Conacci-Sorrell *et al.*, 2005). Several studies on L1-deficient mice have shown errors in axon guidance of corticospinal and retino-collicular neurons, dendritic mis-orientation of cortical pyramidal neurons, smaller hippocampus, abnormal localization of dopaminergic neurons, abnormal cerebellar development, and deficits in spatial learning and sensorimotor gating (Maness and Schachner, 2007). Investigations have revealed that mutations in the L1 gene contribute to different neurological diseases including X-linked hydrocephalus, MASA syndrome (mental retardation, aphasia, shuffling gait, and adducted thumbs), hypoplasia of the corpus callosum, X-linked spastic paraplegia, fetal alcohol syndrome and schizophrenia (Kamiguchi *et al.*, 1998, Kurumaji *et al.*, 2001, Itoh *et al.*, 2004, Katidou *et al.*, 2008). This evidence reflects the critical role of L1 in brain development.

## 1.5. Close homologue of L1 (CHL1)

The close homologue of L1 (CHL1) was identified as a novel member of the L1 family (Holm *et al.*, 1996). Structural studies have shown that CHL1 has 37% homology to the extracellular domain of chicken NgCAM and has 64% homology to the intracellular domain of mouse NrCAM. CHL1 spans the cell membrane and consists of an extracellular portion (1081 amino acids), a transmembrane portion (23 amino acids) and an intracellular tail (105 amino acids). The extracellular domain of CHL1 is composed of six Ig-like domains, followed by four and a half FN III-like repeats. Three specific molecules of CHL1 with molecular weights of 185, 165 and 125 kDa were identified, but only 165 kDa and 125 kDa fragments being proteolytic cleavage products by ADAM<sub>8</sub> (a disintegrin and metalloproteinase) (Holm *et al.*, 1996, Naus *et al.*, 2004). The RGD (Arg-Gly-Asp) motif is a common feature of all members of the L1 subfamily such as L1 (Thelen *et al.*, 2002), NgCAM (Burgoon *et al.*, 1991), neurofascin (Koticha *et al.*, 2005) and CHL1. The RGD motif in CHL1 is located in the second Ig-like domain and interacts with integrins (D'Souza *et al.*, 1991), contributing to cell attachment. Further studies have revealed that, unlike other members of L1 subfamily, CHL1 contains the unique motif of DGEA (Asp-Gly-Glu-Ala) in the sixth Ig domain. DGEA motif of CHL1 interacts with  $\beta$ 1 integrins to promote cell migration and neuritogenesis (Buhusi *et al.*, 2003). A further distinguishing characteristic of CHL1 from other members of L1 family is the reduced fifth FN-like repeat. Two highly conserved parts in the cytoplasmic domain of CHL1 are common for L1 family. One is near to the plasma membrane (amino acid residues 1105-1119), and another is located at the C-terminal tail (amino acid residues 1175-1187) (Holm *et al.*, 1996). Moreover, the RSLE (Arg-Ser-Leu-Gln) motif in the intracellular domain (ICD) of L1 family members is not found in CHL1-ICD. This RSLE signal recruits the L1-CAM protein to the growth cones and interaction of L1 with AP-2 (clathrin adaptor) triggers clathrin-dependent endocytosis of this adhesion molecule (Kamiguchi *et al.*, 1998). The FIGAY motif within the cytoplasmic part of CHL1 contributes to ankyrin recruitment to the plasma membrane (Buhusi *et al.*, 2003). Furthermore, the intracellular section of CHL1 carries the HPD tripeptide that interacts with heat shock cognate protein Hsc70 (Leshchyn'ska *et al.*, 2006). As a glycosylated protein, 20% of CHL1 molecular mass is allocated to the N-glycosylated carbohydrates (Fig.2).

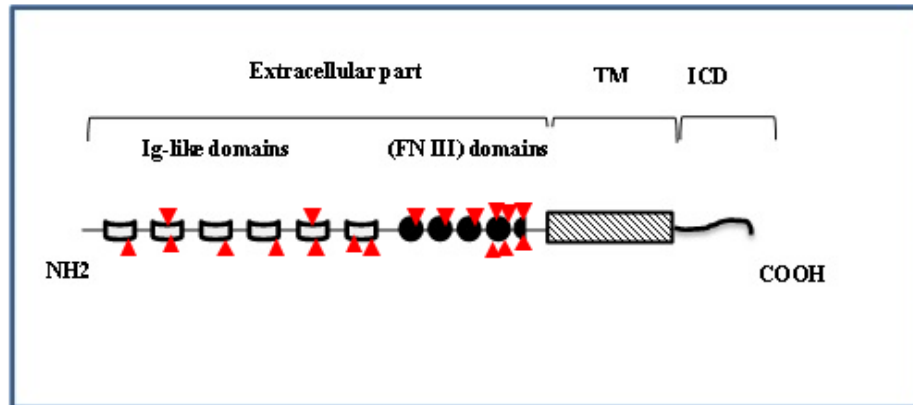


**Figure 2. Structural features of CHL1.**

The close homologue of L1 (CHL1) consists of three parts: (i) an extracellular part consisting of six Ig-like domains and four and a half FNIII-like repeats (ii) the transmembrane domain (TM) and (iii) intracellular domain (ICD). Glycosylation sites are present as triangles at the extracellular domain.

## **1.6. The close homologue of L1 (CHL1): expression pattern and functions**

Although CHL1 expression pattern overlaps with L1 in subpopulations of primary cultures of hippocampal neurons, cortical neurons, mesencephalic neurons and neurons derived from the dorsal root ganglion and spinal cord, notable differences still exist. CHL1 expression was reported in glial cells, while astrocytes only express CHL1 but not L1 (Hillenbrand *et al.*, 1999, Holm *et al.*, 1996). Immunohistochemical analyses detected CHL1 in all areas and layers of the hippocampus, predominantly in the hilus of the dentate gyrus and the mossy fibers in CA3 (Nikonenko *et al.*, 2006). CHL1 protein is expressed in the parallel fibers of molecular layer in the cerebellum. CHL1 provides a new insight in to normal cerebellar development through regulation of Purkinje cell numbers and granule cell proliferation and migration, since 20-23% loss of Purkinje cell and granule cells in the cerebellum of mature CHL1- deficient mice was reported. It has been suggested that reduction in Purkinje cell density in CHL1-/- mice is due to increased caspase-dependent apoptosis (Jakovcevski *et al.*, 2009). Also, over expression of CHL1 in glial scar astrocytes were triggered by basic fibroblast growth factor (FGF-2) in the injured spinal cord (Jakovcevski *et al.*, 2007). CHL1 is involved in synapse formation and function, and high expression level of CHL1 is reported at the early stages of the brain development (Mason *et al.*, 2003, Hillenbrand *et al.*, 1999, Holm *et al.*, 1996). CHL1 regulates migration of neurons (Liu *et al.*, 2000, Buhusi *et al.*, 2003), neuronal positioning (Demyanenko *et al.*, 2004) and neuritogenesis (Hillenbrand *et*

*et al.*, 1999, Dong *et al.*, 2002) during the brain development. CHL1 is involved in axonal regeneration in adult (Chaisuksunt *et al.*, 2000a, Chaisuksunt *et al.*, 2000b, Chaisuksunt *et al.*, 2003, Zhang *et al.*, 2000) and plays a role as a survival factor of the motor neurons (Nishimune *et al.*, 2005), and cerebellar and hippocampal neurons (Chen *et al.*, 1999). Moreover, CHL1 contributes to axon guidance and synaptogenesis, elaboration of neuronal networks and dendrite orientation (Demyanenko *et al.*, 2004, Montag-Sallaz *et al.*, 2002). Mutations in the CALL gene (the human ortholog of CHL1) are associated with mental retardation, epilepsy, schizophrenia and autism spectrum disorders identified by cognition and social behavior deficits (Angeloni *et al.*, 1999, Sakurai *et al.*, 2002, Frints *et al.*, 2003, Chen *et al.*, 2005, Chu and Liu, 2010, Tam *et al.*, 2010, Cuoco *et al.*, 2011, Salyakina *et al.*, 2011, Shoukier *et al.*, 2013). Furthermore, impairments of synaptic transmission, long-term potentiation, working memory, gating of sensorimotor information in CHL1- deficient mice, along with stress response, reactivity to novelty, social and exploratory behavior were reported (Montag-Sallaz *et al.*, 2002, Frints *et al.*, 2003, Pratte *et al.*, 2003, Demyanenko *et al.*, 2004, Demyanenko *et al.*, 2011, Irintchev *et al.*, 2004, Leshchyn'ska *et al.*, 2006, Nikonenko *et al.*, 2006, Morellini *et al.*, 2007, Wright *et al.*, 2007, Kolata *et al.*, 2008, Pratte and Jamon, 2009). Behavioral abnormalities in CHL1- deficient mice could be link to developmental impairments such as aberrant connectivity of hippocampal mossy fibers and olfactory axons (Montag-Sallaz *et al.*, 2002), altered positioning and dendrite orientation of neocortical pyramidal cells (Demyanenko *et al.*, 2004), impaired clathrin-mediated endocytosis in recycling of synaptic vesicles (Leshchyn'ska *et al.*, 2006), as well as improper inhibitory circuitries and synaptic transmission in the hippocampus (Nikonenko *et al.*, 2006). Subsequently, morphological changes in CHL1 deficient mice are revealed: Abnormal branching and orientation of stellate cell axons, decreased numbers of Purkinje and granule cells in mature cerebellum (Montag-Sallaz *et al.*, 2002, Demyanenko *et al.*, 2004, Demyanenko *et al.*, 2011, Nikonenko *et al.*, 2006, Wright *et al.*, 2007, Ango *et al.*, 2008, Jakovcevski *et al.*, 2009), as well as increased numbers of migrating cells in P<sub>7</sub> mice (Jakovcevski *et al.*, 2009). These alterations suggest the critical role of CHL1 in early postnatal brain development and during adulthood.

## 1.7. Interactions of the close homologue of L1 (CHL1)

The mechanisms underlying the functions of CHL1 can be revealed by studying the homo- and heterophilic interactions. The extracellular domain of CHL1 binds to the other CHL1 molecules on adjacent cells lead to homophilic interactions. CHL1 also interacts with other adhesion molecules such as integrins (Buhusi *et al.*, 2003, Katic *et al.*, 2014), NB-3 (Ye *et al.*, 2008), cell surface receptors such as the receptor-type protein-tyrosine phosphatase  $\alpha$  (Ye *et al.*, 2008), and serotonin receptor (Kleene *et al.*, 2015), semaphorin 3A receptor neuropilin1 (Wright *et al.*, 2007) and ephrin A5 receptor (Demyanenko *et al.*, 2011).

The sixth Ig-like motif of CHL1 (DGEA) with mediation of integrins could trigger the Src/PI3-kinase/ MEK/ ERK cascade, which leads to axonal growth and cell migration. Moreover, the first Ig motif (FASNRL) of CHL1 binds to the semaphoring 3A receptor neuropilin-1 and promotes growth cone collapse. A conserved motif in the cytoplasmic domain of CHL1 (FIGAY) induces ankyrin, F-actin and spectrin associations that could be crucial for receptor clustering and signal transduction (Maness and Schachner, 2007). Modulation of CHL1 functions by homo- and heterophilic interactions are reported through a great body of evidence. Studies indicate that FGF-2-mediated expression of CHL1 in astrocytes after spinal cord trauma could limit axonal regrowth and remodeling of neural circuits through CHL1–CHL1 homophilic interaction (Jakovcevski *et al.*, 2007). Another study has reported that CHL1 homophilic interactions modulate differentiation of neuronal progenitor cells at early cerebellar morphogenesis (postnatal day 5), whereas heterophilic interactions between the extracellular domain of CHL1 with vitronectin, integrins, and the plasminogen activator system, promote neurite outgrowth and granule cell migration at a later postnatal stage (day 6-7) of developmental process (Katic *et al.*, 2014). A recent study has demonstrated that CHL1 as a regulator of the serotonergic system could interact with the serotonin 2c receptor (5-HT<sub>2c</sub>) through heterophilic interactions. CHL1 modulates signaling pathways induced by serotonin receptor through molecular associations of PTEN (phosphatase and tensin homolog) and  $\beta$ -arrestin. PTEN interacts with the dephosphorylated 5-HT<sub>2c</sub> receptor in the absence of CHL1, while association of  $\beta$ -arrestin 2 with the phosphorylated 5-HT<sub>2c</sub> receptor occurs in the presence of CHL1. As a consequence, CHL1 influences phospholipase D activity and ERK signaling pathways by interaction with serotonin receptor. The results have shown that the function of 5-HT<sub>2c</sub> receptor is impaired in the absence of CHL1. Since CHL1 and 5-HT<sub>2c</sub> receptor are co-expressed in GABAergic interneurons, hypolocomotion of

CHL1-deficient mice could be a result of locomotor inhibition by the 5-HT<sub>2c</sub> receptor (Kleene *et al.*, 2015).

Various studies have shown that CHL1 involves in two steps of synaptic vesicle recycling. First in endocytosis, the intracellular domain (ICD) of CHL1 interacts with Hsc70 and regulates clathrin release from clathrin-coated synaptic vesicles (Leshchyn'ska *et al.*, 2006). Secondly in exocytosis, the CHL1-ICD interacts with presynaptic chaperones such as SGT, CSP, and Hsc70; mediating SNARE (N-ethylmaleimide-sensitive factor attachment protein receptor) complex refolding (Andreyeva *et al.*, 2010). Furthermore,  $\beta$ II spectrin was identified as a binding partner of CHL1-ICD. Notably, partial disruption of CHL1-spectrin interaction leads to palmitoylation and lipid raft-dependent endocytosis of CHL1, promoting neuritogenesis (Tian *et al.*, 2012).

## **2. Novel binding partners of CHL1**

### **2.1. ALG-2 (apoptosis-linked gene 2): Structure and functions**

In this study, I identified ALG-2 (apoptosis-linked gene 2) as a novel binding partner of CHL1. For this purpose, affinity chromatography and mass spectrometry approaches were used, which will be described in detail over the following next chapters.

ALG-2 also called Programmed Cell Death 6 (PDCD6) is a 22-kD protein, belonging to the penta EF-hand family including calpain, sorcin and grancalcin. ALG-2 has a helix-loop-helix structural domain; forming an anti-parallel dimer conformation *via* paired EF5s (Fig.3). Since ALG-2 forms a dimer, it can bind to two ligands. It bridges two binding proteins or stabilizes the protein complex while playing a role as a calcium-dependent adaptor protein on scaffolds. Structural studies have shown that ALG-2 undergoes conformational changes due to binding to Ca<sup>2+</sup> ions. Although ALG-2-peflin interaction is independent of Ca<sup>2+</sup>, several studies have shown that ALG-2 interacts with different proteins in a calcium-dependent manner (Maki *et al.*, 2011). ALG-2 is a protein expressed in normal brain and highly expressed in an ischemic brain (Jang *et al.*, 2002). ALG-2 has a regulatory role in late apoptosis, where different death pathways converge. Interaction of ALG-2 with death-associated protein kinase 1 (DAPK1) promotes apoptotic cell death *via* the caspase signaling pathway (Lee *et al.*, 2005). Furthermore, binding of ALG-2 to Alix, annexins, TSG101, mucolipin-1 clarified the new

understanding of biological functions of ALG-2 in membrane trafficking (Shibata *et al.*, 2007, Katoh *et al.*, 2005, Vergarajauregui *et al.*, 2009). Recent publications have revealed that ALG-2 interacts with RNA binding motif protein 22 (RBM22). Translocation of ALG-2 from the cytoplasm to the nucleus was triggered after heat shock or thapsigargin treatment (Montaville *et al.*, 2006, Janowicz *et al.*, 2011, Sasaki-Osugi *et al.*, 2013). Recent investigations have reported that ALG-2 is overexpressed in different human cancer types in comparison to normal tissue (la Cour *et al.*, 2003, la Cour *et al.*, 2008, Aviel-Ronen *et al.*, 2008). Taken together, these findings emphasize the critical role of ALG-2 protein in apoptosis and tumor development.

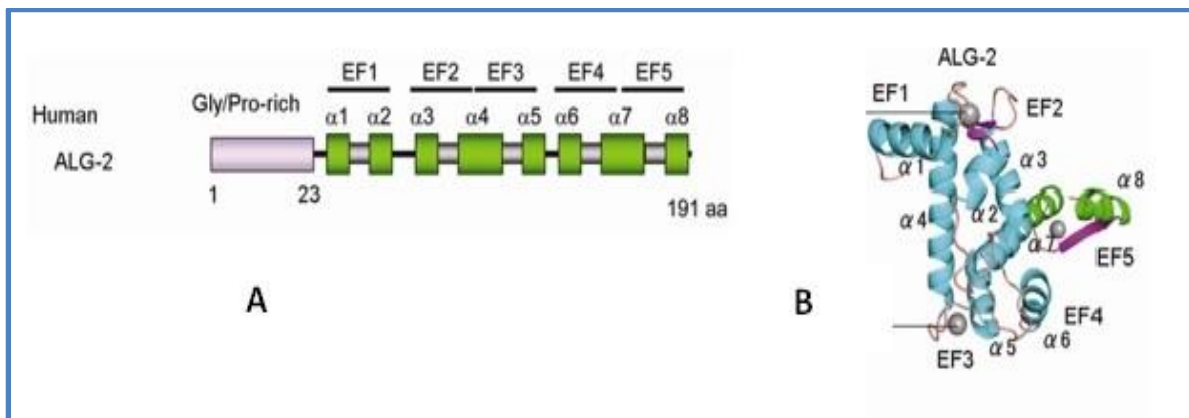


**Figure 3. Schematic structure of human ALG-2 protein.**

(A) ALG-2 includes five EF-hand motifs (EF1–EF5), which are composed of eight  $\alpha$ -helices ( $\alpha$ 1– $\alpha$ 8). (B) Here, the 3D structure of ALG-2 is shown. Helices from EF1- EF4 and EF5 are presented in cyan and in green, respectively. Loops and  $\beta$ -sheet structures are shown in pale pink and magenta, respectively. Calcium atoms are colored as gray spheres. **Presentation was taken from (Maki *et al.*, 2011).**

## 2.2. Synaptogyrin family members

In current study, I identified synaptogyrin-1 and synaptogyrin-3 as novel interacting partners of CHL1. For this purpose, affinity chromatography followed by mass spectrometry approaches were used, which will be described in detail in the following next chapters.

Synaptogyrin family consists of two neuronal (synaptogyrin 1 and 3) and one ubiquitous (cellugyrin) isoforms. Several studies have identified synaptogyrins as synaptic vesicle proteins that contribute to the regulation of neurotransmitter release (Belizaire *et al.*, 2004).

Because Synaptogyrin-3 is expressed only in distinct populations of synapses, therefore the interaction of CHL1 and synaptogyrin-3 was further investigated in this study. Synaptogyrin-3 as a new synaptic vesicle protein interacts with the dopamine transporter (DAT) to positively regulate DAT activity. Synaptogyrin-3 promotes the physical and functional interactions of DAT with the vesicular monoamine transporter 2 (VMAT2) in dopamine vesicular storage systems. These interactions lead to refilling of the vesicles with extracellular dopamine after release (Egana *et al.*, 2009).

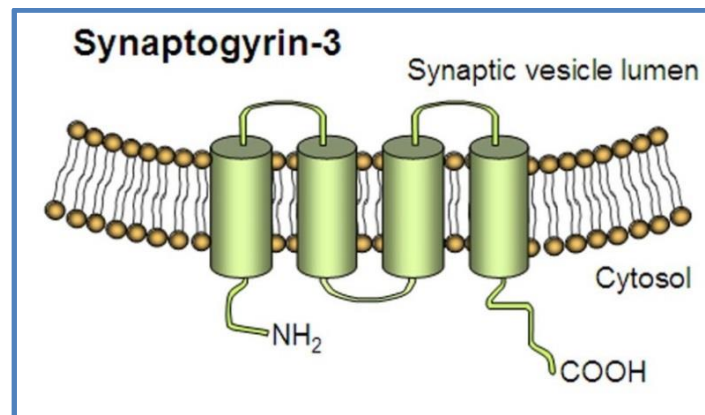


**Figure 4. Schematic illustration of the synaptic vesicle protein: synaptogyrin-3.**

Synaptogyrin-3 contains four transmembrane domains with cytoplasmic N and C termini. **Presentation was taken from (Egana *et al.*, 2009).**

### **2.3. Dopamine transporter (DAT) as a novel binding partner of CHL1**

Since synaptogyrin-3 interacts with DAT and CHL1, I investigated whether CHL1 also interacts directly with DAT. This interaction was identified through different experiments and will be described in more detail in the next chapters.

#### **2.3.1. Dopamine transporter: structure and interactions**

Dopamine transporter belongs to the SLC6 family (solute carrier family 6) of transporters which uptakes dopamine by Na<sup>+</sup> symport mechanism. DAT is a presynaptic plasma membrane protein with 12 transmembrane domains, and a long glycosylated loop between the third and fourth domains. DAT cytoplasmic N- and C-terminal sections are critical sites for post-translational modifications and regulation, as well as binding sites for protein

partners. While the C terminus is S-palmitoylated, the N terminus undergoes phosphorylation and ubiquitylation (Vaughan and Foster, 2013). Several proteins have been identified that interact with different domains of the DAT and regulate its function. Recent studies have shown that cellular processes such as synaptic distribution, targeting to specific compartment, trafficking, recycling and functions of the DAT that could be regulated by interacting proteins such as: the focal adhesion protein Hic-5, synuclein, syntaxin, protein interacting with C kinase-1 (PICK1), receptor for activated C kinase-1 (RACK1), and protein phosphatase PP2A (Torres, 2006).

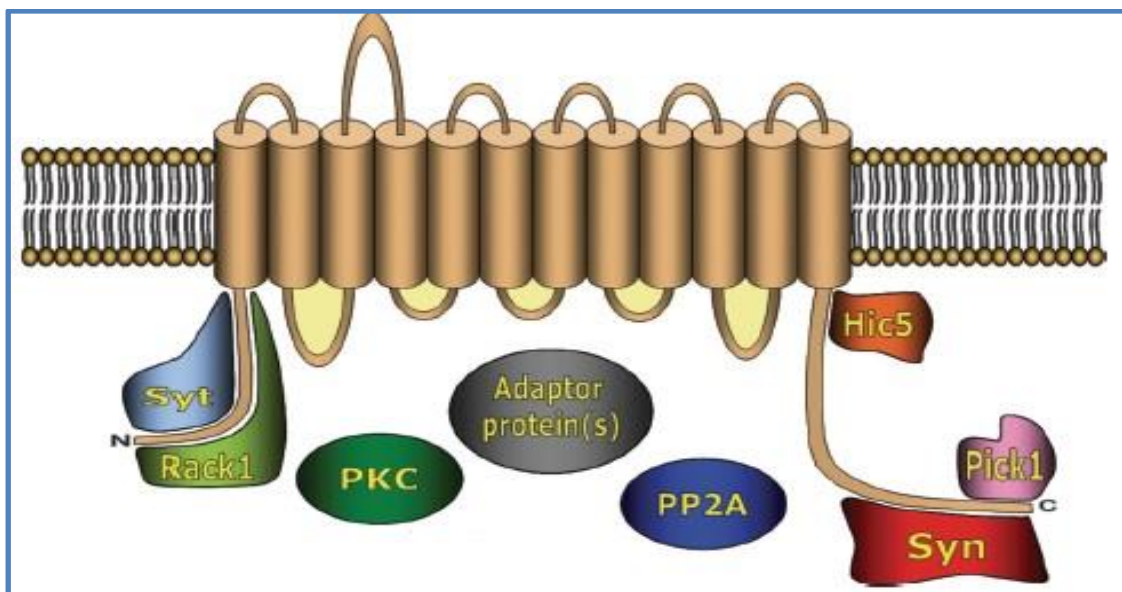


**Figure 5. Interaction of dopamine transporter with binding partners.**

Depicted proteins interact with different domains of the DAT. Syntaxin 1A (Syt) and RACK1 bind to the N-terminus, and synuclein (Syn), Hic-5 and PICK1 bind to the C-terminus. The association between DAT and PKC or PP2A may be direct or involve adaptor protein(s). **Presentation was taken from (Torres, 2006).**

### 2.3.2. Dopamine transporter function

Immunohistochemistry studies of mouse brain showed extensive dopamine transporter (DAT) expression in the striatum, cell bodies of the substantia nigra, ventral tegmental area (VTA), nucleus accumbens, olfactory tubercle, nigrostriatal bundle and lateral habenula.

Dopamine contributes to many physiological functions including movement, cognitive processes, mood and rewarding behavior. DAT is a presynaptic plasma membrane protein that mediates re-uptake of dopamine from synaptic cleft into presynaptic terminals, and thus

is essential for homeostasis of dopamine at the synapse. DAT function and dopamine transmission contribute to neurological and psychiatric diseases including Parkinson's diseases, depression, schizophrenia, attention deficit hyper activity disorder (ADHD), tourette syndrome and bipolar disorder. In addition, DAT plays an important role in addiction and is the principle target for psychostimulants, such as cocaine and amphetamine (AMPH) (Torres *et al.*, 2003b). A growing number of studies have suggested that different mechanisms are involved in regulation of DAT function. Since oligomerization of DAT seems to be crucial for the trafficking of transporter to the cell membrane, N-linked glycosylation is involved in normal expression of transporters at the cell surface, but not for ligand binding or translocation of dopamine (Torres *et al.*, 2003a). DAT is not a static molecule as it dynamically cycles to and from the plasma membrane *via* the trafficking machinery. Since recent studies have suggested that internalized DAT recycles back to the plasma membrane, other studies have shown that DAT degrades following internalization. DAT trafficking has been studied in various neuronal and non-neuronal cell lines, as well as midbrain culture. Two different mechanisms for DAT endocytosis were detected: Basal and PKC-stimulated internalizations. Although DAT constitutively internalizes and recycles, a great body of evidence has shown that DAT undergoes phosphorylation by protein kinase C (PKC), which induces DAT endocytosis, leading to cell surface loss and downregulation of transporter. Recent studies have reported that constitutive DAT endocytosis is independent of dynamin, occurs equivalently from lipid raft and non-raft micro domains, while PKC-stimulated DAT internalization is dynamin-dependent and appears particularly from lipid raft domains. In the second mechanism, dynamin acts in association with actin cytoskeleton (Gabriel *et al.*, 2013)

## **II. Aims of the study**

Since CHL1 is linked to mental retardation, schizophrenia, major depression, epilepsy, and autism spectrum disorders in humans, investigations of CHL1 interactions may help to understand cellular and molecular mechanisms associated with neurological and psychiatric diseases. Several studies have shown that ablation of CHL1 in mice leads to impairments in synaptic transmission, long term potentiation, working memory, gating of sensorimotor information and stress response as well as alterations in social and exploratory behavior. Therefore, studying the functional interplay of CHL1 with binding partners would shed new light to further understanding the mechanisms underlying CHL1 functions in the brain. The aims of this study are:

- Identification and characterization of putative binding partners of CHL1 intracellular domain by affinity chromatography and mass spectrometry.
- Verification of physical interaction between CHL1 and binding partners by alternative approaches such as co-immunoprecipitation, pull down assay, immunofluorescence staining and co-localization studies
- Functional studies of CHL1 and binding proteins using a variety of methods that specifically designed for the respective interacting partner

### III. Materials

#### 1. Antibodies

##### 1.1. Primary antibodies

Name and epitope	Source	Species	Application
ALG-2 (FL-191)	Santa Cruz (sc-292580)	polyclonal rabbit	WB , IP,IF
ALG-2 (AA8)	Santa Cruz (sc-101209)	Monoclonal Mouse	WB , IP,IF
CHL1(C-18), raised against C-terminus	Santa Cruz (sc-34986)	Polyclonal goat	IP, IF, proximity ligation assay
CHL1, raised against the extracellular domain	R&D systems (AF-2147)	Polyclonal goat	WB
Dopamine transporter	Millipore (MAB369)	Monoclonal rat	WB
Dopamine transporter (H-80)	Santa Cruz (sc-14002)	polyclonal rabbit	IF, IP, proximity ligation assay
NCAM180 (D3) against intracellular domain of NCAM180	Schlosshauer <i>et al.</i> , 1989	Monoclonal Mouse	WB
Synaptogyrin-3 (E-11)	Santa Cruz (sc-271046)	Monoclonal Mouse	WB , IP,IF, proximity ligation assay
TH (tyrosine hydroxylase)	Millipore (AB152)	polyclonal rabbit	IF

**Table 1. Primary antibodies are listed in alphabetical order.**

The acronyms are: WB: Western blot; IF: Immunofluorescence; IP: Immunoprecipitation.

## 1.2. Secondary antibodies

All horseradish peroxidase (HRP) secondary antibodies were purchased from the Jackson Laboratory (Dianova. Hamburg. Germany). HRP-coupled antibodies were used in a dilution of 1:10,000 in 4% skim milk powder in phosphate buffered saline solution pH 7.4 (PBS) containing 0.05% Tween 20 (PBST) for immunoblotting. Cy2-, Cy3- and Cy5-coupled antibodies were used in a dilution of 1:200 in PBS for immunostaining.

## 2. Chemicals

Cyanogen bromide-activated-Sepharose (Sigma Aldrich, C9142) was used for affinity chromatography. Fura-2 AM (Invitrogen, F1221), Phorbol 12-myristate13-acetate (PMA) (Tocris, 1201), calcein AM (Molecular Probes, Leiden, the Netherlands) and Turbofect (Thermofischer-R0531) were provided.

## 3. Buffers and solutions

Ampicillin stock (1000x)	100 mg/ml in H <sub>2</sub> O, store in aliquots in - 20°C
Blocking buffer (affinity chromatography)	0.2 M Glycine (pH 8.0)
Blocking buffer (WB.)	4% skim milk powder in PBST
Blotting buffer	25 mM Tris (pH 8.3) 190 mM Glycine 20% Methanol
Cell-line medium (NIH-3T3 and HEK293 )	10% Fetal calf serum (FCS) 2 mM L-glutamine 1 mM Sodium pyruvate 5 U/ml Penicillin/Streptomycin All in high glucose Dulbecco modified Eagle's (DMEM)

Cerebellum medium	1 mM L-glutamine 1 mM Sodium pyruvate 5 U/ml Penicillin/Streptomycin 0.1% Bovine serum albumin (BSA) 10 µg/ml Insulin 4 nM L-Thyroxine 100 µg/ml Bovine transferrin, Holo 30 nM Sodium-selenite 1x B-27 Supplement All in Neurobasal A (Life Technologies)
Coupling buffer (affinity chromatography)	0.1 M NaHCO <sub>3</sub> (pH 8.3) 0.5 M NaCl
Digestion solution	135 mM NaCl 5 mM KCl 7 mM Na <sub>2</sub> HPO <sub>4</sub> 4 mM NaHCO <sub>3</sub> 25 mM HEPES (pH 7.4)
Dissection solution	4 mM NaHCO <sub>3</sub> 10 mM HEPES 6 mg/ml D-glucose 5 µg/ml gentamycin 3 mg/ml BSA 12 mM MgSO <sub>4</sub>  All in Hanks's balanced salt solution (HBSS)
Elution buffer (affinity chromatography)	0.1 M Glycine (pH 2.3)

Elution buffer for the pQE-system	50 mM NaH <sub>2</sub> PO <sub>4</sub> 300 mM NaCl 300 mM imidazole
Hippocampus medium	2 mM L-glutamine 1x B-27 supplement 12 ng/ml bFGF All in Neurobasal A
Homogenization buffer (affinity chromatography)	50 mM Tris-HCl (pH7.4) 0.32 M Sucrose 1 mM CaCl <sub>2</sub> 1 mM MgCl <sub>2</sub>
IPTG (1M) stock solution (1000x)	238 mg/ml in H <sub>2</sub> O, store in aliquots in - 20°C
Kanamycin stock (1000x)	25 mg/ml in H <sub>2</sub> O, store in aliquots in - 20°C
LB-medium	10 g/l Bacto-tryptone, pH 7.4 10 g/l NaCl 5 g/l Yeast extract
LB-ampicillin medium	100 mg/l Ampicillin in LB-medium
LB-kanamycin medium	25 mg/l Kanamycin in LB-medium
Lysis buffer for the pQE-system	50 mM NaH <sub>2</sub> PO <sub>4</sub> (pH 8) 300 mM NaCl 10 mM Imidazole
PBS (phosphate buffered saline)	137 mM NaCl 2.7 mM KCl 8 mM Na <sub>2</sub> HPO <sub>4</sub> 1.5 mM KH <sub>2</sub> PO <sub>4</sub> (pH 7.4)

PBST	PBS+ 0.05% Tween 20
Radio immunoprecipitation assay (RIPA) buffer	50 mM Tris-HCl (pH 7.4) 180 mM NaCl 1 mM Na <sub>4</sub> P <sub>2</sub> O <sub>7</sub> 1% NP-40
Resolving gel 12% (SDS-PAGE)	1.3 ml H <sub>2</sub> O 2.3 ml 1 M Tris-HCl (pH 8.8) 0.06 ml 10% SDS 0.015 ml 10% ammonium persulfate (APS) 2.4 ml 30% acrylamide / 0.8% bisacrylamide 6 µl TEMED
SDS running buffer (10x)	250 mM Tris-HCl (pH 8.3) 1.9 M Glycine 1% SDS
SDS sample buffer (5x)	62.5 mM Tris-HCl, pH 6.8 40 % (w/v) Glycerol 2 % SDS 5 % 2-Mercaptoethanol 0.04 % Bromphenol blue
Stacking gel (5 %) (SDS-PAGE)	1.6 ml H <sub>2</sub> O 0.4 ml 30% acrylamide / 0.8% bisacrylamide 0.3 ml 1M Tris-HCl (pH 6.8) 30 µl 10% SDS 15 µl 10% APS 6 µl TEMED

TAE buffer (50x)	2 M Tris-acetate (pH8.0)
	100 mM EDTA
Nuclei extraction buffer (Roeder C buffer)	10 mM Tris-HCl (pH 8)
	0.5 mM EDTA
	2 mM MgCl <sub>2</sub>
	300 mM NaCl
	10% Glycerol

**Table 2. Buffers and solutions in alphabetical order.**

## 4. Molecular weight ladder

### 4.1. DNA ladder

**GeneRuler 1 kb Plus DNA Ladder**

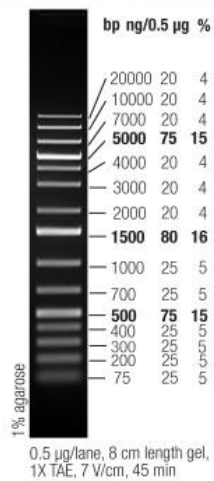


**Figure 6 . GeneRuler™ 1kb DNA Ladder Plus (Fermentas, SM1331).**  
Representative image was taken from Fermentas webpage.

## 4.2. Protein ladder

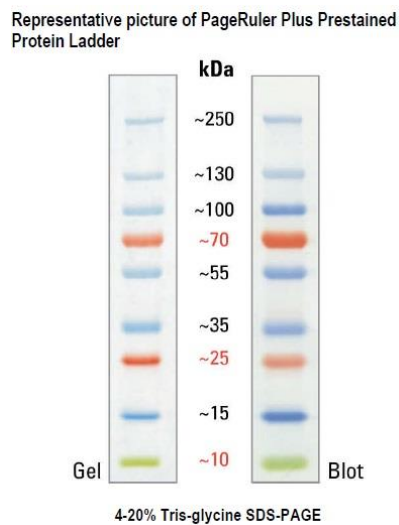


**Figure 7. SDS-PAGE band profile of the PageRuler protein Ladder, (Thermofisher, 26619)**  
Representative image was taken from Thermofisher webpage.

## 5. Animals

CHL1-deficient mice (Montag-Sallaz *et al.*, 2002) that have been generated on a C57BL/6J background by breeding for more than eight generations. Also, the same age wild-type C57BL/6J mice were bred and maintained at the Universitäts klinikum Hamburg-Eppendorf. Mice were kept at 25°C, on a 12 h light/12 h dark cycle with *ad libitum* feeding. Wild-type and CHL1-deficient mice of a postnatal day 0 to 2 or P5, and adult 12 to 16 weeks-old of either sex were used.

## 6. Bacterial strains

*Escherichia coli* M15 (pREP4) (QIAGEN)

*Escherichia coli* competent cells (638909, Clontech cloning kit, USA)

## 7. Plasmids

### Plasmid

### Information

**CFP-synaptogyrin-3**

Mammalian expression vector

Kind gift from Dr. Gonzalo Torres, USA

<b>YFP-Dopamine transporter (DAT)</b> Kind gift from Dr. Gonzalo Torres, USA	Mammalian expression vector
<b>pAcGFP-CHL1</b> Newly constructed plasmid for this study	Mammalian expression vector of GFP-tagged full length CHL1
<b>pCAG-IRES- DAT/CHL1</b> Newly constructed plasmid for this study	Bicistronic mammalian vector included IRES element that co-expresses dopamine transporter (DAT) and CHL1
<b>pCAG-IRES-DAT</b> Newly constructed plasmid for this study	Bicistronic mammalian vector included IRES element that expresses dopamine transporter (DAT)
<b>pcDNA-CHL1</b> Available in the lab	Mammalian expression of full length CHL1
<b>DsRed-ALG-2</b> Kind gift from Dr. Joachim Krebs, Germany	Mammalian expression of red fluorescent - tagged full length ALG-2
<b>CHL1-ICD</b> (Leshchyn'ska et al., 2006)	Prokaryotic expression vector for His-tagged intracellular domain of CHL1
<b>NCAM180-ICD</b> Available in the lab	Prokaryotic expression vector for His-tagged intracellular domain of NCAM180

**Table 3. Expression vectors used for mammalian and bacterial systems.**

## 8. Primers

Oligonucleotide	Sequence
Forward primer for linearization of GFP vector	5'-ACC GGT CAT GGT GAG CAA-3'
Reverse primer for linearization of GFP vector	5'-TCT GAC GGT TCA CTA AAC-3'
Forward primer for amplification of CHL1insert with 15bp extensions homologous to GFP vector end	5'-TAG TGA ACC GTC AGA ATG ATG GAA TTG CCA TTA TGT-3')
Reverse primer for amplification of CHL1insert with 15bp extensions homologous to GFP vector end	5'-CTC ACC ATG ACC GGT TGC CCG GAG TGG GAA GGT-3'
Forward primer for linearization of pCAG vector	5'-AGC GGC CGG CCG CCA GCA CAG TGG-3')
Reverse primer for linearization of pCAG vector	5'-CGG GGC GAA GGC AAC GCA GCG ACT-3'
Forward primer for amplification of IRES element	5'-ATG GTA ATC GTG CGA GAG G-3'
Reverse primer for amplification of IRES element with extension homologous to CHL1	5'-TGG CAA TTC CAT CAT GGT TGT GGC CAT ATT ATC AT-3')
Forward primer for amplification of DAT with extension homologous to pCAG vector end	5'-GTT CGC CCC GAT GAG TAA GAG CAA ATG CTC CGT G-3'
Reverse primer for amplification of DAT with extensions homologous to IRES	5'-CAC GAT TAC CAT TGA CAC CTT GAG CCA GTG GCG G-3'
Forward primer for amplification of CHL1	(5'-ATG ATG GAA TTG CCA TTA TGT-3')
Reverse primer for amplification of CHL1 with extension homologous to pCAG vector end	5'-TGG CGG CCG GCC GCT TCA TGC CCG GAG TGG GAA-3'

**Table 4. List of the primers that used for cloning.**

## 9. Kits

InFusion Cloning Kit	Clontech, 638909
NucleoSpin® Plasmid isolation kit	Macherey-Nagel
PCR clean-up gel extraction kit	Clontech
PLA proximity ligation assay	Duolink

## IV. Methods

### 1. Molecular biology methods

#### 1.1. Molecular cloning and PCR

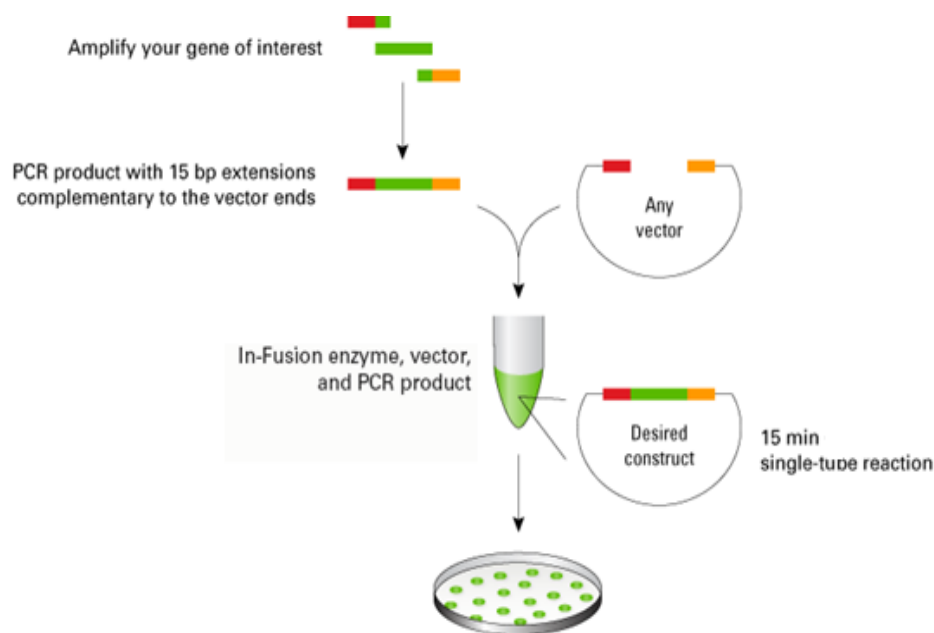


**Figure 8. Protocol overview of cloning with InFusion Cloning Kit (Clontech)**

The protocol steps are summarized here: The vector was linearized by PCR using specific primers. To amplify the gene of interest, proper primers were designed with 15bp extensions that are complementary to the ends of the linearized vector. Then, the PCR products were purified with spin-column and the In-Fusion cloning reaction was prepared according to the manufacturer's instructions. Competent cells were transformed with reaction mixture and bacteria were plated on LB plates. **Presentation was taken from Clontech webpage.**

### **1.1.1. Sub-cloning of CHL1 from pcDNA-CHL1 construct in to GFP vector**

For the creation of a vector expressing GFP-tagged CHL1, the insert was amplified from the pcDNA3-CHL1 vector containing the full length CHL1 (Holm et al., 1996).

**1.** For linearization of GFP vector the forward primer (5'-ACC GGT CAT GGT GAG CAA-3') and the reverse primer (5'-TCT GAC GGT TCA CTA AAC-3') were used in the PCR reaction.

**2.** Gene of interest (CHL1) was amplified by PCR reaction. For this purpose, forward primer (5'-TAG TGA ACC GTC AGA ATG ATG GAA TTG CCA TTA TGT-3') and reverse primer (5'-CTC ACC ATG ACC GGT TGC CCG GAG TGG GAA GGT-3') with 15bp extensions complementary to GFP vector ends were designed.

#### **3. Polymerase chain reaction (PCR)**

Amplification of DNA fragments was performed in a 25 µl reaction mix in PCR tubes in PCR cyclers. Polymerase enzyme (CloneAMP HiFi PCR Premix) was obtained from In-Fusion HD Cloning Kit (638909, Clontech). The following reaction mixture was prepared: 100 ng template, 1µl forward primer (10 pM), 1µl reverse primer (10 pM), 12.5 µl CloneAMP HiFi PCR Premix enzyme and dH<sub>2</sub>O up to 25 µl.

The PCR was performed with the following step gradient:

- a) Initial denaturing 98°C, 5 min
- b) Denaturing 98°C, 10 sec
- c) Annealing 58°C, 30 sec
- d) Synthesis 72°C, 45 sec/ 1kb DNA
- e) Termination 72°C, 7 min
- f) Cooling 4°C

The amplification procedure (steps b-d) was repeated 35 times.

**4.** Following PCR, the amplified products were run on agarose gel electrophoresis. Target fragments of linearized vector and CHL1 insert were cut and isolated with PCR clean-up gel extraction kit that is provided in Clontech InFusion Cloning Kit. After purification, fusion

reaction was prepared by adding 2  $\mu$ l InFusion enzyme provided in the kit, 100 ng linearized vector, 100 ng CHL1 insert and d H<sub>2</sub>O up to 10  $\mu$ l. The reaction was incubated for 15 min at 50°C and continued with bacteria transformation procedure.

### **1.1.2. Cloning of CHL1 and Dopamine transporter (DAT) in bicistronic IRES Vector**

1. Linearization of pCAG vector was performed by using forward primer (5'-AGC GGC CGG CCG CCA GCA CAG TGG-3') and reverse primer (5'-CGG GGC GAA GGC AAC GCA GCG ACT-3'). For amplification of the IRES element, the IRES forward primer (5'-ATG GTA ATC GTG CGA GAG G-3') and IRES reverse element with extension complementary to CHL1 (5'-TGG CAA TTC CAT CAT GGT TGT GGC CAT ATT ATC AT-3') were applied.

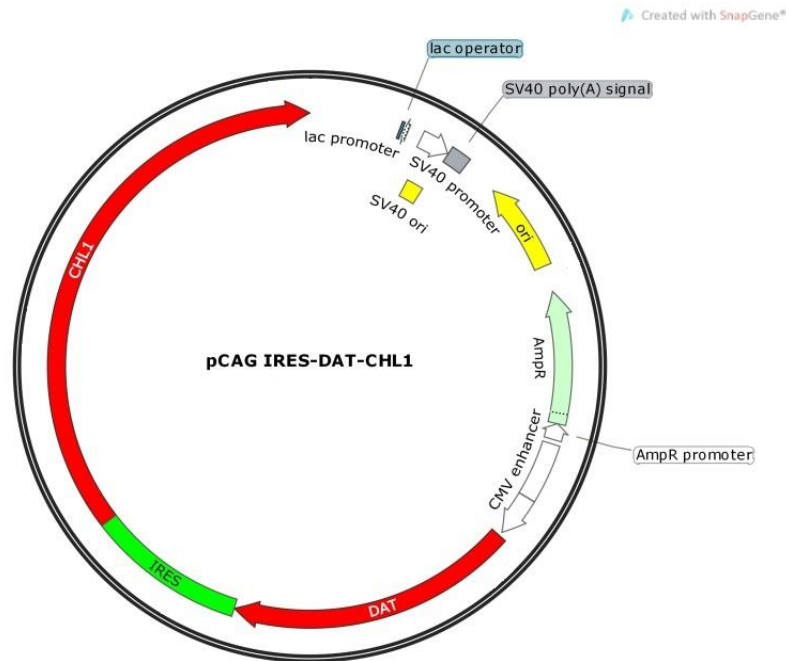
2. DAT construct was a kind gift from Dr. Gonzalo Torres. Forward primer for amplification of DAT with extension complementary to pCAG vector end (5'-GTT CGC CCC GAT GAG TAA GAG CAA ATG CTC CGT G-3') and reverse primer for amplification of DAT with extension complementary to IRES (5'-CAC GAT TAC CAT TGA CAC CTT GAG CCA GTG GCG G-3') were designed. Also, in order to amplify CHL1-coding cDNA (Holm *et al.*, 1996) by PCR reaction, forward primer (5'-ATG ATG GAA TTG CCA TTA TGT-3') and reverse primer for CHL1 with extension complementary to pCAG vector end (5'-TGG CGG CCG GCC GCT TCA TGC CCG GAG TGG GAA-3') were used.

3. Following PCR, the amplified products were run on agarose gel electrophoresis. Target fragments of linearized vector and CHL1 and DAT inserts were cut and isolated with PCR clean-up gel extraction kit. After purification, a fusion reaction was prepared by adding 2  $\mu$ l InFusion enzyme provided in the kit, 100 ng linearized vector, 50 ng CHL1 insert, 50 ng DAT insert and d H<sub>2</sub>O up to 10  $\mu$ l. The reaction was incubated for 15 min at 50°C and continued to bacteria transformation procedure.

4. The bicistronic IRES Vector created from the fusion of the pCAG with DAT and CHL1 could co-express the dopamine transporter and CHL1 from the same mRNA. The bicistronic IRES vector resulted from the fusion of the pCAG with DAT fragment was applied for single expression of the dopamine transporter (Kleene *et al.*, 2015).

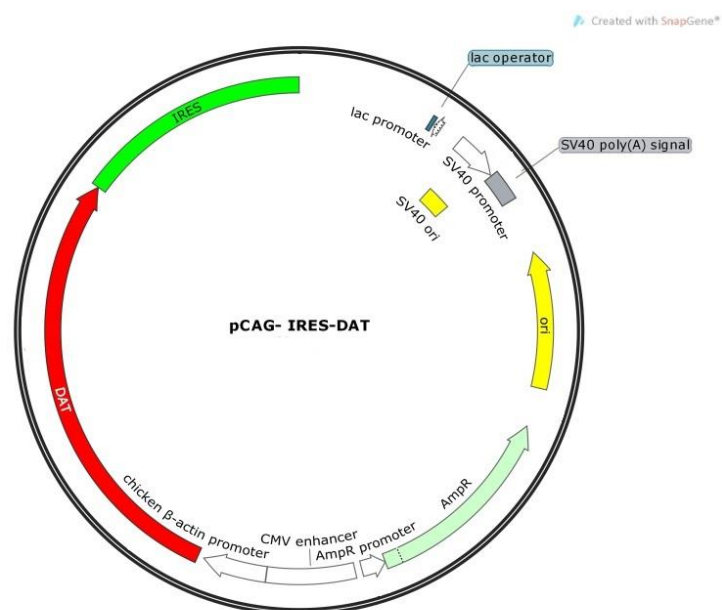
### Construct 1: pCAG-IRES-DAT/CHL1

The fused fragment of pCAG-CHL1 was incubated with DAT-IRES fragment in order to create construct 1 with final molecular weight of 10.1 Kb that simultaneously co-expresses dopamine transporter and CHL1 from the same mRNA.



### Construct 2: pCAG-IRES-DAT

Through infusion of pCAG (3.7Kb), IRES (1 Kb) and DAT (1.8 Kb) fragments, construct 2 with final molecular weight of 6.5 Kb was created, which expresses dopamine transporter alone.



## **1.2. Horizontal agarose gel electrophoresis of DNA**

Agarose powder was boiled in TAE buffer. The solution was cooled down. Immediately, 5 µl Roti-GelStain (Carl Roth, 3865) was added to 100 ml agarose and mixed gently. The gel was casted in an electrophoresis chamber (BioRad) and 0.8-1% gel was prepared. The DNA samples were diluted with 5x sample buffer containing orange-G and loaded in to the wells of the gel. The samples were run at constant 100 V and the bands were viewed under UV light.

## **1.3. Determination of DNA concentration**

DNA concentration was determined by absorption measurement at 260 nm using the NanoDrop (Spectrophotometer ND-1000, Peqlab). The ratio of A<sub>260</sub>/A<sub>280</sub> is used to evaluate the purity of DNA and value of 1.8 is acceptable as a pure DNA. It should be considered that contamination with protein and phenol increases the absorbance at 280 nm and decreases the DNA purity. Furthermore, the ratio of 260/230 could be used as a second measure of DNA purity. The values in the range of 2.0-2.2 could indicate the absence of contaminations at 230 nm.

## **1.4. Transformation of bacteria**

50-100 ng of plasmid DNA was added to 100 µl of competent cell and incubated for 30 min on ice. Following a heat shock (2 min, 42°C), the samples were incubated on ice (3 min). After 30 min incubation at 37°C with 800 µl SOC-medium (provided in the kit), bacteria were plated on LB plates containing the appropriate antibiotics. Plates were incubated overnight in a 37°C incubator.

## **1.5. Plasmid isolation from *Escherichia coli* culture**

A culture of 3 ml LB medium containing appropriate selective antibiotic (25 µg/ml of kanamycin or 100 µg/ml ampicillin) was inoculated with a single colony and incubated overnight at 37°C. Bacteria were then harvested by centrifugation at 12000 g for 1 min at room temperature. The plasmid was isolated with Miniprep kit according to the manufacturer instructions (Macherey-Nagel) and eluted by 50 µl of TE buffer. To prepare large amounts of

plasmid DNA, 500 ml bacteria culture were taken to isolate plasmids using the Maxiprep kit with the same principle.

## **1.6. DNA sequencing**

Sequencing was carried out with fluorescent dideoxy terminators according to Sanger ("*DNA sequencing with chain-terminating inhibitors*". *Proc. Natl. Acad. Sci. U.S.A.* 74 (12): 5463–7.) and analysis was performed on an ABI 3130 Genetic Analyzer with Sequence Analysis v 5.4 software (Applied Biosystems) at the bioanalytics facility, ZMNH, Hamburg.

## **2. Protein biochemistry methods**

### **2.1. Production of recombinant proteins**

#### **2.1.1 Expression of recombinant proteins in *E. coli*.**

M15 *E. coli* strain was transformed with the expression constructs such as His-tagged CHL1-ICD and NCAM180-ICD. Then, LB culture containing the appropriate antibiotics (Kan and Amp) was inoculated by a single colony and incubated at 37°C under constant agitation until the optical density of culture had reached to 0.6. Protein expression was induced by adding IPTG (f.c.1mM) to the culture with further incubation for 4-6 h at 37°C. Bacteria were collected by centrifugation (4000 x g, 10 min, 4°C). The pellet was lysed in lysis buffer using a sonicator (Branson Sonifier B15, level 6, 50% pulse, 5 x 20 s, on ice). The debris was removed by centrifugation and the supernatant was subjected to purification steps.

#### **2.1.2. Purification of recombinant proteins**

The cleared lysates were incubated with Ni-NTA agarose beads (Qiagen). Recombinant proteins attached to beads *via* their His-Tag. Purification was done according to the manufacturer's instructions. Different washing steps were performed by a gradient of imidazole 10 to 300 mM. Finally, the His-tagged proteins were eluted from the beads by 300 mM imidazole. Then, purified proteins were applied on SDS-PAGE gel.

## **2.2. Determination of protein concentration**

The protein concentration was measured with a bicinchoninic acid (BCA) assay. In a 96-well plate, 10  $\mu$ l of the sample or 10  $\mu$ l of the bovine serum albumin (BSA) standard in different concentrations (50  $\mu$ g/ml; 100  $\mu$ g/ml; 200  $\mu$ g/ml; 400  $\mu$ g/ml; 600  $\mu$ g/ml; 800  $\mu$ g/ml; 1000  $\mu$ g/ml) were placed. Reagent A and B were mixed in a ratio of 50:1 (v/v) according the BCA kit (Pierce) instructions, then added to the samples and incubated for 30 minutes at 37°C. Finally, the absorption was determined at 560 nm with ELISA reader (BioTek, Bad-Friedrichshall, Germany) and the protein concentration calculated by comparison to the BSA standard curve.

## **2.3. SDS -PAGE**

SDS-PAGE (sodium dodecyl sulfate-polyacrylamide gel electrophoresis) is applied for separation of proteins based on molecular weight. Discontinuous acrylamide gels composing a stacking gel (4% acrylamide) and a resolving gel (8% - 12% acrylamide) were prepared. Protein samples were boiled in SDS-sample buffer for 10 minutes at 95°C and loaded into the wells of the stacking gel. BioRad electrophoresis chambers were maintained at 100 V until the bromophenol blue line reached down to the bottom of the gel. Gels were either stained with Coomassie blue or subjected to Western blot analysis.

## **2.4. Coomassie staining of polyacrylamide gels**

SDS-PAGE was removed from glass, stained in Roti-Blue staining solution (30 ml H<sub>2</sub>O; 10 ml methanol; 10 ml 5x Roti-Blue staining solution (Carl Roth) with constant agitation. Destaining of gels was done with H<sub>2</sub>O until the background of the gel appeared transparent. Coomassie blue staining is able to detect bands containing about 0.2  $\mu$ g protein or more.

## **2.5. Western blot**

For Western blot analysis, a Mini Transblot apparatus (BioRad) was used to transfer proteins from the acrylamide gel onto a nitrocellulose membrane (Schleicher and Schuell) in order to detect separated proteins with corresponding antibodies. The electro blotting “sandwich” was assembled according to the manufacturer’s instructions and electrophoretic transfer of

proteins was completed in 90 minutes at constant 100 V on ice. Next, the nitrocellulose membrane was blocked for one hour in blocking solution (4% skim milk powder in PBST) at room temperature. The membrane was incubated with primary antibody at appropriate dilution in PBST overnight at 4°C under agitation. To reduce non-specific binding, the membrane was washed 3 times for 15 minutes with PBST at room temperature. Then, diluted horseradish peroxidase (HRP)-conjugated secondary antibody was applied. The secondary antibody solution was discarded and the membrane washed 3 times with PBST. Immunoreactivity was visualized using the enhanced chemiluminescence detection system (ECL) and detected with ImageQuant™ LAS 4000 mini (GE Healthcare).

## **2.6. Brain homogenization**

Mice from wild-type C57BL/6J or CHL1-deficient were decapitated; the brains were removed from the skulls and immediately homogenized by applying up-and-down in glass homogenizer on ice. The suspension was subjected to affinity chromatography or immunoprecipitation or sub-fractionation.

## **2.7. Isolation of subcellular fractions**

Fresh brains of adult mice were homogenized in homogenization buffer (50 mM Tris-HCl (pH7.4), 0.32 M sucrose, 1 mM CaCl<sub>2</sub>, 1 mM MgCl<sub>2</sub>) by applying up-and-down in glass homogenizer. All steps were carried out at 4 °C. After centrifugation at 17,000 × g for 30 min at 4 °C, the supernatant collected as a cytoplasmic fraction. Following addition of 1% CHAPS to the suspension; the ‘cytoplasmic’ fraction was loaded on the affinity column. For the isolation of the membrane fraction, the 17,000 × g pellet was homogenized in 20% OptiPrep and loaded onto a discontinuous OptiPrep gradient of 35%, 25%, and 20%, and centrifuged at 10,000 × g for 40 min. The OptiPrep 35/25% interphase was saved for nuclei extraction that will be described later. The two upper phases of OptiPrep 25 and 20% are collected for membrane fractionation and diluted five times with homogenization buffer and subsequently centrifuged at 100,000g for 30 min. The pellet considered as ‘membrane’ fraction included both plasma and synaptic membranes. To make it soluble, the pellet was resuspended in homo buffer plus 1% CHAPS. Also, nuclei were collected from the OptiPrep 35/25% interphase (described above), diluted with 2 volumes of homogenization buffer, and centrifuged at 1,000 × g for 10 min. The nuclear pellet was then resuspended in nuclei

extraction buffer, Roeder C buffer (10mM Tris-HCl (pH 8), 0.5mM EDTA, 2mM MgCl<sub>2</sub>, 300mM NaCl, 10% glycerol, pH 7.5, protease inhibitor mixture) and incubated on ice for 30 min. After centrifugation at 12,000 × *g* for 5 min, the supernatant was collected as ‘soluble’ nuclear protein extract, and the pellet was nominated as ‘insoluble’ nuclear protein fraction (Lutz *et al.*, 2012, Loers *et al.*, 2012).

## **2.8. Affinity chromatography**

### **2.8.1. Preparation of cyanogen bromide-activated-Sepharose and ligand immobilization**

For affinity chromatography, recombinant CHL1-ICD or NCAM180-ICD were produced, purified and immobilized on CN-Br activated-Sepharose by covalent conjugation *via* primary amino groups of the proteins. Steps were performed according to the manufacturer’s instructions (Sigma Aldrich, C 9142).

Briefly, the coupling processes were performed as following steps:

- a.** The calculated amount of freeze-dried CN-Br-Sepharose powder was suspended in 1mM HCl, and then the active CN-Br-Sepharose was allowed to swell completely.
- b.** The buffer was exchanged against coupling buffer containing the ligand either CHL1-ICD or NCAM180-ICD.
- c.** Protein-gel suspension was incubated overnight at 4°C with constant agitation.
- d.** Remaining active groups of the gel were blocked by addition of 0.2 M glycine buffer.
- e.** Coupling process was finished by alternate washing with basic coupling buffer pH 8.3 or acidic acetate buffer pH 4 .These washing cycles were repeated four to five times.

For affinity chromatography purpose, a ligand-immobilized sepharose gel was transferred into an empty column or batch, and placed at 4°C.

## **2.8.2. Affinity chromatography**

Isolation of subcellular fractions was performed according to the method described in the previous section. Sub-fractions were applied to the CN-Br affinity columns either containing CHL1- ICD or NCAM180-ICD-conjugated beads and incubated overnight at 4°C. After extensive washing with homogenization buffer, proteins were eluted using 0.1M Glycin buffer (pH 2.3). Proteins bound to the individual bait proteins were separated on the SDS-PAGE and stained with colloidal Coomassie blue dye. Bands specifically found in the CHL1-ICD and NCAM180-ICD eluates were cut and sent to Universitätsklinikum Hamburg-Eppendorf (UKE) facilities for the mass spectrometry analysis. Finally, the lists of new putative CHL1 and NCAM-180 binding partners were identified (Richter, M. 2002, PhD dissertation).

## **2.9. Binding protein assays**

### **2.9.1. Co-Immunoprecipitation (Co-IP)**

Brains from wild-type or CHL1-deficient mice were homogenized with a glass homogenizer in RIPA buffer containing protease inhibitor. Tissue debris was spun down by centrifugation at (1,000 g; 10 minutes; 4°C). Following treatment with 2 mM CaCl<sub>2</sub> or 1 mM EGTA, the clear supernatant (1 mg/ml) was incubated with 2 µg of primary antibody or unspecific IgGs from the species which the primary antibodies were raised (as a control). Next, 20 µl protein A/G agarose beads (Santa Cruz) were added to the samples and incubated overnight at 4°C. Beads were precipitated together with the antibodies and protein complex by centrifugation (1,000 g; 5 minutes; 4°C), washed twice with RIPA buffer and once with PBS. Proteins were eluted from the beads with SDS sample buffer and subjected to SDS-PAGE followed by Western blot analysis.

### **2.9.2. Pull-down assay**

In pull-down experiment, a recombinant tagged protein is used as the bait to pull-down proteins that bind to it. Following centrifugation of brain homogenate, the cleared supernatant was incubated with His-tagged CHL1-ICD. Afterwards, Ni-NTA agarose beads (Qiagen) were added to the sample to pull down His-tagged proteins. The beads along with bait-prey complex were precipitated by centrifugation (1,000 g; 5 minutes; 4°C), washed twice with

RIPA buffer and once with PBS, eluted with sample buffer and subjected to SDS-PAGE and Western blot analysis.

### **3. Cell biology**

#### **3.1. Cell line culture**

NIH-3T3 and HEK293 cells were grown in 25 ml cell medium (Dulbecco modified Eagle's medium (DMEM), 1 mM sodium pyruvate, 1 mM L-glutamine, 10% fetal calf serum (FCS), 5 U/ml penicillin/streptomycin) in 175 cm<sup>2</sup> culture flasks or 6 well plates (Sarstedt) in a 37°C incubator with 95% humidity and 5% CO<sub>2</sub>. Every three days, cells were passaged when they reached 80% confluency. During this procedure, cells were washed with pre-warmed (37°C) HBSS without calcium and magnesium (PAA Laboratories) and incubated for 5 minutes with Trypsin-EDTA (PAA Laboratories) and resuspended in fresh medium and seeded in a new flask or 6-well plate in a dilution of 1:10.

#### **3.2. Transfection of cell-lines with TurboFect**

For transient transfection, one million cells per ml of medium were seeded onto PLL-coated glass cover slips or in 6-well plates. After growing to 50-80% confluency, a transfection mixture was prepared. For one million cultured cells, 4 µg plasmid DNA was mixed with 6 µl Turbofect transfection reagent in 400 µl culture medium without serum according to the manufacturer's instructions. The transfection solution was mixed, kept for 20 minutes at room temperature and added drop wise to the cells. Following transfection, cells were maintained in culture for a further 24 to 48 hours.

#### **3.3. Primary culture**

##### **3.3.1. Cell culture of primary hippocampal neurons**

For hippocampal cell culture, wild-type mice (C57BL/6J) of a postnatal day 0 to 2 were decapitated and their brain removed from the skulls. The brains were cut along the midline. The two hippocampi were isolated, cleaned, and split into 1 mm pieces. The hippocampi were washed once with dissection solution and treated with digestion solution containing trypsin and DNase I for five minutes at room temperature. After removal of the digestion

solution, the digestion reaction was stopped by adding trypsin inhibitor in dissection solution, followed by two times washing with dissection solution. The hippocampi were dispersed in dissection solution containing DNase I with glass Pasteur pipettes. Afterwards, the homogeneous suspension was centrifuged for 15 minutes at 4°C and 1000 g. The cell pellet was resuspended in hippocampus medium and the cells were counted in a Neubauer chamber. Cells were plated on PLL-coated glass cover slips for immunostaining purposes.

### **3.3.2. Primary culture of cerebellar granule neurons**

Wild-type (C57BL/6J) mice of postnatal day 6 to 7 were decapitated and their cerebellums were pinched off with forceps from the skulls. The cerebella sections were washed twice with ice cold HBBS (PAA Laboratories) and treated with trypsin and DNase I in HBSS for 15 minutes at room temperature. After elimination of the trypsin solution, the cerebella pieces were washed three times with ice cold HBBS, triturated in HBSS containing DNase I by pipetting up and down. Then, cells were transferred into ice cold HBSS and centrifuged for 15 minutes at 4°C with 100 g. The cell pellet was suspended in cerebellum medium and the cells were counted in a Neubauer chamber. Two million cells were plated on poly-L-lysine (PLL)-coated glass cover slips for immunostaining. Cells were maintained in a 5% CO<sub>2</sub>, 37°C incubator.

### **3.3.3. Coating of glass cover slips with poly-L-lysine**

Glass cover slips were treated with 3 M HCl for 30 minutes at room temperature with gentle shaking. Following two times washing with H<sub>2</sub>O, coverslips were incubated for 3 hours under gentle agitation with acetone at room temperature. Cover slips were rinsed five times with H<sub>2</sub>O, and twice with ethanol respectively. Then, they were kept sterilized at 200°C. Afterward, the cover slips were submerged in PLL solution (0.01% in H<sub>2</sub>O) at 4°C under gently shaking. Finally, cover slips were rinsed three times with H<sub>2</sub>O, dried under the laminar hood and incubated for 30 minutes under UV light.

## **3.4. Immunocytochemistry**

Hippocampal or cerebellar neurons (one million cells per ml) were seeded onto PLL-coated glass cover slips and maintained in culture for 24 or 48 hours. Cells were fixed with 4%

paraformaldehyde (PFA) in PBS for 15 minutes at 37°C. Subsequently, the cells were washed with PBS, permeabilized and blocked with 0.2% Triton X-100, 2% donkey serum and 1% BSA in PBS for one hour at room temperature. Primary antibodies were applied over night at 4°C. Following washing with PBS, the cells were incubated with secondary antibodies diluted with a ratio of 1:200 in PBS for 30 minutes at room temperature. Cells were rinsed three times with PBS for 5 minutes at room temperature. Coverslips were mounted with Roti-Mount Fluor Care DAPI (Carl Roth, Karlsruhe, Germany). Confocal images were taken with an Olympus Fluoview FV1000 confocal laser-scanning microscope (Hamburg, Germany) in sequential mode.

### **3.5. Live cell staining**

For live cell staining, primary antibody against CHL1 was applied to live cells for 10 minutes at 37°C. Then, the corresponding Cy-conjugated secondary antibody was added to the cells for another 10 minutes. Cells were fixed with 4% PFA in PBS for 15 minutes at 37°C, washed 3 times with PBS, permeabilized and blocked with 0.2% Triton X-100, 2% goat serum and 1% BSA in PBS for one hour at room temperature and incubated overnight at 4°C with primary antibodies against binding partners of CHL1. Following three washes with PBS, the cells were incubated with the corresponding Cy-labeled secondary antibodies diluted 1:200 in PBS for 30 minutes at room temperature. After rinsing the cells with PBS, coverslips were mounted with Roti-Mount Fluor Care DAPI (Carl Roth, Karlsruhe, Germany). Confocal images were taken with an Olympus Fluoview FV1000 confocal laser-scanning microscope (Hamburg, Germany) in sequential mode.

### **3.6. Immunohistochemistry**

Brains from adult mice were fixed with 4% formaldehyde in 0.1 M cacodylate buffer, pH 7.3, at room temperature. The brains were post-fixed overnight at 4°C in the formaldehyde solution, submerged in 15% sucrose solution in 0.1 M cacodylate buffer, pH 7.3, for 2 days at 4°C, followed by freezing by immersion for 2 min in precooled 2-methyl-butane (isopentane) and kept in liquid nitrogen. Serial coronal 25- $\mu$ m-thick sections were cut in a cryostat (Leica CM3050, Leica Instruments, Wetzlar, Germany) and collected on SuperFrost Plus glass slides (Carl Roth, Karlsruhe, Germany). Antigen retrieval was performed by incubating the sections in 10 mM sodium citrate solution (pH 9.0) for 30 min at 80°C. Blocking of non-

specific binding sites was performed with phosphate buffered saline, pH 7.3 (PBS) containing 0.2% Triton X-100, 0.02 % sodium azide, and 5% normal donkey serum for 1 h at room temperature. The sections were incubated with primary antibodies diluted 1:100 in PBS overnight at 4°C in a humidified chamber. Following washing in PBS (3× 15 min at room temperature), the section were incubated at room temperature with donkey Cy-conjugated secondary antibodies diluted in PBS for 2 hours. After subsequent washing, the sections were mounted with Roti-Mount Fluor Care DAPI and images were taken with an Olympus Fluoview FV1000 confocal laser-scanning microscope in sequential mode.

### **3.7. Tyrosine hydroxylase (TH) immunostaining**

Serial coronal 25- $\mu$ m-thick sections of adult Wt and Ko perfused brains were cut in a cryostat (Leica CM3050, Leica Instruments, Wetzlar, Germany) and collected on SuperFrost Plus glass slides (Carl Roth, Karlsruhe, Germany). Sections were blocked for 1 h with 10% normal goat serum and 0.25% Triton X-100. Next, the sections were incubated overnight at 4 °C with the TH (tyrosine hydroxylase) primary antibody (1:1000, millipore, AB152). The next day, the sections were washed with 0.1% Triton X in PBS and incubated with a biotinylated anti-rabbit secondary antibody (1:500, Vector Laboratories, USA) for 1 h at room temperature. The intensity signal was then amplified by incubating the sections with the Avidin/Biotin ABC reagent (Vector Laboratories, USA). Finally, the immunostaining was revealed by incubation with the chromogen diaminobenzidine (DAB), producing a brown color visible in bright-field light microscopy.

### **3.8. Proximity ligation assay**

Duolink immunoassay is a highly specific technique that allows protein-protein interactions studies *in situ*. Tissue or cells should be fixed on a glass slide for microscopy and pre-treated according to immunohistochemistry procedure. Cartoon presentation of proximity ligation assay is presented (Fig.9).

Briefly, the principles of the proximity ligation assay are described in four steps:

**A.** Fixed cells or tissue slices was incubated with primary antibodies from two different species.

**B.** A pair of secondary antibodies attached to oligonucleotides (PLA probe MINUS and PLA probe PLUS) were incubated with sample.

**C.** The ligation solution containing two oligonucleotides and ligase were added to the sample. When the PLA probes are in close proximity, oligonucleotides will hybridize to the two PLA probes and form a closed circle by enzymatic ligation.

**D.** Oligonucleotides were amplified *via* rolling circle amplification using the ligated circle as a template, generating a repeated sequence. In this study, sections were mounted with Roti-Mount Fluor Care DAPI stained nuclei. The red signal is easily visible as distinct fluorescent spots and analyzed by fluorescence microscopy.

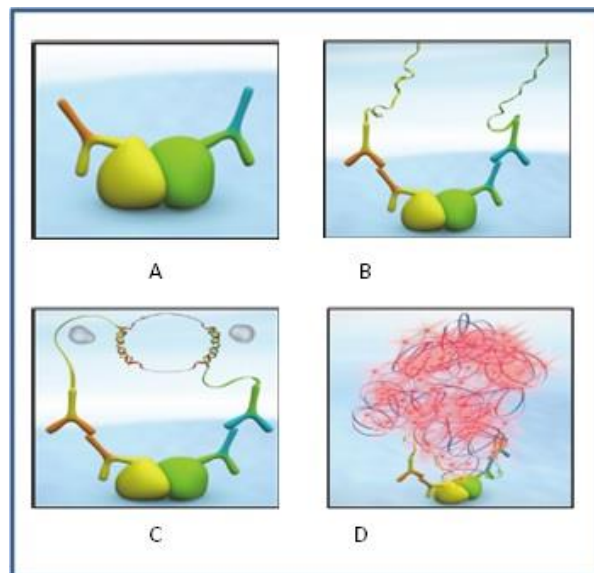


**Figure 9. Schematic illustration of proximity ligation assay.**

**The presentation was taken from Abnova.**

### **3.9. MTT assay**

MTT is a colorimetric assay that widely used to assess cytotoxicity and cell viability. MTT is taken up by live cells and metabolized to purple salt.

In this study, the cells were cultured in 48 well plates for 24-48 h. Then, cells were treated with 25  $\mu$ l of MTT stock solutions (5 mg/ml in PBS), followed by incubation for 4 h. Solutions were aspirated and cells were treated with lysis buffer (10% SDS in 10 mM HCl),

followed by absorbance reading at 560 nm with an ELISA reader. Results were expressed as a percentage of MTT reduction relative to the control cells. All measurements were made in triplicates.

### **3.10. Staining of live cells with calcein**

Cells were seeded and transfected with appropriate expressing vectors. For induction of cell death, cells were incubated with 1  $\mu$ M thapsigargin (TG) for 16 h. While calcein stains only live cells, viability of cells was assessed by comparison of calcein positive cells versus total cells. For calcein staining, cells were treated with 1  $\mu$ g/mL calcein for 1 h at 37°C. The images from randomly chosen areas of a microscopic field (magnification 20X) in each well were taken, as well as three wells for each treatment condition.

### **3.11. Calcium imaging**

Hippocampal neurons were seeded onto PLL-coated glass cover slips with a density of one million cells per ml, and maintained in culture for 48 hours. During live imaging, cells were kept in an incubation chamber (37°C, 5% CO<sub>2</sub>, 70% humidity). Neurons were loaded with 5  $\mu$ M Fura-2 AM (Invitrogen, F1221). At a defined time point (60 sec), stimulation with CHL1-Fc (10  $\mu$ g/ml) was performed. The intensity of Fura-2 signal within the cell soma before and after CHL1-Fc application and the changes in fluorescent calcium signals in response to calcium binding were recorded by epi-fluorescence microscopy using a special filter for the 340/380 measurement. Fura-2 saturated with calcium is excitable at a wavelength of 340 nm; While Fura-2 that is free of calcium could be excited only at a wavelength of 380 nm. Therefore, the concentration of intracellular calcium could be determined from the ratio of fluorescence emission or excitation at distinct wavelengths. Also, the ratio of 340/380 is independent of the amount of Fura-2 that was loaded into the cells and also independent of bleaching of the dye.

### **3.12. Fluorescence resonance energy transfer (FRET)**

FRET is a powerful technique for detecting protein-protein interactions. When two chromophores are in proper relative orientation and sufficient proximity (2 to 10 nm), a non-

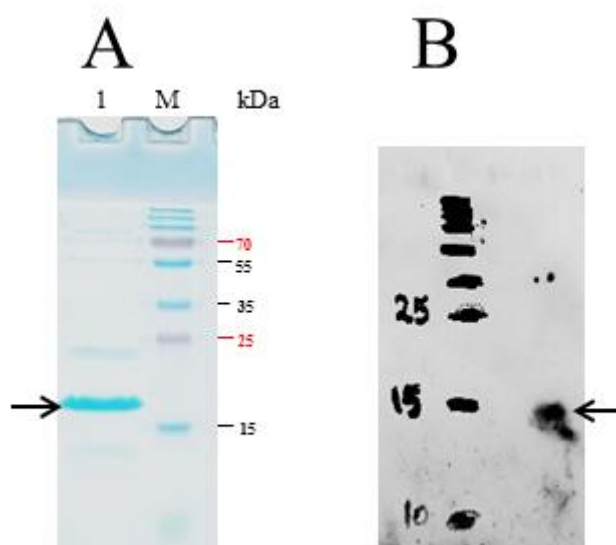
radiative transfer of energy from an excited state donor fluorophore to an adjacent acceptor occurs. This phenomenon is called *FRET*, which is used for measuring molecular interactions. In this study, NIH-3T3 cells were grown in 20 ml cell medium. Cells were passaged when they reached 80% confluency and seeded on PLL coated coverslips, transfected with CFP-synaptogyrin-3 and GFP-CHL1. During live imaging, the cover slip was transferred into a petri dish with 3 ml pre-warmed medium and cells were kept in an incubation chamber (37°C, 5% CO<sub>2</sub>, 70% humidity). FRET analysis was performed with the confocal laser-scanning microscope Olympus FV1000 using the sensitized emission method. In this experiment, CFP- synaptogyrin-3 was used as a donor while the acceptor was the GFP-CHL1.

## V. Results

### 1. Identification of potential binding partners of CHL1 and NCAM180 by affinity chromatography

#### 1.1. Expression and purification of recombinant CHL1-ICD and NCAM180-ICD

M15 E.coli competent cells were transformed with expression vectors coding for either CHL1-ICD or NCAM180-ICD. Protein expression was induced by IPTG, leading to production of His-tagged fusion proteins that consist of the intracellular domain (ICD) of either CHL1 or NCAM180. To purify the proteins, the bacteria were collected, lysed and the soluble supernatant applied to a Ni-NTA batch. After extensive washing steps, recombinant proteins were eluted using a high concentration of imidazole. The purified intracellular domains of CHL1 and NCAM180 were isolated. Predominant bands with molecular weight of 18 kDa (CHL1-ICD) and 80 kDa (NCAM180-ICD in dimer form) were detected in the Coomassie blue stained gels and Western blot analysis (Fig.10).



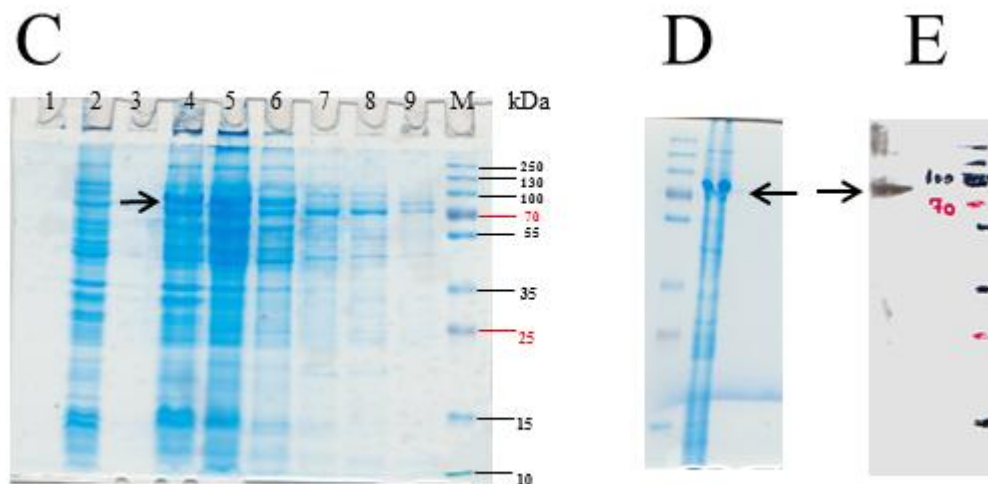


**Figure 10. Production of recombinant intracellular domains of CHL1 and NCAM180.**

**(A):** Competent cells were transformed with expression plasmid containing CHL1-ICD gene. After induction with IPTG, the intracellular domain of CHL1 was expressed. For purification of fusion protein *via* the His-Tag, the clear supernatant was applied to Ni-NTA batch. Non-specific proteins were washed out and the fusion protein was eluted by using high imidazole concentration buffer. The purified intracellular domain of CHL1 was applied to SDS-PAGE and an apparent band with an approximate molecular mass of 18kDa was observed (Lane1). **M** indicates molecular weight marker **(B):** Western blot analysis was carried using C18 antibody against intracellular domain of CHL1, detecting a protein with molecular weight of 18 kDa.

**(C):** Competent cells transformed with expression vector of NCAM180-ICD were analyzed on SDS-PAGE. Lysate before induction (Lane 1: supernatant; Lane2: pellet), Lysate after IPTG induction, showed the predominate expression of NCAM180-ICD with molecular mass of 80 kDa in dimer form (Lane 3: supernatant; Lane4: pellet). After lysis of the bacteria, soluble supernatant was applied on Ni-NTA batch for purification purpose (Lane 5). Following a four step wash (Lane 6-9), non-specific proteins were removed. **(D):** Isolated NCAM180-ICD was subjected to SDS-PAGE. A band with 80 kDa molecular weight indicates dimer form of intracellular domain of NCAM180. **(E):** Western blot analysis was performed using antibody D3 against intracellular domain of NCAM180. Arrows indicate the position of recombinant protein.

## 1.2. Affinity chromatography of brain homogenates using immobilized CHL1-ICD and NCAM180-ICD

For identification of putative binding partners of CHL1, recombinant intracellular domains (ICD) of CHL1 and the neural cell adhesion molecule isoform 180 (NCAM180) were immobilized on CN-Br activated sepharose by covalent conjugation. Preparation of beads is explained in the methods chapter with more detail (Richter, M. 2002, PhD dissertation). NCAM180-ICD was used as a control to identify CHL1-ICD specific binding partners. Wild

type brains were applied to the CN-Br affinity columns either containing CHL1-ICD or NCAM180-ICD conjugated beads and incubated overnight at 4 °C. After extensive washing, proteins were eluted using elution buffer. Proteins bound to the individual bait proteins were separated on the SDS-PAGE and stained with colloidal Coomassie blue dye. Bands specifically found in the CHL1-ICD eluate in comparison to NCAM180-ICD eluate were cut. Mass spectroscopy was performed by UKE facility in order to detect and identify the potential interaction partners of the intracellular domains of CHL1 or NCAM180.

### 1.3. Detection and identification of the CHL1 and NCAM180 binding proteins

#### 1.3.1. Isolation of CHL1 binding partners from crude brain homogenate

Brains from wild-type mice were homogenized on ice with a glass homogenizer in homogenization buffer. The homogenate was cleared from tissue debris by centrifugation (1,000 g; 10 minutes; 4°C). The supernatant of brain homogenate was incubated with either CHL1-ICD or NCAM180-ICD conjugated beads. The eluted fractions were subjected to the SDS-PAGE and visualized by Coomassie blue staining. In comparison to NCAM180-ICD eluate, distinct bands in the CHL1 eluate indicating putative binding partners of CHL1 were excised and sent for mass spectroscopy analysis.

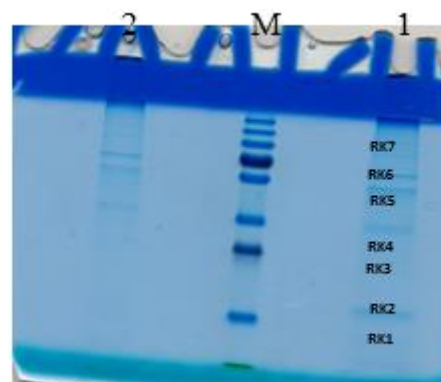


**Figure 11. Isolation of CHL1 binding partners.**

The crude brain fraction was allowed to interact with either immobilized CHL1-ICD or NCAM180-ICD. Eluents were separated by SDS-PAGE. In comparison to NCAM180-ICD eluate (Lane2), seven specific bands from the CHL1-ICD eluate (Lane1) were cut and sent for mass spectrometry analysis.

### 1.3.2. List of potential interaction partners of CHL1 identified in Mass spectroscopy analysis

The isolated proteins were sequenced using the Quadrupole-time-of-flight (*QTOF*) mass spectrometer by Universitätsklinikum Hamburg-Eppendorf facilities (harder@uke.de). Finally, new putative CHL1 binding partners were identified. The mass spectrometry results are confirmed by earlier findings. Among the mass spectrometry list of CHL1 binding partners, SNAP-25 and Vamp2 have already been published as CHL1 interacting proteins (Andreyeva *et al.*, 2010). Notably, several other interesting yet unknown interaction partners of CHL1 were identified in this study, the following could be listed: Sorcin, programmed cell death protein 6 (PDCD6) also called apoptosis-linked gene-2 protein (ALG-2), peflin1 (PEF-1), synaptogyrin-1, synaptogyrin-3, the Ras-related proteins Rab 1A and Rab14.

Name:		R.Kleene		host:		mouse	
Institut:		ZMNH		E-mail:		ralf.kleene@zmnh.uni-hamburg.de	
Arbeitsgruppe:		Kleene		erledigt am:		23/10/13	
Eingang:		07/10/13		Operator:		sönke	
Kostenstelle:				E-mail:		harder@uke.de	
Probenanzahl:		7		Verdau:		Trypsin (6ng/yl), Standardverdau	
Daten unter:		Kleene-7-10-13		Modifikation:		Cysteine mit DTT u. Jodacetamid	
Versuch:		GST-konstrukt/ AFFI-Chromat		Gerät:		Q-Tof II	
<b>Ergebnisse:</b>							
Probenname	Masse M/Z	Ergebnis/Kürzel	Accnr.SwissProt	Größe Da.	Proteinsequenzen		
RK1	492.7036	<b>Pdcd6</b>	P12815	21854	R.SIISMFDR.E		
	721.8036				K.AGVNFSEFTGVWK.Y		
	833.3036	Vamp2	P63044	12683	R.ADALQAGASQFETSAAK.L		
	944.9036				R.LQQTQAQVDEVVDIMR.V		
	752.9036	<b>Sorcin</b>	Q6P069	21613	K.ITFDDYIACCVK.L		
RK2	729.8036	Protein hfq	C4ZR49	11160	K.GQSLQDPFLNALR.R		
Rk3	637.8036	Hbb-b1	P02088	15830	R.LLVVYPWTQR.Y		
	647.8036				K.DFTPAQAQAFQK.V		
	626.8036	Hba-a1	P01942	15076	K.FLASVSTVLTSK.Y		
	461.7036	30S ribosomal protein S15	A7ZS62	10263	R.YTQLIER.L		
RK4	603.8036	<b>Pef1</b>	Q8BFY6	29209	R.IDVAGFSALWK.F		
	782.8036				K.VCTQLQVLTEAFR.E		
	778.8036	GAPDH	Q569X5	35787	R.VPTPNVSVVDLTCR.L		
	890.9036				K.LISWYDNEYGYSNR.V		
RK5	685.8036	<b>Synaptogyrin-3</b>	Q8R191	24545	R.TTPGPGTAQAGDAAR.A		
	604.8036				R.AGAAFDPVSFAR.R		
	612.8036	SNAP-25	Q96FM2	23300	R.EQMAISGGFIR.R		
	838.8036				R.TLVMLDEQGEQLER.I		
	636.8036	<b>Synaptogyrin-1</b>	O55100	25636	K.DNPLNEGDAAR.A		
	801.8036	Triose-phosphate isomerase	P17751	32171	K.VVLAYEPVWAIGTK.T		
	658.8036	Ras-related protein Rab 1A	P62821	22663	K.LQIWDTAGQER.F		
RK6	658.8036	Ras-related protein Rab-14	Q91V41	23882	K.LQIWDTAGQER.F		
	812.8036				R.NLTNPNTVILIGNK.A		
Rk7	723.8036	ADP/ATP translocase 1	P48962	32883	R.YFPTQALNFAFK.D		
	585.8036				K.EQGFLSFWR.G		

Table 5. List of potential interaction partners of CHL1 identified by mass spectrometry.

### 1.3.3. Isolation of CHL1 and NCAM180 binding partners from subcellular fractions

Wild-type mouse brain homogenates were subjected to subcellular fractionation. Cytoplasmic, nuclear and membrane fractions were isolated and applied to the CN-Br affinity batches either containing CHL1-ICD or NCAM180-ICD conjugated beads. Afterwards the beads were washed and bound proteins were eluted using an elution buffer. Following SDS-PAGE, gels were stained in Coomassie blue in order to detect predominant bands that were achieved by the affinity approach.

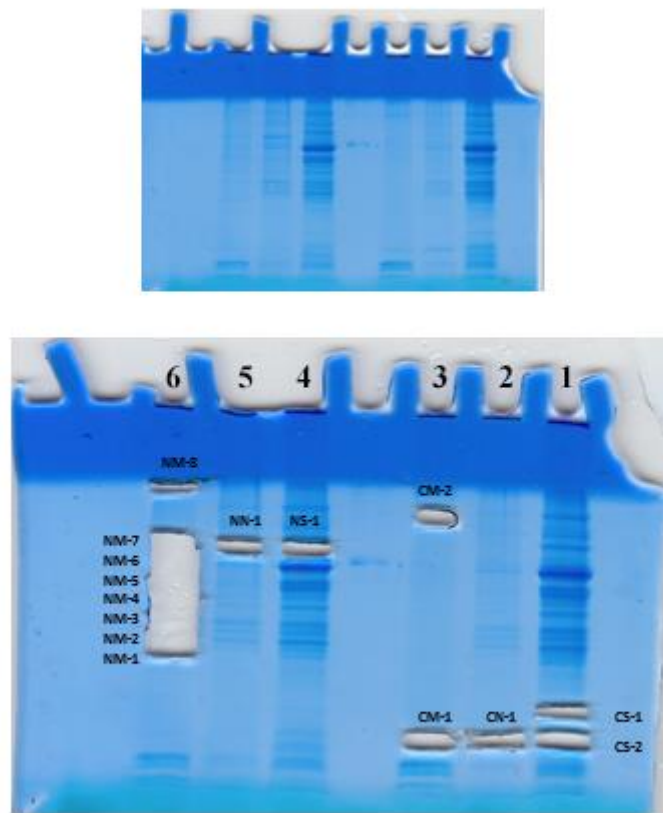


**Figure 12. Isolation of interacting partners of CHL1 and NCAM180.**

Subcellular fractions of brain homogenate including the cytoplasmic fraction (S), nuclear fraction (N) and membrane fraction (M) were incubated with either CHL1-ICD (Lane 1,2,3) or NCAM180-ICD (Lane 4,5,6) conjugated beads. Non-specifically bound proteins were removed by extensive washing. Proteins bound to CHL1-ICD or NCAM180-ICD were eluted and separated by SDS-PAGE. Specific bands were cut, and the proteins were sequenced using QTOF-mass spectroscopy. The acronyms are: **CS**, cytoplasmic fraction incubated with CHL1-ICD; **CN**, nuclear fraction incubated with CHL1-ICD; **CM**, membrane fraction incubated with CHL1-ICD; **NS**, cytoplasmic fraction incubated with NCAM180-ICD; **NN**, nuclear fraction incubated with NCAM180-ICD; **NM**, membrane fraction incubated with NCAM180-ICD.

### 1.3.4. Mass spectroscopy analysis of the potential interaction partners of CHL1 and NCAM180 corresponds to subcellular fractions of the brain

The interaction of programmed cell death protein 6 (PDCD6) and CHL1 seems very interesting since programmed cell death protein 6 also called apoptosis-linked gene-2 (ALG-2) was identified twice in two individual mass spectrometry analyses, providing the first hints for physical interaction between ALG-2 and CHL1, which was verified by further approaches.

Tabelle1					
Name:	R. Kleene	host:	maus		
Institut:	ZMNH	E-mail:	ralf.kleene@zmnh.uni-hamburg.de		
Arbeitsgruppe:	AG Schachner	erledigt am:	12.03.14		
Eingang:	29.01.14	Operator:	Sönke		
Kostenstelle:		E-mail:	harder@uke.de		
Probenanzahl:	15	Verdau:	Trypsin (6ng/yl), Standardverdau(Shevschenko)		
Daten unter:	Kleene-29-1-14	Modifikation:	Cysteine mit DTT u. Jodacetamid		
Versuch:	Afficromat (proben in e-coli gemacht)	Gerät:	Q-toff II		
Bemerkung:					
<b>Ergebnisse:</b>					
Probenname	Masse M/Z	Ergebnis/Kürzel	Acnr.SwissProt	Größe Da.	Proteinsequenzen
cs1	798.9036	Peroxioredoxin-2	Q61171	21765	K.SAPDFTATAVVDGAFK.E
	554.7036				K.SLSQNYGVLK.N
	722.8036	Rps5	P97461	22875	R.VNQAIWLLCTGAR.E
	823.5036				K.NIAECLADELINAAK.G
	669.8036	Rps7	P62082	22113	K.AIIIFVVPVQLK.S
	582.7036	Rpl17	Q9CPR4	21409	R.YSLDPENPTK.S
	868.9036	TS-HMG	P40630	27970	R.SAYNIYVSEFQEA.K.D
	604.8036	StARD9	Q80TF6	499932	K.YSQNLEWLR.L
	671.8036	StARD4	Q99JV5	25563	M.ADPESPWSQIGR.K
	cs2	670.8036	Cofilin-1	P18760	18548
669.8036					R.YALYDATYETK.E
702.8036		Rpl23a	P62751	17684	R.LAPDYDALDVANK.I
570.8036					K.FPLTTESAMK.K
632.8049		RNA-binding protein FUS	P56959	52642	K.AAIDWFDGKESGNIK.V
511.7036					K.AAIDWFDGK.E
706.8036		Dcx	O88809	40587	R.SLSDNINLPQGV.R.Y
610.8036					R.SFDALLADLTR.S
670.8036		Programmed cell death protein 6	P12815	21854	K.YITDWQNVFR.T
678.8036					R.LSDQFHDILIR.K
610.8036		Cirbp	P60824	18596	K.YGQISEVVVK.D
856.9036		CRIP-1	Q5M8N0	18601	R.VVYTGIDYDEGVPTK.S
522.8036		Sfrs3	P84104	19318	R.AFGYYGPLR.S
541.7036		Rpl26	P61255	17248	K.FNPFVTSDR.S
678.8036		MRP-L22	Q8BU88	23790	K.LVEGPPPPPEVPK.T
721.8036		Rps10	P63325	18904	K.AEAGAGSATEFQFR.G
622.8036		Tubulin beta-2A chain	Q7TMM9	49875	R.ISEQFTAMFR.R
cm1	966.1036	Histone H2A type	Q6GSS7	14087	K.VTIAQGGVLPNIQAVLLPK.K
	495.7036	Histone H4	Q5T006	11360	K.VFLENVIR.D
cm 2	641.8036	200 kDa neurofilament protein	P19246	116924	K.MALDIEIAAYR.K
cn1	689.8036	ROA2	O88569	37380	R.GGGGNFGPGGPNFR.G
nn1	890.2049	N-CAM-1	Q9R2A7	119353	K.ASPAPTPTPAGAASPLAAVAAPATDAPQAK.Q
	625.8036				K.NPPEAATAPASPK.S
ns1	890.2049	N-CAM-1	Q9R2A7	119353	K.ASPAPTPTPAGAASPLAAVAAPATDAPQAK.Q
	625.8036				K.NPPEAATAPASPK.S
	642.8036	PABP-1	P29341	70626	K.EFSPFGTITSAK.V

Tabelle1				
	641.8036			
	600.8036	Hsc70	Q3U9G0	70827
	825.9036			
	668.8036	FUSE-binding protein 1	Q91WJ8	68497
	677.8036			
	677.8036	FUSE-binding protein 2	Q3U0V1	76728
nm1	647.8036	VDAC-2	Q60930	31713
	714.8036			
	700.8036	VDAC-1	Q60932	32331
	607.3036			
nm2	607.3036	VDAC-1	Q60932	32331
	714.8036	VDAC-2	Q60930	31713
	808.9036	Syntaxin-1B	P61264	33224
	565.8036	Tubb2	Q7TMM9	49875
	848.9036			
nm3	607.3036	VDAC-1	Q60932	32331
	714.8036	VDAC-2	Q60930	31713
	665.8036	hnRNP C1/C2	Q9Z204	34364
	714.9036	L-xylulose reductase	Q91X52	25729
	752.9036	hnRNP A/B	Q99020	30812
	627.8036	VDAC-3	Q60931	30733
	835.9036	Stomatin-like protein 2	Q99JB2	38361
nm4	566.8036	Actin, cytoplasmic 1	Q6ZWM3	41710
	581.8036			
	848.9036	Tubb2	Q7TMM9	49875
	718.9036	Rbmxrt	Q91VM5	42136
	744.9036	hnRNP D0	Q60668	38330
nm5	848.9036	Tubb2	Q7TMM9	49875
	615.3036			
	862.9036	Galectin-9	O08573	40010
nm6	567.8036	Alpha-intemexin	P46660	55349
	528.8036			
	722.9036	Vimentin	P20152	53655
	779.9036			
	874.9936	Neurofilament light polypeptide	P08551	61471
	648.8036			
nm7	809.9036	Mitofilin	Q8CAQ8	83848
	786.9036			
	625.8036	NCAM-1	Q9R2A7	119353
	661.8036			
	744.9036	Hsp70A1	Q61696	70036
	516.8036	Nestin	Q6P5H2	207000
	615.8036	Tubb2	Q7TMM9	49875
nm8	817.9036	ASH2-like protein	Q91X20	68207
	918.0036	Low-sulfur keratin	P25690	46034
	526.8036	keratin, type I microfibrillar	3358093	45770

Seite 2

**Table 6. List of potential binding partners of CHL1-ICD and NCAM180-ICD.**

Subcellular fractions of a brain homogenate including the cytoplasmic fraction (S), nuclear fraction (N) and membrane fraction (M) were incubated with CHL1-ICD (C) or NCAM180-ICD (N) conjugated beads. The acronyms are described in Fig.12 caption.

## 2. Study the interaction of CHL1 with ALG-2

### 2.1. Verification of the CHL1- ALG-2 interaction by Co-IP

The potential interaction between CHL1-ICD and apoptosis-linked gene 2 protein (ALG-2) also called programmed cell death protein 6 (PDCD6) was noted in two individual mass spectrometry reports. To verify the interaction of CHL1 and PDCD6 (ALG-2), co-immunoprecipitation from brain homogenate was performed. For this purpose, the wild-type or CHL1-deficient mice brains were homogenized in RIPA buffer. The homogenates were cleared from tissue pieces by centrifugation (1,000 g; 10 minutes; 4°C). The pre-cleaned lysates were incubated with antibody against ALG-2 or non-specific IgGs (as a control). Protein complex was precipitated with protein A/G agarose beads, and then eluted with Laemmli buffer. Samples were separated by SDS-PAGE followed by Western blot. The result indicate that CHL1 was successfully precipitated in the presence of 2 mM calcium from brain lysate, while no signals were detected with CHL1 antibody in the absence of calcium or control IgG, indicating that the interaction between CHL1 and ALG-2 is calcium dependent.

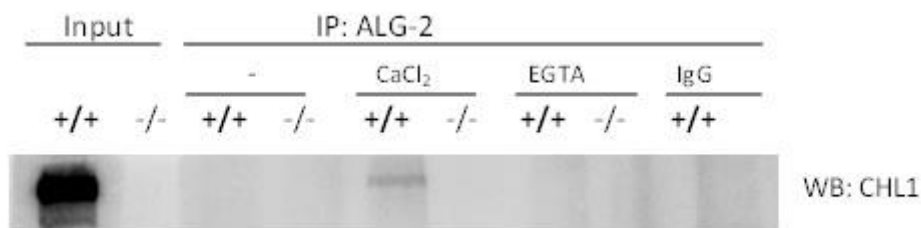


**Figure 13. Co-immunoprecipitation of CHL1 with the ALG-2 antibody from mouse brain lysate.**

Wild-type and CHL1 KO mice homogenate (input materials) and ALG-2 immunoprecipitates (IP) from brain lysate were separated by SDS-PAGE and analyzed by Western blot (WB) with the CHL1 antibody. Control IP with non-specific IgG antibody served as a control. CHL1 was precipitated with the ALG-2 antibody from wild-type brain homogenate in a calcium dependent manner.

### 2.2. Investigation of CHL1- ALG-2 interaction by pull down assay

To further study the interaction of CHL1 with ALG-2, recombinant intracellular domain of CHL1 containing His-Tag was used as a bait to precipitate ALG-2 from mouse brain homogenates. Western blot analysis of the precipitates has shown that the ALG-2 antibody

recognized a band of 25 kDa in the presence of EGTA, while no band is detectable in other conditions, suggesting that recombinant peptide of CHL1-ICD could precipitate the monomer of ALG-2 with molecular weight of 25 kDa in the absence of calcium. This can possibly be explained by the presence of the ‘His-Tag’ in the recombinant intracellular domain of CHL1, which could alter the conformational properties of recombinant ICD in compare to the native CHL1.

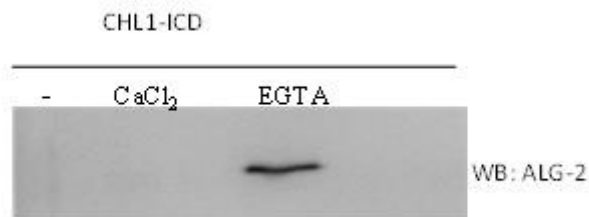


**Figure 14. ALG-2 is pulled down with the intracellular domain of CHL1.**

CHL1-ICD was incubated with mouse brain homogenate followed by a pull-down with Ni-NTA beads. Precipitates were detected by Western blot (WB) analysis with ALG-2 antibody. Here, the interaction between CHL1-ICD and ALG-2 occurred in the presence of EGTA.

### **2.3. Immunostaining of ALG-2 and CHL1 in cerebellar neurons (Fixed cells)**

The primary neuron culture was used to investigate the interaction between ALG-2 and CHL1. Cerebellar of postnatal 6-days old mice were prepared, dissociated and cultured on PLL-coated glass coverslips for 1 day. Following fixation and permeabilization, the cells were incubated with primary antibodies against ‘extracellular’ domain of CHL1 and anti-ALG-2. After incubation with donkey Cy2-or Cy-3-conjugated secondary antibodies, coverslips were mounted with Roti-Mount Fluor Care DAPI. The immunostaining of cerebellar neurons showed that there is no specific co-localization between two proteins in ‘fixed’ cells.

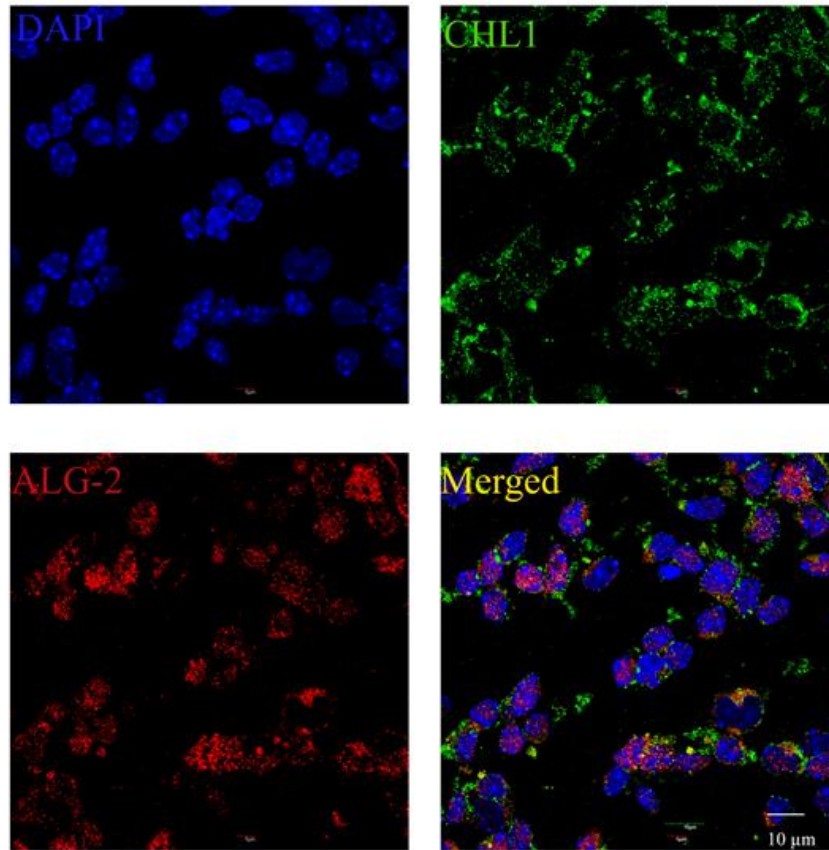


**Figure 15. Immunostaining of CHL1 and ALG-2 in primary cerebellar neurons after fixation**

Cerebellar neurons from 6-days old mice were stained with antibody against extracellular epitope of CHL1 and anti-ALG-2 antibody. Double labeling resulted in an overlay image (merged). Nuclei are stained with DAPI (blue). No specific co-localization exists between the two proteins in fixed cells.

#### **2.4. Prominent co-localization of CHL1 and ALG-2 in primary cerebellar neurons (Live cells)**

Since no co-localization of CHL1 and ALG-2 was detected in fixed cells, it was interesting to investigate if co-localization could be observed in live cerebellar neurons staining. Living cells were pre-incubated with primary antibody against ‘extracellular’ domain of CHL1, followed by incubation with corresponding secondary antibody. Afterwards, the cells were fixed with 4% PFA, permeabilized and stained with anti-ALG-2 antibody. The prominent co-localization of CHL1 and ALG2 suggests that clustering of CHL1 on cell surface due to application of CHL1 antibody could trigger ALG-2 accumulation in defined areas, resulting

in close interaction of CHL1 and ALG-2 along neurites. This observation is in agreement with published data regarding clustering of NCAM and CHL1 on cell surface upon application of antibody against their extracellular epitope (Westphal *et al.*, 2010, Tian *et al.*, 2012).

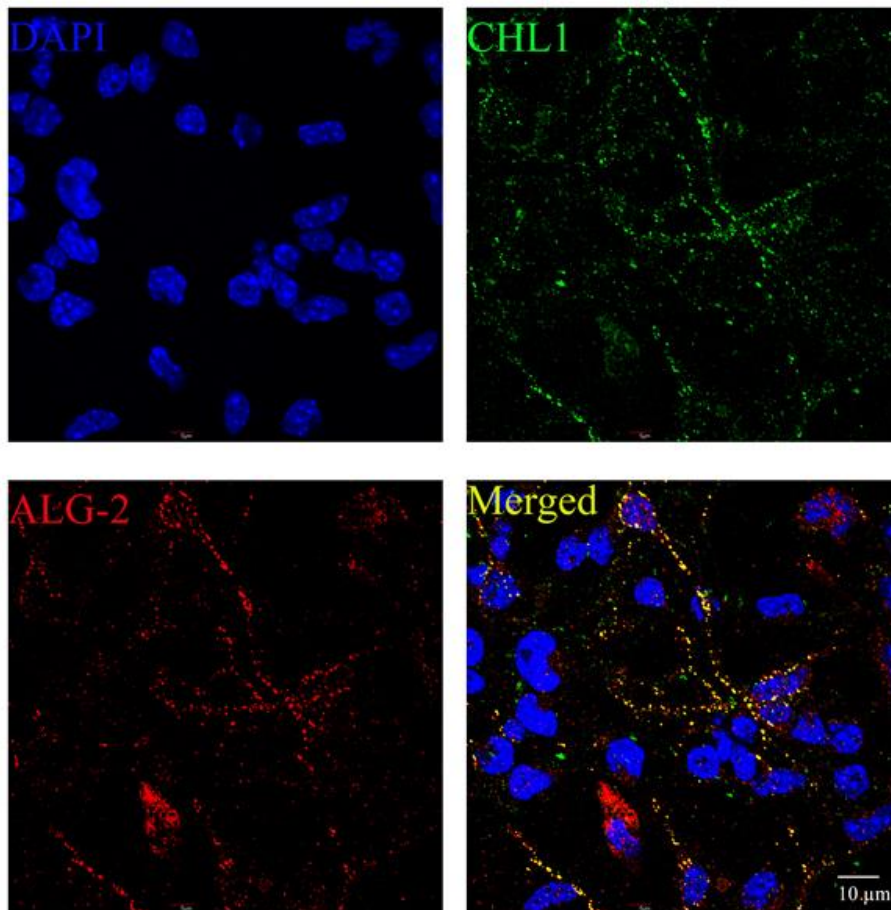


**Figure 16. CHL1 co-localizes with ALG-2 in primary cerebellar neurons (Live cells)**

Immunostainings were performed with cerebellar neurons from P6 wild-type mice maintained for 24 hours in culture. CHL1 was clustered on living cells with the polyclonal antibody against an epitope in the extracellular region. After live staining, the cells were fixed with 4% PFA, permeabilized and stained for ALG 2. Nuclei are stained with DAPI. Yellow staining indicates strong co-localization of CHL1 and ALG-2 along neurites.

## 2.5. Partial co-localization of CHL1 and ALG-2 in primary cerebellar neurons stimulated with CHL1-Fc

Since clustering of CHL1 induced CHL1 co-localization with ALG-2 in live cells, it was interesting to examine if stimulation with CHL1-Fc could also influence the interaction of these two proteins. For this purpose, cells were treated with or without 5  $\mu\text{g/ml}$  of CHL1-Fc, or L1-Fc. Non-stimulated cells also were used as a control. Following fixation, the cells were incubated with antibodies against ALG-2 and against ‘intracellular’ domain of CHL1. The results indicated that partial co-localization between CHL1 and ALG-2 occurs after stimulation with CHL1-Fc.

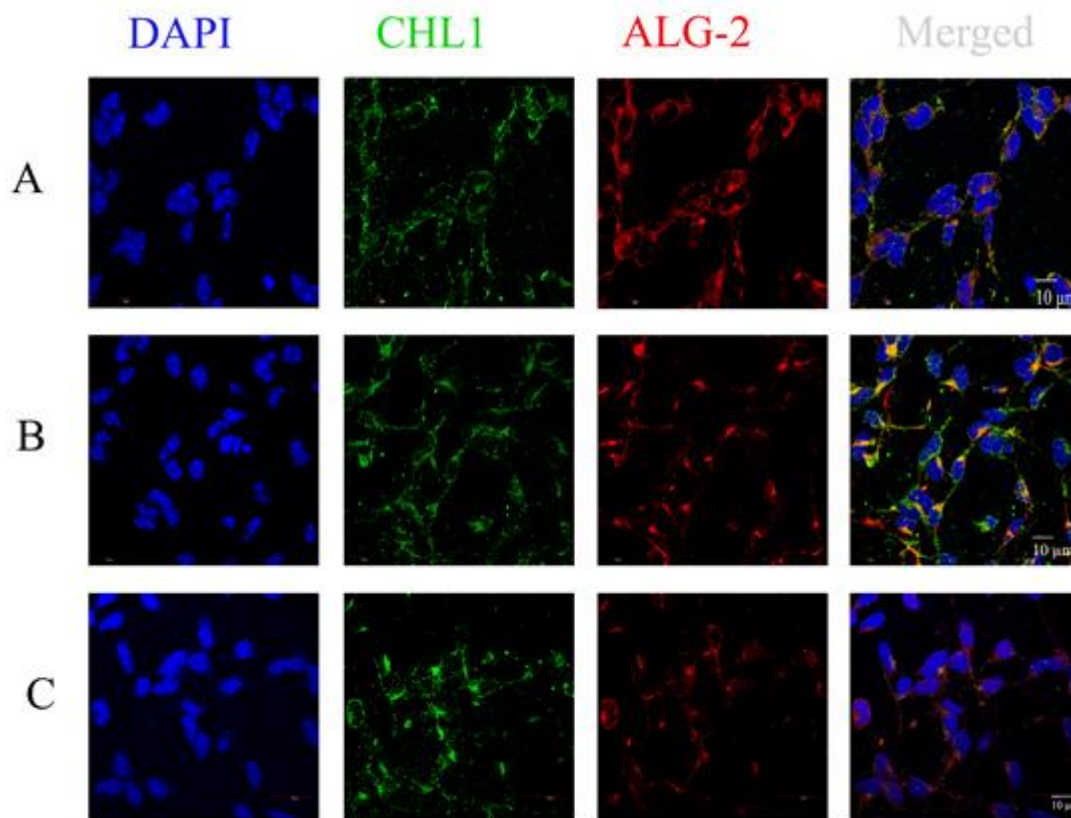


**Figure 17. CHL1 partially co-localizes with ALG-2 after treatment of cerebellar neurons with CHL1-Fc**

Cerebellar neurons that were maintained in culture for 24 hours were treated for 1 hour with 5  $\mu\text{g/ml}$  of either CHL1-Fc or L1-Fc. Afterwards; the cells were fixed, permeabilized and stained with antibodies against ALG-2 and against intracellular domain of CHL1. **(A)**: Non-treated cerebellar neurons were used as a control. The merged image showed no co-localization between two proteins in non-stimulated cells.

**(B)**: Cerebellar neurons were treated for 1 hour with CHL1-Fc. Yellow regions represent partial co-localization between CHL1 and ALG-2 in comparison to non-stimulated cells. **(C)**: No co-localization was observed in cerebellar neurons treated with L1-Fc.

## 2.6. CHL1 interacts with ALG-2 *in situ* (cerebellar and hippocampal tissues)

The interaction between CHL1 and ALG-2 was further assayed by immunostaining of mouse brain tissues. Proximity ligation assay was performed to detect close protein interactions with high sensitivity and specificity. Primary antibodies against CHL1 and ALG-2 were applied on cerebellar and hippocampal tissues. When the primary antibodies attach to their antigens in close proximity (less than 40 nm), a pair of oligonucleotide-labeled secondary antibodies amplify the fluorescent signals, suggesting a close interaction between CHL1 and ALG-2 presents in the cerebellum and the hippocampus. When tissues from CHL1-deficient mice (negative control) were incubated with antibodies against CHL1 and ALG-2, no fluorescent signal was detectable. Confocal images indicate that CHL1 and ALG-2 are in close proximity in the CA3 region of hippocampus. Notably, intensive red signals in the cerebellum indicate the interaction between CHL1 and ALG-2 in parallel fiber of the cerebellum, which is consistent with high level of CHL1 expression in parallel fibers (Jakovcevski *et al.*, 2009).

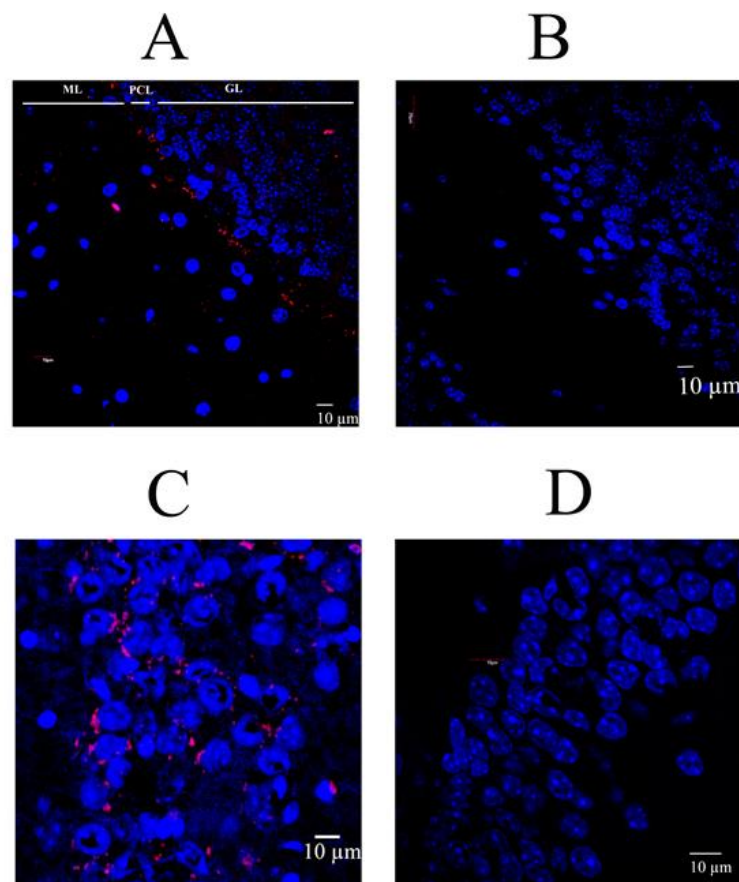
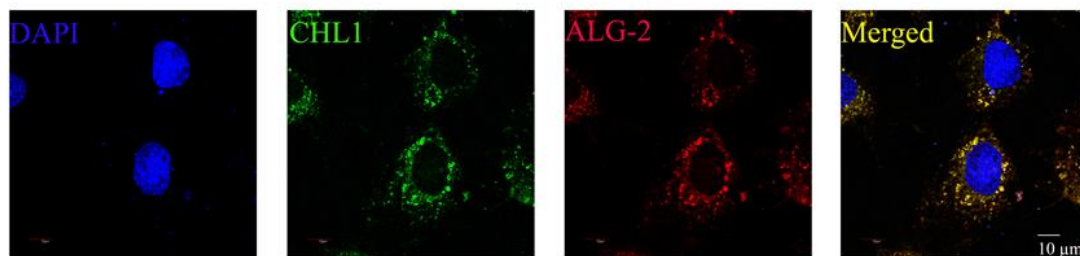


Figure 18. Close interaction between CHL1 and ALG-2 in the cerebellum and the hippocampus.

Brain slices from wild-type (A,C) and CHL1-deficient (B,D) mice were used in proximity ligation assays with antibodies against CHL1 and ALG-2. Confocal fluorescent images from the cerebellum cortex (A,B) and hippocampus CA3 region (C,D) are presented. Nuclei are stained with DAPI (blue) and spots of intense fluorescent signals (red) demonstrate close CHL1-ALG-2 interaction in parallel fibers of cerebellum and the CA3 region of hippocampus. The acronyms are: **ML**, molecular layer; **PCL**, Purkinje cell layer; **GL**, Granular layer.

## 2.7. CHL1 co-localizes with ALG-2 in transfected NIH- 3T3 cells

NIH-3T3 cells were plated on coverslips and cultured at 37°C and 5% CO<sub>2</sub> followed by transfection with specific green fluorescent and red fluorescent expression vectors of GFP-CHL1 and DsRed-ALG-2. Transfected cells were allowed to express both fluorescent proteins for 48h. Image outputs from confocal microscopy suggested that overexpression of both CHL1 and ALG-2 for 48h promoted their co-localization in granule-like structures in the cytoplasm.



**Figure 19. Interaction of CHL1 and ALG-2 in transfected NIH- 3T3 cells**

NIH- 3T3 cells were co-transfected with DsRed-ALG-2 and GFP-CHL1 following seeding on coverslips. 48h after transfection, the cells were fixed and analyzed by confocal microscopy. Microphotographs show that overexpression of ALG-2 and CHL1 for 48h resulted in their co-localization in granule-like structures in the cytoplasm.

## 2.8. Treatment of NIH-3T3 cells with thapsigargin induces nuclear import of ALG-2, but not CHL1

The majority of ALG-2 (apoptosis-linked gene-2) is localized in the cytoplasm. Various studies have shown that ALG-2 translocated to the nucleus under stress induced by thapsigargin or heat shock (Montaville *et al.*, 2006, Janowicz *et al.*, 2011, Sasaki-Osugi *et al.*, 2013). Thapsigargin elevates cytosolic calcium by blocking the endoplasmic reticulum (ER) calcium-ATPase and leads to ER stress-induced apoptosis.

Since ALG-2 interacts with CHL1, the question arises whether CHL1 could be imported to the nucleus in response to ER-stress. To address this question, two days after transfection with DsRed -ALG-2 and GFP-CHL1 plasmids, cells were treated with 1  $\mu$ M thapsigargin (TG) for 16 hours. In this experiment, the translocation of ALG-2 into the nucleus could be observed under stress condition which is consistent with previous studies (Montaville *et al.*, 2006, Janowicz *et al.*, 2011), while CHL1 subcellular distribution did not change after TG treatment. Consequently, no co-localization between CHL1 and ALG-2 was observed in the nucleus.

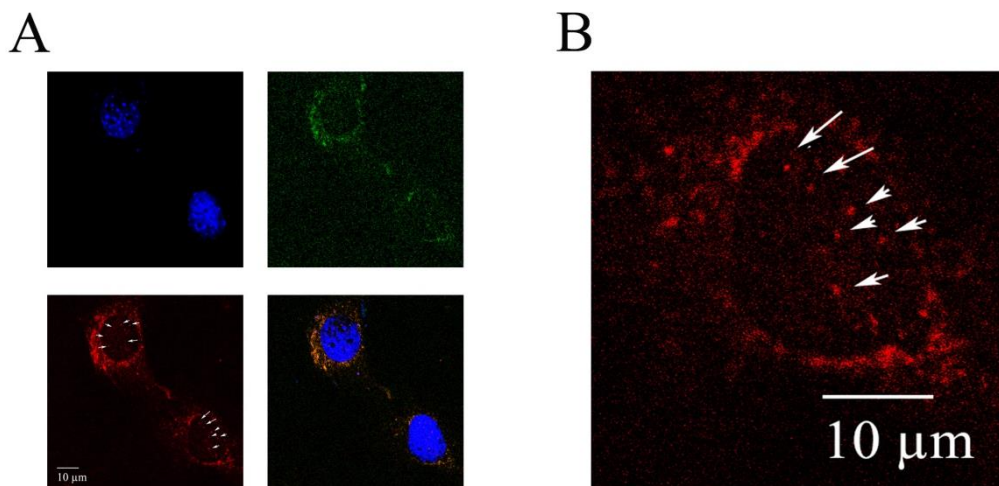


**Figure 20. Thapsigargin triggers nuclear import of ALG-2, but not CHL1.**

(A): When NIH-3T3 cells expressing fluorescent DsRed-ALG-2 and GFP-CHL1 exposed to thapsigargin-induced stress at 37°C for up to 16 hours, only ALG-2 signals were observed in the nucleus, but not CHL1 signals. (B): DsRed-ALG2 channel was magnified in the respective large panel. Solid arrows: appearance of

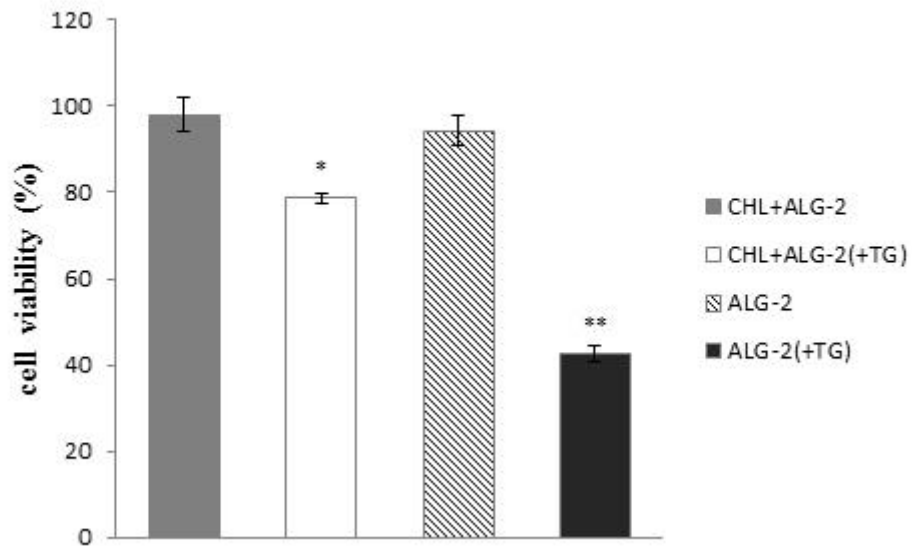
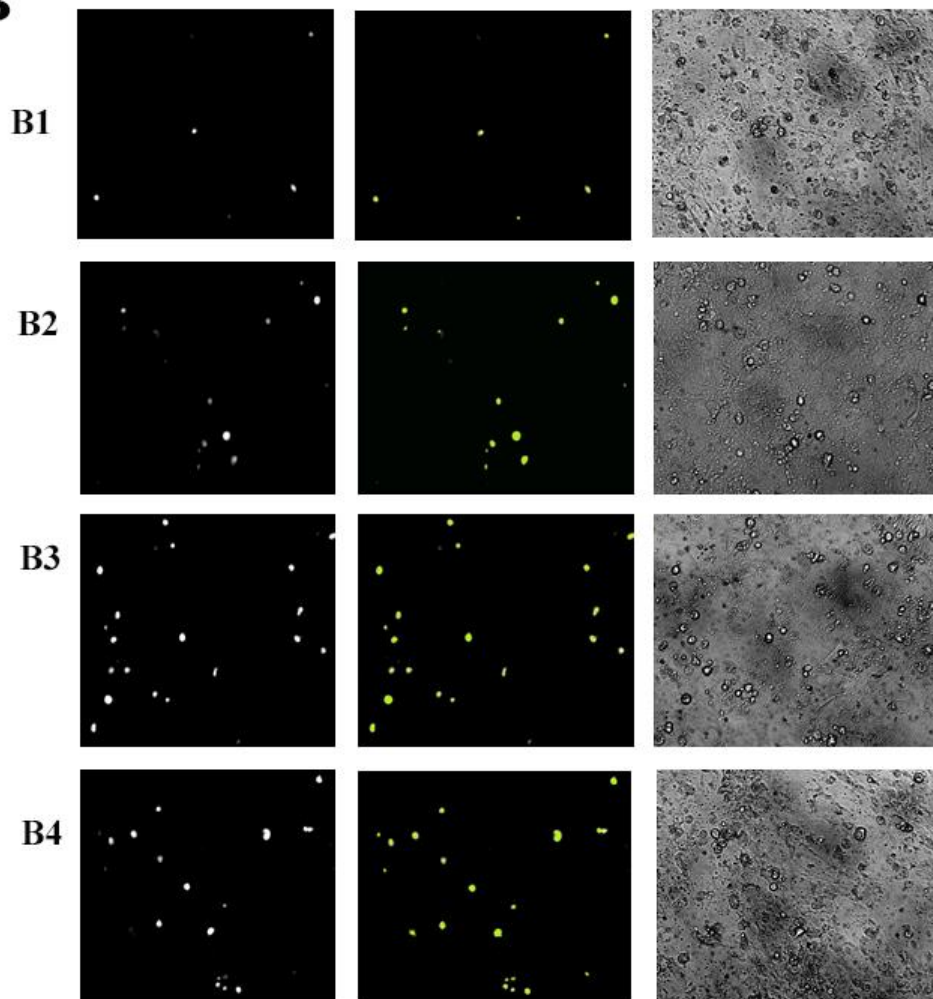
ALG-2 puncta in nucleus after TG stress. There is no co-localization between CHL1 and ALG-2 in the nucleus, indicating CHL1 did not translocate to the nucleus following stress.

## **2.9. CHL1 protects NIH-3T3 cells from TG-induced apoptosis**

NIH-3T3 cells were transfected with expression vectors coding for CHL1 and ALG-2. For induction of cell death, cells were treated with 1 $\mu$ M thapsigargin (TG) and cell viability assessed after a further 16 h culture period. Results obtained by MTT assay (Fig.21A) revealed that incubation of cells with TG leads to a significant decrease in cell viability as compared to the controls. Furthermore, the presence of CHL1 significantly enhanced cell viability of cells co-expressing both CHL1 and ALG-2. This was not the case in cells that expressed only ALG-2, which suggests that CHL1 enhances cell survival upon TG treatment.

Quantitative analyses of cell viability using a colorimetric assay with MTT was performed in parallel to cell imaging using calcein (a viability stain) and live cell fluorescence microscopy. For calcein staining, cells were treated with 1  $\mu$ g/mL calcein for 1 h at 37°C. The images from randomly chosen areas of a microscopic field (magnification 20X) in each well, as well as three wells for each treatment condition were taken. Here, NIH-3T3 cells were transfected with ALG-2 (B1) or co-transfected with CHL1 and ALG-2 (B2) and were treated with 1 $\mu$ M thapsigargin for 16h (B1, 2). Cells transfected with ALG-2 alone (B3) or co-transfected with both ALG-2 and CHL1 (B4) were considered as untreated controls. Consistent with MTT results, the calcein stained images showed that co-expression of CHL1 with ALG-2 (B-2) enhanced number of calcein positive cells in TG treated cells compared with cells expressing ALG-2 alone (B-1).

By combining both biochemical MTT assay and cell imaging, it is revealed that CHL1 promotes cell survival under thapsigargin-induced stress which is consistent with protection role of CHL1 against apoptosis in neurons (Chen *et al.*, 1999, Nishimune *et al.*, 2005, Jakovcevski *et al.*, 2009).

**A****B**

**Figure 21. CHL1 enhances NIH-3T3 cell survival under TG treatment.**

**(A):** Following NIH-3T3 cells transfection with expression plasmids of CHL1 and/or ALG-2, cells were exposed to TG for 16 h. MTT analysis showed that cell survival was significantly enhanced to 78% in cells co-expressed both CHL1 and ALG-2, while cell viability reduced to 42% in the cells expressed only ALG-2. Results are expressed as % of the control. Data are presented as mean values and analyzed by Student's *t*-test. \* *P*-value<0.01; \*\**P* <0.001 were considered as statistically significant in compare to untreated control cells.

**(B):** NIH-3T3 cells were transfected with ALG-2 (B1) or co-transfected with CHL1 and ALG-2 (B2) exposed to thapsigargin for 16 hr (B1, 2). Cell survival was visualized by comparison of calcein positive cells versus total number of cells (right column). Control Cells were transfected with ALG-2 alone (B3) or co-transfected with both ALG-2 and CHL1 (B4) and cultured as untreated controls (B3, 4). The original black and white images (left column) and green colored images (middle column) of calcein positive cells are shown. In accordance with MTT results, the calcein- stained images confirm that co-expression of CHL1 with ALG-2 (B2) enhances cell survival in cells treated with TG as compared to the cells expressing ALG-2 alone (B1). Images were taken by Kontron microscope.

### **3. Study the interaction of CHL1 with synaptogyrin**

As novel interaction partners of CHL1, synaptogyrin-1 and synaptogyrin-3 were identified by affinity chromatography followed by mass spectrometry analysis.

Synaptogyrins consist of two neuronal isoforms (synaptogyrin1 and 3) and belong to a family of tyrosine-phosphorylated proteins (Belizaire *et al.*, 2004). Furthermore, the evolutionary conservation of synaptogyrins but not synaptophysins has been reported. Previous studies have revealed that synaptogyrins have a role in the regulation of neurotransmitter release (Zakharenko *et al.*, 2001). Although synaptogyrin 1 and 3 were identified as synaptic vesicle proteins, it is very interesting that synaptogyrin-3 (syg-3) is expressed only in the brain (Belizaire *et al.*, 2004). In contrast to synaptogyrin-1, which is found in most synapses, synaptogyrin-3 is found only in a few synaptic brain regions, indicating a special function for syg-3 in distinct areas of synapses. It is well known that the regulation of synaptic vesicle exocytosis and synaptic plasticity includes protein–protein interactions. In other words, synaptogyrins carry out functions by interacting with other synaptic proteins. In regards to mass spectrometry results and the potentially interesting role of synaptogyrin-3 in brain, the interaction of CHL1 and synaptogyrin-3 was further analyzed in this study.

### 3.1. Co-IP of CHL1 and synaptogyrin-3 from mouse brain lysate

To verify the interaction of CHL1 with synaptogyrin-3, a co-immunoprecipitation assay was performed. Adult wild type and CHL1 deficient mice brains were homogenized. The lysates were pre-cleaned. Then, either 2mM CaCl<sub>2</sub> or 1mM EGTA was added and the lysates were incubated with antibody against CHL1, or non-specific IgGs as a control. Protein complex was precipitated with A/G agarose beads. Proteins were eluted from the beads with SDS sample buffer and subjected to SDS-PAGE followed by Western blot analysis using specific antibody against synaptogyrin-3. Results revealed that CHL1 and synaptogyrin-3 are associated with each other in the presence of 2 mM CaCl<sub>2</sub>.

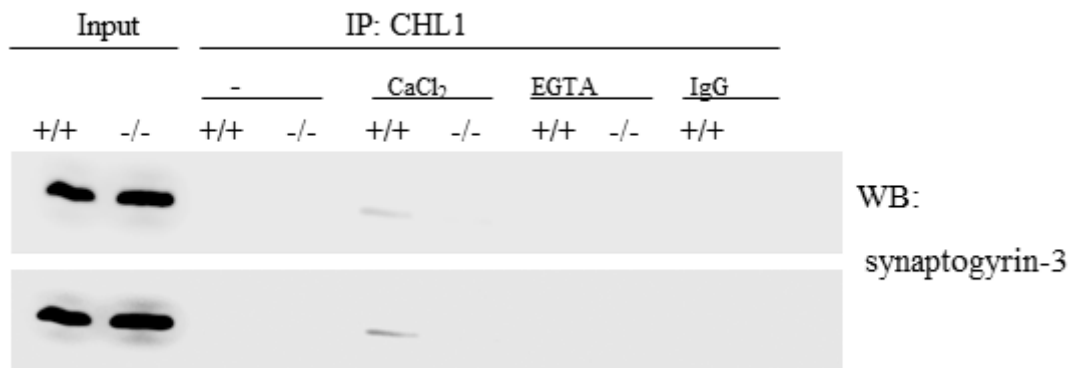


**Figure 22. Interaction of CHL1 and synaptogyrin-3 is calcium dependent.**

Brain extracts from wild-type (+/+) and CHL1-deficient mice (-/-) as input materials were subjected to immunoprecipitation (IP) with the CHL1 antibody and Western blot analysis (WB) with the synaptogyrin-3 antibody. Finally, the 25 kDa band of synaptogyrin-3 in the CHL1 immunoprecipitates from wild-type brain in the presence of 2 mM CaCl<sub>2</sub> was recognized. Two images were captured from the same blot. To get visible band for synaptogyrin-3 which is weak in compare to inputs, different exposure times were used. The upper image was taken using shorter exposure times. The blot was then imaged again using longer exposure times resulted in signal saturation of input bands. Immunoreactivity was visualized using the enhanced chemiluminescence detection system (ECL) and detected with ImageQuant™ LAS 4000 mini (GE Healthcare).

### 3.2. Synaptogyrin-3 is pulled down with the CHL1-ICD

As a further confirmation of the interaction between CHL1 and synaptogyrin-3, a pull down assay was performed. Mouse brain homogenate was incubated with CHL1-ICD, followed by a pull down with Ni-NTA beads. Precipitated proteins were subjected to SDS-PAGE. Western blot analysis using synaptogyrin-3 antibody recognized a predominant band of 25 kDa in the non-treated and 2 mM CaCl<sub>2</sub> treated CHL1-ICD precipitates, indicating the interaction of CHL1 and synaptogyrin-3 occurs at normal physiological calcium concentration present in the brain lysate, and up to higher concentrations of 2 mM CaCl<sub>2</sub>.

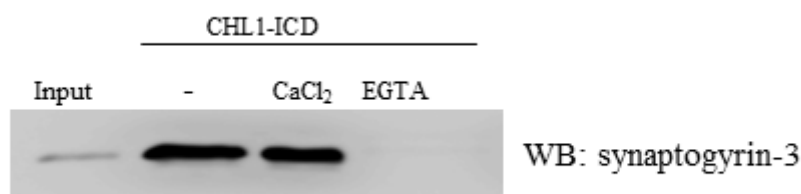


**Figure 23. Synaptogyrin-3 is pulled down with the ICD of CHL1.**

Brain homogenate was incubated with recombinant CHL1-ICD, followed by a pull down with Ni-NTA beads. The pulled down proteins were subjected to SDS-PAGE. Western blot analysis was performed using the synaptogyrin-3 antibody, indicating the interaction of CHL1 and synaptogyrin-3 occurs at normal physiological calcium concentration present in brain lysate, and up to higher concentrations of 2 mM CaCl<sub>2</sub>.

### 3.3. CHL1 prominently co-localizes with synaptogyrin-3 in cultured cerebellar and hippocampal neurons only after stimulation with CHL1-Fc

Primary cerebellar neurons were maintained on PLL. The cells were pre-treated with 5 µg/ml of CHL1-Fc, or L1-Fc. Non-treated neurons also were used as a control. The cells were fixed, permeabilized and stained with antibody against intracellular domain (ICD) of CHL1 and anti synaptogyrin-3 antibody. It is suggested that treatment of neurons with CHL1-Fc could trigger calcium release, resulting in CHL1 and synaptogyrin-3 interaction in the presence of calcium.

Consistent with above results, primary cultured hippocampal neurons also were pre-incubated with 5 µg/ml CHL1-Fc. Following fixation and permeabilization, neurons were co-stained with antibodies against intracellular domain (ICD) of CHL1 and anti synaptogyrin-3.

Yellow staining indicates CHL1 and synaptogyrin-3 are likely to interact with each other after stimulation with CHL1-Fc.

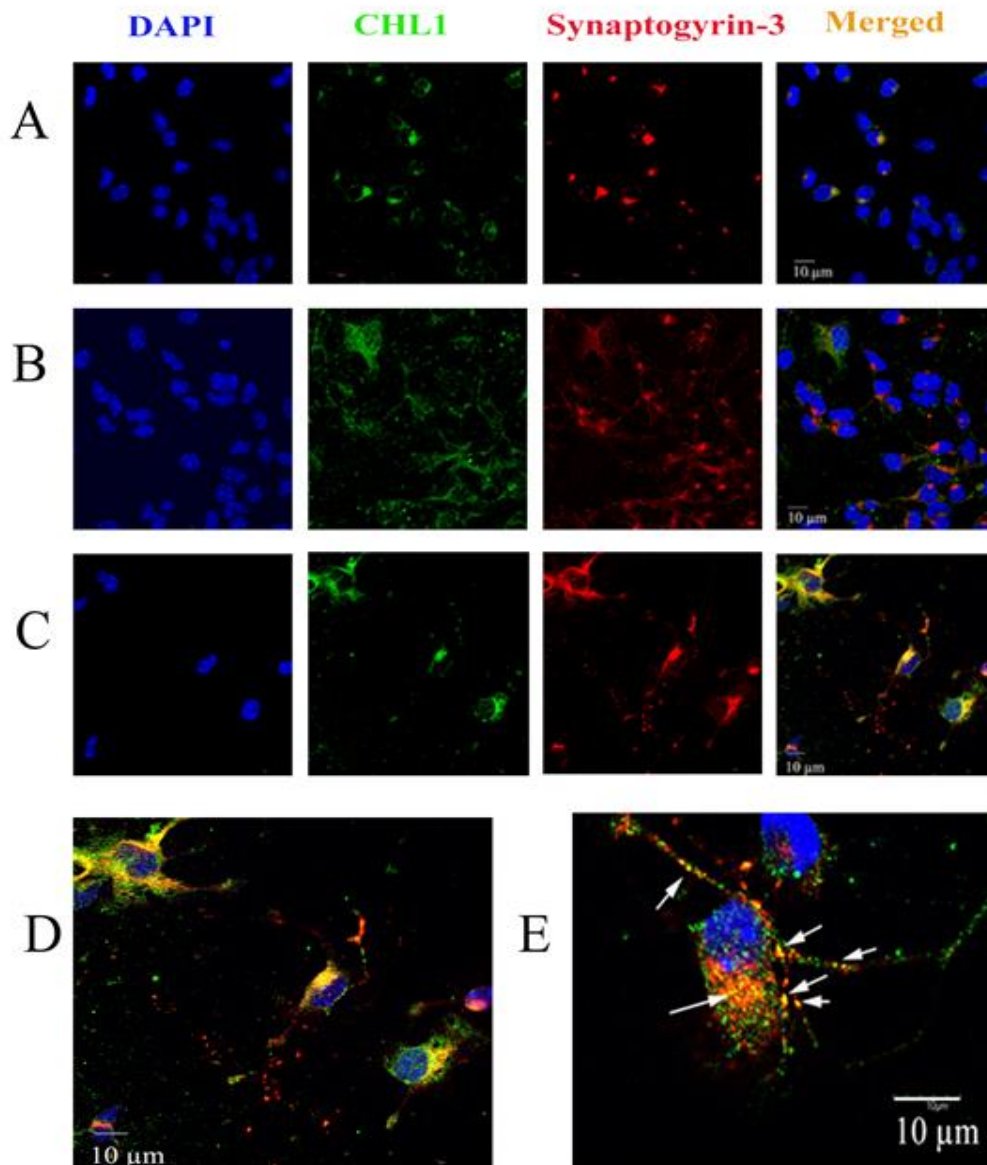


**Figure 24. Co-localization of CHL1 and synaptogyrin-3 in cerebellar and hippocampal neurons treated with CHL1-Fc**

The co-localization of endogenous CHL1 with synaptogyrin-3 was investigated in primary cerebellar neurons. Non-treated cells were considered as control (A). The cerebellar cells were incubated with L1-Fc (B) or CHL1-Fc (C). After fixation and permeabilization of cells, antibodies against intracellular domain (ICD) of CHL1 and anti synaptogyrin-3 were applied. Fixed cells were then incubated with secondary antibodies coupled to the fluorescent dyes Cy3 or Cy2. Only after stimulation of neurons with CHL1-Fc co-localization was observed as yellow signals. The merged image of cerebellar neurons was magnified in the respective large panel (D). Dissociated hippocampal neurons were incubated with CHL1-Fc, revealing co-localization of CHL1 and synaptogyrin-3 in the soma and neurites (arrows). The merged image of hippocampal neurons is a z-stack with a

greater depth of field, composed of 36 individual source images (E). Coverslips were mounted with Roti-Mount Fluor Care DAPI and confocal images were taken with an Olympus Fluoview FV1000 confocal laser-scanning microscope.

### 3.4. Treatment of hippocampal neurons with the extracellular domain of CHL1 triggers a calcium response

Several studies have been shown that application of L1 or NCAM synthetic peptide or antibody, which binds to the extracellular domain of cell adhesion molecule triggers calcium signaling (Ronn *et al.*, 2002, Kiryushko *et al.*, 2006, Von Bohlen Und Halbach *et al.*, 1992).

In the previous experiment, it was suggested that CHL1-Fc could trigger calcium release, resulting in CHL1 and synaptogyrin-3 interaction in the presence of calcium. To test this hypothesis, calcium imaging was performed. Hippocampal neurons were seeded on PLL-coated glass cover slips with a density of one million cells per ml and maintained in culture for 48 hours. Cells were loaded with 5  $\mu$ M Fura-2 AM as an intracellular calcium indicator. Stimulation with CHL1-Fc (10  $\mu$ g/ml) was performed at a defined time point (60 sec). The intensity of Fura-2 signal within the cell soma before and after CHL1-Fc application, as well as changes in fluorescent calcium signals were recorded. Calcium imaging shows that incubation of hippocampal neurons with CHL1-Fc triggers calcium release that could promote the interaction of CHL1 with synaptogyrin3 since their interaction is calcium dependent.

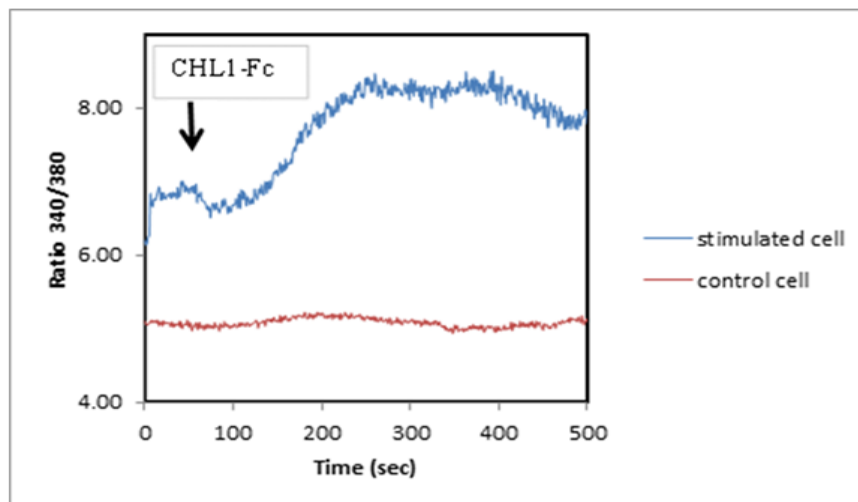


**Figure 25. Application of CHL1-Fc enhances intracellular calcium levels in cultured hippocampal neurons.**

The graph shows the intensity of Fura-2 AM signal in primary hippocampal neurons before and after stimulation with CHL1-Fc. The live cell records were taken with epi-fluorescence microscopy with a special filter for the 340/380 measurement. Fura-2 is excitable at a wavelength of 340 nm, but only if Fura-2 is saturated with calcium. If Fura-2 is free of calcium, it can only be excited at a wavelength of 380 nm. Therefore, the ratio of 340/380 is independent of the amount of Fura-2 that was loaded in to the cells and also independent of bleaching of the dye. Calcium imaging indicates that incubation of hippocampal neurons with CHL1-Fc promotes calcium release that mediates the interaction of CHL1 with synaptogyrin-3 in a calcium dependent fashion.

**3.5. Co-localization of CHL1 and synaptogyrin-3 in striatal tissue**

The interaction between CHL1 and synaptogyrin-3 was further analyzed by immunohistochemistry of the adult mouse brain tissue. Double-labeling with goat antibody against CHL1 and mouse antibody against the synaptogyrin-3 showed a considerable number of yellow spots, indicating the co-localization of CHL1 and synaptogyrin-3 in the striatum.

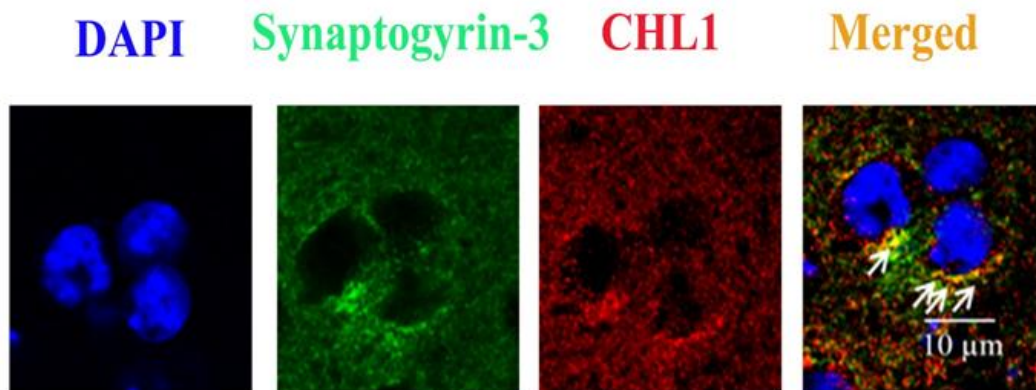


**Figure 26. Immunostaining of CHL1 and synaptogyrin-3 in the striatum**

Striatal slice from wild-type mouse was incubated with antibodies against CHL1 and synaptogyrin-3. Then, secondary antibodies coupled with Cy2 or Cy3 were applied. Merged image indicates co-localizations in yellow spots (arrows).

**3.6. Close interaction between CHL1 and synaptogyrin-3 *in situ***

To investigate direct interaction of CHL1 with synaptogyrin-3 in intact adult mouse brain, the striatal tissue was incubated with primary antibodies against CHL1 and synaptogyrin-3 for proximity ligation assay which detects close protein interactions within a distance less than

40 nm. Red fluorescent signals were observed throughout the striatum, indicating these two proteins are in close interaction with each other.

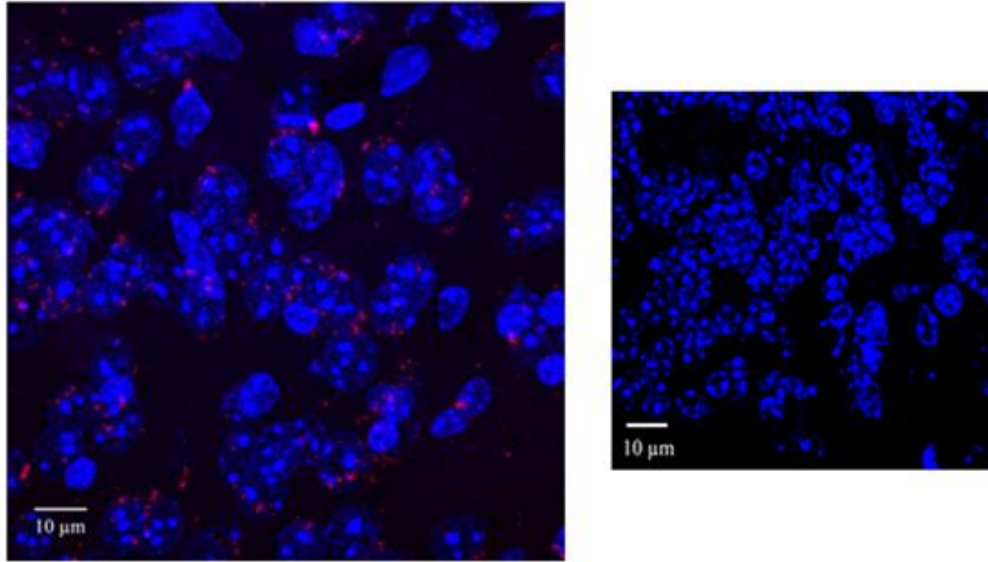


**Figure 27. Close interaction between CHL1 and synaptogyrin-3 *in situ*.**

Tissue from wildtype (left panel) and CHL1-deficient mice (right panel) were subjected to proximity ligation assay with the CHL1 and synaptogyrin-3 antibodies. Nuclei were stained with DAPI (blue). Spots of fluorescent signals (red) were observed in confocal fluorescent images (left panels), indicating CHL1 co-localizes with its binding partner synaptogyrin-3 in the striatum.

### **3.7. Verification of CHL1 and synaptogyrin-3 interaction by FRET**

Because of its sensitivity to distance, Fluorescence resonance energy transfer (FRET) has been used to investigate proteins interactions at the molecular level. FRET measures molecular proximity of less than 10 nm. In this study, the plasmids of cyan fluorescence protein (CFP) and green fluorescence protein (GFP) were applied. NIH-3T3 cells were co-transfected with CFP-synaptogyrin-3 as a donor and GFP-CHL1 as an acceptor. Two days after transfection, the cover slip was transferred into a petri dish with 3 ml pre-warmed medium. During live imaging, cells were kept in an incubation chamber (37°C, 5% CO<sub>2</sub>, 70% humidity). FRET analysis was performed with the confocal laser-scanning microscope Olympus FV1000 using sensitized emission method. The result indicating CHL1 and synaptogyrin-3 are in a close vicinity of approximately 5 nm.

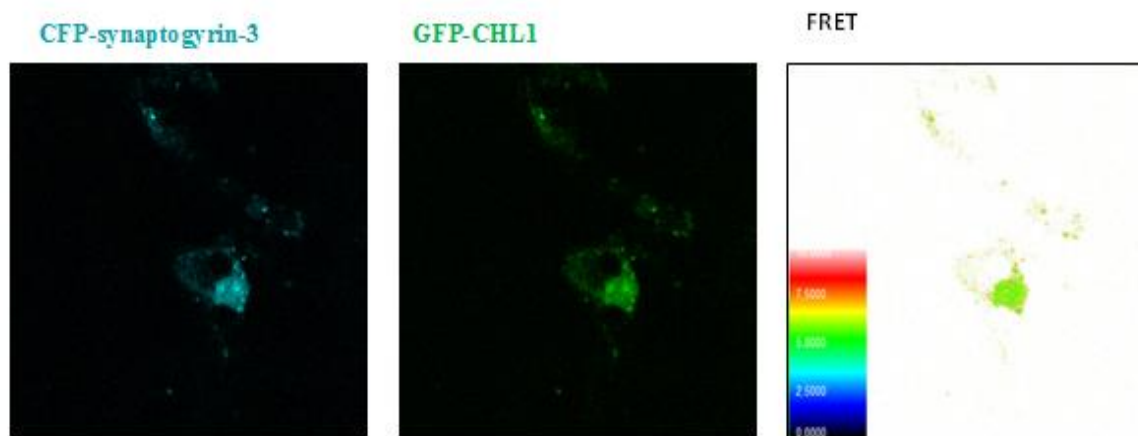


**Figure 28. Verification of CHL1 and synaptogyrin-3 interaction by FRET using sensitized emission method**

NIH-3T3 cells were transfected with CFP-synaptogyrin-3 and GFP-CHL1 constructs. The FRET imaging was performed with a confocal laser scanning microscope (Olympus FV1000). Color scale represents distance (nm) between two proteins. The observations revealed that CHL1 and synaptogyrin-3 are in a close vicinity of approximately 5 nm.

#### **4. Study the interaction of CHL1 with dopamine transporter (DAT)**

Although synaptogyrin-3 is involved in neurotransmitter release, other studies have shown that synaptogyrin-3 interacts with dopamine transporter (DAT) to positively regulate DAT activity (Egana *et al.*, 2009). DAT is a presynaptic plasma membrane protein that regulates the re-uptake of dopamine back into nerve terminals and thus is essential for homeostasis of dopamine at the cleft. DAT function and dopamine signaling contribute to neurological and psychiatric diseases. Furthermore, DAT plays an important role in addiction and is the principle target for psychostimulants, such as cocaine and amphetamine (AMPH).

Since synaptogyrin-3 interacts with DAT and CHL1, I was interested whether CHL1 also interacts directly with DAT. Investigation of the CHL1 interaction with both DAT and synaptogyrin-3 would shed light understanding the cellular and molecular mechanisms associated with DAT trafficking and functions regulated by CHL1 with the objective of maintaining dopaminergic tone at the synapse. Therefore, study the interaction of CHL1 and DAT was a major focus of my study.

#### 4.1 Analysis of CHL1-DAT interaction *in situ*

As an alternative method to confirm CHL1-DAT interaction *in situ*, proximity ligation assay (PLA) was applied to mouse striatum tissue. The interaction between two proteins was detected using the corresponding two primary antibodies. When the PLA probes are in close proximity (<40 nm), fluorescent signals were generated and amplified. Red fluorescent spots indicate close interaction between CHL1 and DAT.

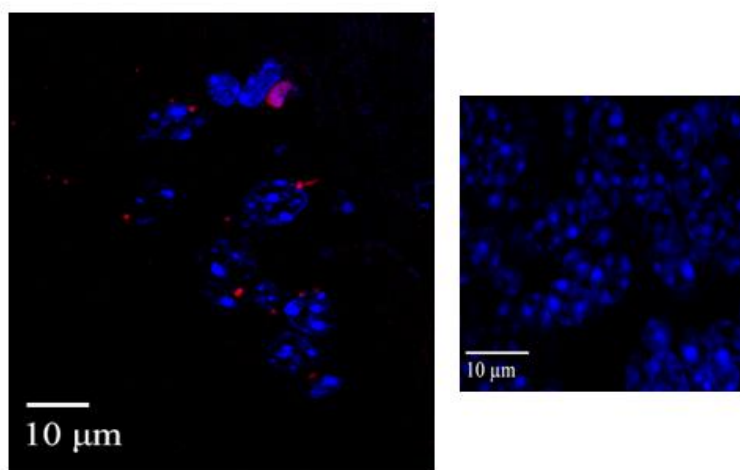


**Figure 29.** Close interaction of CHL1 and DAT *in situ*.

Striatum tissue subjected to proximity ligation assay with antibodies against CHL1 and DAT. Nuclei were stained with DAPI (blue). Red Spots of intense fluorescent signals indicate close protein interaction between DAT and CHL1.

#### 4.2. Verification of ‘CHL1-DAT-Synaptogyrin-3’ association by Co-IP

An immunoprecipitation experiment was performed to examine whether there is a direct interaction between CHL1 and dopamine transporter (DAT). For this purpose, striatum brain homogenates from wildtype and CHL1-deficient mice were incubated with the CHL1 antibody followed by incubation with protein A/G agarose beads to precipitate the potential association of ‘CHL1-DAT-Synaptogyrin-3’. After SDS-PAGE, Western blot analyses were done using DAT and synaptogyrin-3 (syg-3) antibodies. DAT and synaptogyrin-3 were co-immunoprecipitated from wild-type brain homogenate in the presence, but not in the absence of calcium, indicating that the interactions between CHL1, DAT, synaptogyrin-3 are calcium-dependent (Fig.30A). The inverse immunoprecipitation with the DAT antibody

demonstrated that CHL1 was also successfully precipitated in the presence of calcium from brain homogenate (Fig.30B). Taken together, the results suggest that ‘CHL1-DAT-Synaptogyrin-3’ are associated in a calcium dependent manner and could form a complex *in vitro*.

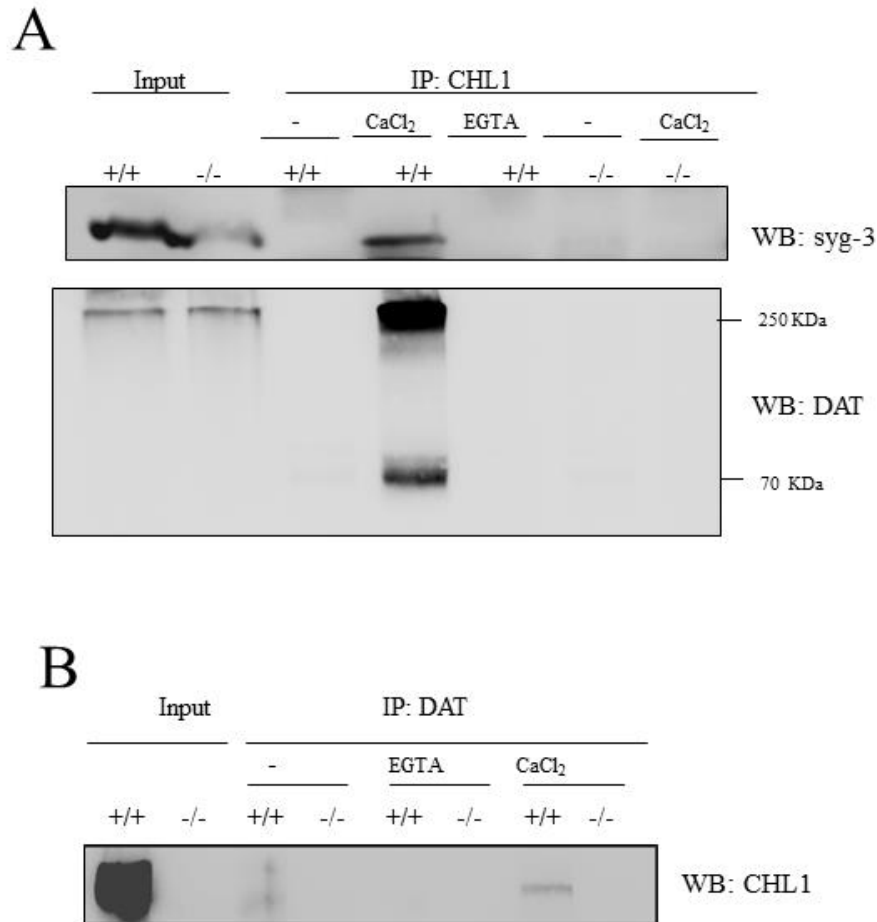


**Figure 30. Verification of ‘CHL1-DAT-Synaptogyrin-3’ complex by Co-IP.**

**(A):** Wildtype or CHL1-deficient brain homogenates were subjected to immunoprecipitation with the CHL1 antibody and were probed with the synaptogyrin-3 and DAT antibodies. Western blotting with DAT antibody revealed two distinct bands with molecular weights of 70 kDa and 250 kDa correspond to monomer and oligomer forms of DAT (Chen and Reith, 2008). **(B):** Immunoprecipitation with anti-DAT antibody followed by Western blotting with anti-CHL1 was performed. The results indicated synaptogyrin-3 and DAT were co-immunoprecipitated with the CHL1 antibody, whereas CHL1 was also precipitated with the DAT antibody in an inverse fashion. Co-immunoprecipitation experiments suggested that ‘CHL1-DAT Synaptogyrin-3’ could form a complex in a calcium dependent manner.

### 4.3. Co-localization of ‘CHL1-DAT-Synaptogyrin-3’ complex in striatum

The *in vitro* findings of Co-IP have revealed the direct interactions of CHL1 with DAT and synaptogyrin-3. To test this possibility *in vivo*, immunostainings of striatal tissues with antibodies against CHL1, DAT and synaptogyrin-3 were performed. Co-localization of triple labeled proteins appeared in white spots in the merged panel. These results provided evidence for protein association composed of CHL1, DAT and synaptogyrin-3 *in vivo*.

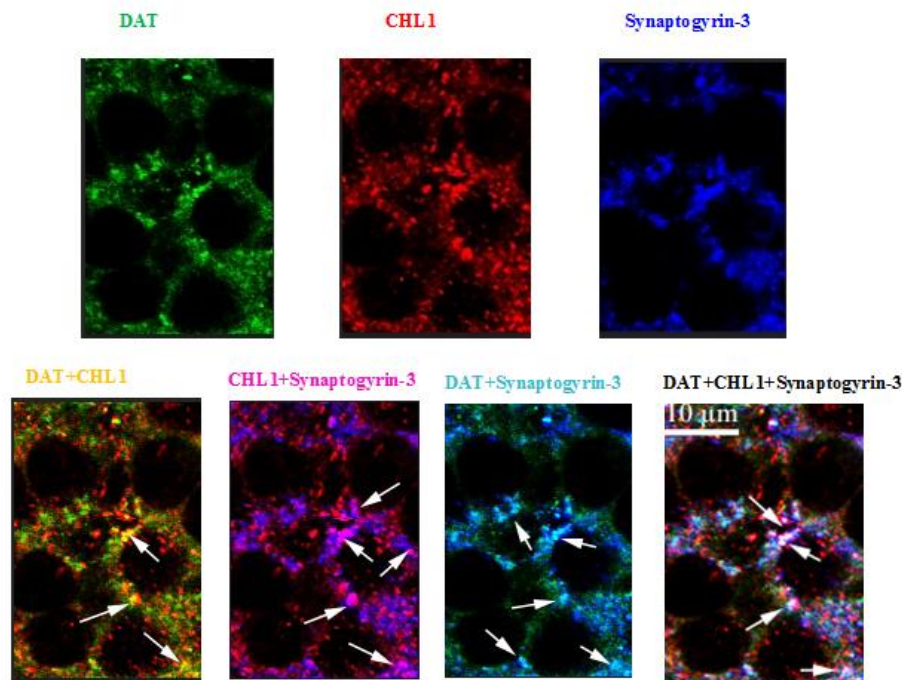


**Figure 31. CHL1 co-localizes with both synaptogyrin-3 and DAT in striatal tissue.**

Striatal tissue was incubated with antibodies against CHL1, synaptogyrin-3 and DAT followed by Cy3, Cy5 Cy2, conjugated secondary antibodies, respectively. Co-localization of CHL1 with DAT is shown in yellow. Co-localization of CHL1 with synaptogyrin-3 is shown in pink. Co-localization of DAT with synaptogyrin-3 is shown in turquoise. Co-localization of three proteins ‘CHL1, DAT and synaptogyrin-3’ is seen in white. Co-localized spots are shown by arrows.

## **5. Functional analysis of the interaction between CHL1 and dopamine transporter**

Dopamine is a critical neurotransmitter in the CNS that plays role in locomotor function, reward and cognition mechanisms. Impairments in the dopamine system contribute to schizophrenia, Parkinson's disease and attention deficit hyperactivity disorders. The plasma membrane transporter DAT regulates extracellular dopamine levels by re-uptake dopamine from cleft back to presynaptic terminal. This re-uptake is very critical to limit the lifetime of dopamine signaling in the brain. Although DAT is a therapeutic molecule for treatment of neurological disorders, it is highly targeted by addictive substances such as cocaine and amphetamine (AMPH).

### **5.1. Internalization of CHL1 with DAT after stimulation by PMA in transfected HEK cells**

Numerous studies have been shown DAT is a dynamic molecule on the cell surface; it cycles from the plasma membrane through endocytosis (internalization) under both basal and protein kinase C (PKC) stimulated conditions or cycles back to the membrane *via* exocytosis (fusion). Activation of PKC by phorbol esters, such as PMA (Phorbol 12-myristate 13-acetate) is well established, causing acute internalization of the DAT in cell lines (Daniels and Amara, 1999; Melikian and Buckley, 1999; Blakely and Bauman, 2000; Granas et al., 2003; Miranda et al., 2007; (Eriksen *et al.*, 2009).

Over various studies, several DAT interacting proteins have been identified (Torres, 2006), assuming that trafficking and functional properties of DAT can be regulated *via* protein–protein interactions. Therefore, it was interesting to investigate whether CHL1 plays a role in trafficking of DAT. To address this question, CHL1 and DAT gene were cloned in a bicistronic vector containing the internal ribosome entry site (IRES), which allows the simultaneous expression of two proteins from the same mRNA. For internalization study, HEK cells were plated on coverslips, transfected with DAT/CHL1 bicistronic mammalian vector. Afterwards, cells were incubated in the presence or absence of 1  $\mu$ M PMA for 30 min at 37°C. The coverslips were fixed in 4% PFA for 1hr at RT, and then washed three times with PBS for 5 min at RT. While plasma membrane distribution of both CHL1 and DAT was

observed within non-treated cells, PMA treatment triggered the appearance of intracellular vesicular structures resulted by internalization of CHL1 with DAT. Coverslips were mounted with Roti-Mount Fluor Care DAPI and confocal images were taken with an Olympus Fluoview FV1000 confocal laser-scanning microscope in sequential mode.

This observation indicate that CHL1 internalizes with DAT in response to PKC stimulation, which is in agreement with published data regarding endocytosis of CHL1 through lipid raft domain (Tian *et al.*, 2012).

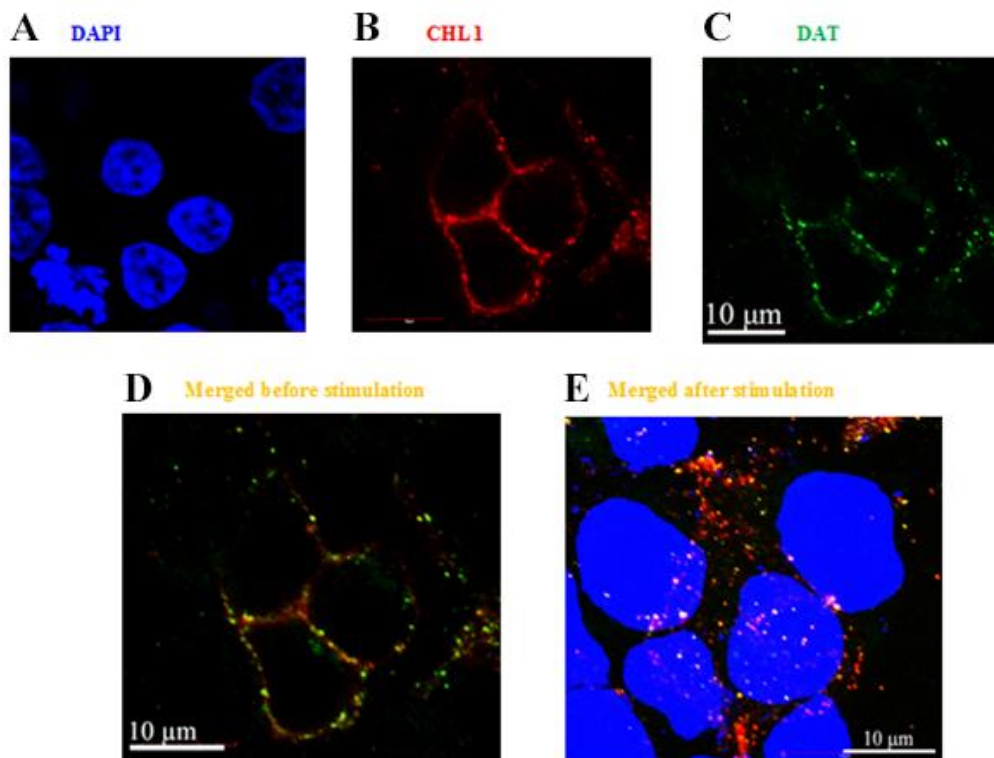


**Figure 32. Visualization of CHL1 internalization with DAT in transfected HEK 293 cells.**

HEK cells were transfected with DAT/CHL1 bicistronic mammalian vector. The cells were incubated in the absence (A-D) or presence (E) of 1 μM PMA for 30 min at 37°C, as PMA promotes internalization of DAT. As shown in images (A-D), DAT and CHL1 are labeled only in the plasma membrane before incubation with PMA. After treatment with PMA, CHL1 co-localizes with internalized DAT that can be apparent in intracellular vesicular structures.

## 5.2. Immunohistochemical staining of the midbrain dopaminergic system in wildtype and CHL1-deficient mice

Dopamine plays a critical role in the regulation of locomotion, cognition, reward and emotional behavior, while CHL1 ablation is associated with mental retardation, epilepsy, schizophrenia and autism disorders accompanied by alteration in working memory, stress response, reactivity to novelty, social and exploratory behavior. To further investigate the implication of CHL1 in dopaminergic system, mice midbrains were analyzed. For this purpose, serial coronal 25- $\mu\text{m}$ -thick sections of adult wildtype and CHL1-deficient tissues were incubated with the TH (tyrosine hydroxylase) primary antibody, followed with DAB staining. In CHL1-deficient mice, immunohistochemical stains for TH revealed obvious loss of midbrain dopamine neurons based on the lower density of TH-positive cells in substantia nigra (SN) as compared to the wild-type tissue. This observation is in agreement with a previous statistical analysis in our lab, which indicates an ‘age-dependent’ loss of dopamine neurons in CHL1-deficient mice (Thilo, B.E. 2005, PhD dissertation). Taken together, the strong evidence of dopamine neurons loss in CHL1-deficient mice was gained.

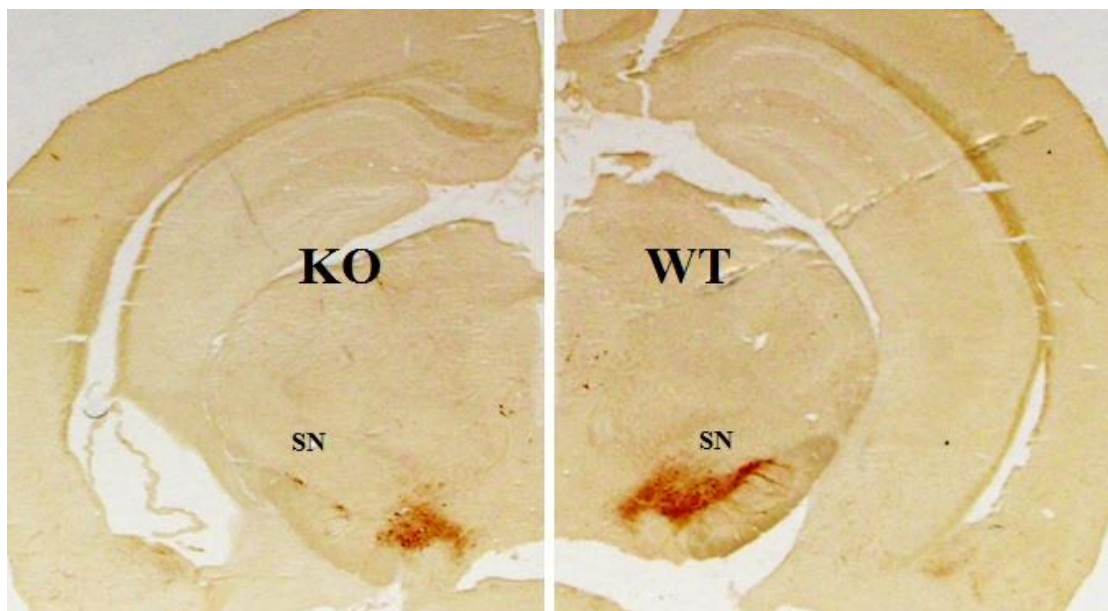


**Figure 33. Tyrosine hydroxylase (TH) immunostaining of the midbrain dopamine neurons in wildtype and CHL1-deficient mice.**

Tyrosine hydroxylase (TH) expression in the midbrain of adult wildtype and CHL1 knockout mice was probed by immunostaining. The density of dopamine neurons in substantia nigra (SN) of CHL1-deficient mice has shown a marked reduction versus wildtype tissue.

## **VI. Discussion:**

### **6.1. Identification of potential binding partners of CHL1 and NCAM180**

In this study, novel cytosolic interacting partners of CHL1 and the neural cell adhesion molecule isoform 180 (NCAM180) were identified by affinity chromatography followed by mass spectrometry. For this purpose, recombinant intracellular domains (ICDs) of CHL1 and NCAM180 were produced and purified *via* the His-Tag. NCAM180.ICD was used as control to identify CHL1-ICD specific binding partners. The purified ICDs were immobilized on CN-Br resin and wild type brain homogenates were then applied to the immobilized ICDs. Proteins bound to the individual bait proteins were separated on SDS-PAGE and stained with colloidal Coomassie blue dye. Bands specifically found in the CHL1-ICD eluate were cut and sent to the mass-spectrometry. Among the mass spectrometry list of putative binding partners of CHL1, following proteins appeared to be the most interesting ones: Synaptosomal-associated protein-25 (SNAP-25), vesicle-associated membrane protein 2 (Vamp2), programmed cell death protein 6 (PDCD6) also called apoptosis-linked gene-2 protein (ALG-2), peflin1 (PEF-1), sorcin, synaptogyrin-1, synaptogyrin-3, the Ras-related proteins Rab 1A and Rab 14, also cofilin and doublecortin. Since SNAP-25 and Vamp2 have been published as CHL1 binding partners (Andreyeva *et al.*, 2010), this method is certainly a reliable approach to gain first hints of potential protein-protein interactions.

### **6.2. Investigation of CHL1-ALG-2 physical and functional interaction**

From two individual mass spectrometry analyses, indications were obtained for a possible interaction between CHL1 and programmed cell death protein 6 (PDCD6) also called apoptosis-linked gene-2 protein (ALG-2). Further, this interaction was verified using additional techniques.

Physiological interaction between CHL1 and ALG-2 was determined by a co-immunoprecipitation experiment. Since CHL1 precipitated with the ALG-2 antibody from brain homogenate only in the presence of 2 mM CaCl<sub>2</sub>, it is likely that CHL1-ALG-2 interaction is calcium dependent. This result is consistent with previous studies, which

reported that ALG-2, being a calcium binding protein and a member of the penta EF-hand family, interacts with different proteins such as scotin, Alix and TSG101, annexin A11 and annexin A7, human PLSCR3, sec31A and CHERP in a calcium- dependent manner (Draeby *et al.*, 2007, Okumura *et al.*, 2009, Satoh *et al.*, 2002, Shibata *et al.*, 2008, Shibata *et al.*, 2007, Sasaki-Osugi *et al.*, 2013).

However, the interaction of CHL1 with ALG-2 occurred in the absence of calcium in a pull-down experiment. One can assume that the presence of the ‘His-Tag’ in the recombinant intracellular domain of CHL1 could alter the interaction conditions either due to its charge or by steric hindrance. Also, the recombinant intracellular domain of CHL1 applied in pull-down may possess a different folding or other conformational properties than the native full length CHL1 present in the Co-IP. Therefore, the binding affinity between recombinant CHL1-ICD and ALG-2 could vary with respect to buffer additives such as calcium.

The combined results from the Co-IP and pull-down assays suggest a strong physical interaction between CHL1 and ALG-2 *in vitro*.

In present study, immunostaining of CHL1 and ALG-2 in fixed cerebellar neurons showed that there is no specific co-localization between these two proteins. Surprisingly, application of antibody against the extracellular domain of CHL1 in live cerebellar neurons induced the prominent co-localization between CHL1 and ALG-2. This can possibly be explained by clustering of CHL1 with binding of the antibody on the cell surface, which could mimic homophilic interactions of CHL1. This result raises the question, which kind of signal is induced during the CHL clustering. It has been reported that clustering of L1 and NCAM by antibodies both could induce Ca<sup>2+</sup> influx *via* voltage-dependent calcium channels (VDCC) (Williams *et al.*, 1992, Niethammer *et al.*, 2002), but especially CHL1 antibody-treatment induces Ca<sup>2+</sup> influx *via* L-type VDCCs (Tian *et al.*, 2012). These observations are in agreement with our hypothesis that clustering of CHL1 followed by calcium influx results in co- localization of ALG-2 and CHL1 along neurites if the calcium levels have been elevated. This point was also confirmed by *in vitro* Co-IP assay, which revealed that the association between CHL1 and ALG-2 is calcium dependent.

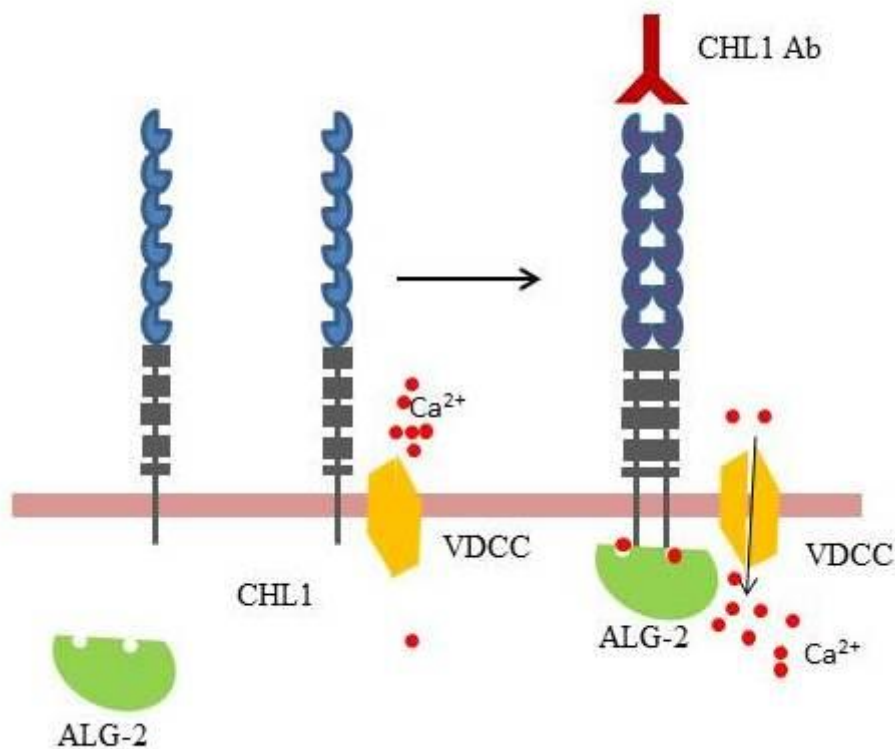


**Figure 34. Clustering of CHL1 on cell surface, calcium influx and interaction with ALG-2.**

Clustering of CHL1 on cell surface followed by Ca<sup>2+</sup> influx via L-Type VDCC (Tian *et al.*, 2012) could facilitate the CHL1-ALG-2 interaction at high levels of cytoplasmic calcium.

Using Duolink, red fluorescence signals throughout CA3 region of hippocampus and along the parallel fibers of cerebellum could be observed, indicating that endogenous CHL1 and ALG-2 are in close proximity in these areas. To our knowledge, this observation is the first report regarding the presence of ALG-2 as a calcium binding protein in the cerebellum. Also the potential ALG-2-CHL1 interaction in parallel fibers is a new observation not yet reported so far.

This finding is in agreement with published data showing high level expression of CHL1 in parallel fibers of the cerebellum, while ablation of CHL1 in climbing and parallel fiber in CHL1-deficient mice influence the survival of purkinje cells, affecting targeting and function of early synaptic connections in the spiny branchlets of climbing and parallel fibers during normal development (Jakovcevski *et al.*, 2009). On the other hand, expression of the large

family of EF-hand calcium-binding proteins (such as calretinin, calbindin D-28k and parvalbumin) in the cerebellum have been previously observed, suggesting that calcium binding proteins possess critical roles in calcium homeostasis and in the regulation of cerebellar neuronal excitability (Gall *et al.*, 2005). Indeed, the presence of EF-hand calcium-binding proteins in parallel fibers is expected to modulate excitatory synaptic transmission, information processing and synaptic plasticity. In this context, an excessive calcium concentration during excitatory stimulation could lead to lipid and protein degradation and cell death in parallel fibers, one of the major excitatory afferents converging on to Purkinje cells.

In previous studies, the anti-apoptotic effect of CHL1 has been described (Chen *et al.*, 1999, Nishimune *et al.*, 2005, Jakovcevski *et al.*, 2009). Since ALG-2 (apoptosis-linked gene-2) promotes apoptotic cell death (Chen and Sytkowski, 2005), and since ALG-2 as an EF-hand calcium binding protein interacts with CHL1 in parallel fibers, these data motivated me to explore the possible functional interaction between CHL1 and ALG-2.

One well-known cellular response to thapsigargin (TG) is the cytosolic calcium elevation followed by ER stress-induced apoptosis. In this work, results obtained by the MTT assay revealed that incubation of transfected NIH-3T3 cells with TG leads to a significant decrease in cell viability as compared to the controls. Furthermore, the presence of CHL1 significantly enhanced the cell viability of cells co-expressing both CHL1 and ALG-2. This was not the case in cells that expressed only ALG-2, which suggests that CHL1 enhances cell survival under thapsigargin-induced stress and calcium overload toxicity. One could speculate whether CHL1 plays role as a ‘neuroprotective’ molecule during calcium overload and excitotoxicity in parallel fibers. This idea is supported by the above findings, as CHL1 is able to protect cells from cell death.

It has been reported that ALG-2 translocated from the cytoplasm to the nucleus after thapsigargin treatment (Montaville *et al.*, 2006, Janowicz *et al.*, 2011). While fragments of the cell adhesion molecules L1 and NCAM were found in the nucleus (Lutz *et al.*, 2012, Westphal *et al.*, 2016), I address the question whether CHL1 as a cell adhesion molecule could be also imported to the nucleus in response to TG stress. From immunofluorescence staining, only nuclear ALG-2 immunoreactivity signals were observed upon TG treatment, but the nuclear localization of CHL1 could not be detected.

### **6.3. Investigation of the interaction of CHL1 and synaptogyrin-3**

The mass spectroscopy analysis indicated the potential interaction between CHL1 and synaptogyrin-1 and synaptogyrin-3. Synaptogyrins were identified as synaptic vesicle proteins which contribute to the regulation of neurotransmitter release. Notably, synaptogyrin-3 is expressed only in the brain and in the distinct populations of synapses in contrast to synaptogyrin-1. It is well known that the regulation of synaptic vesicle exocytosis and synaptic plasticity includes protein–protein interactions. In other words, synaptogyrins carry out their functions by interacting with other synaptic proteins. Considering the special function of synaptogyrin-3 in the brain, the interaction of CHL1 and synaptogyrin-3 was further analyzed in this study.

Co-localization of endogenous CHL1 with synaptogyrin-3 was confirmed in the brain tissue, where the yellow signals were detectable in the merged image using double labeling with both cy-2 and cy-3. In addition to this, intensive red signals were also detectable in a proximity ligation assay, indicating that CHL1 is in close contact with synaptogyrin-3 in the intact tissue. In this context, the result from FRET analysis using CFP-synaptogyrin-3 and GFP-CHL1 constructs has shown that CHL1 and synaptogyrin-3 are in close vicinity of approximately 5 nm.

The evidence for the physical binding of CHL1 to synaptogyrin-3 in the presence of calcium was obtained by a co-immunoprecipitation assay. Furthermore, using CHL1-ICD in a pull down assay, it could be observed that synaptogyrin-3 precipitated either from untreated brain lysate or from brain lysate treated with 2mM calcium. Hence, CHL1-synaptogyrin-3 interaction occurs at normal physiological calcium concentration present in the brain homogenate, and up to higher concentrations of 2 mM CaCl<sub>2</sub>, indicating that the CHL1-synaptogyrin-3 interaction is calcium dependent. This presumption was supported by the immunocytochemical analysis of CHL1 and synaptogyrin-3 in cerebellar and hippocampal neurons, revealing that the co-localization of CHL1 and synaptogyrin-3 is likely to occur after stimulation with CHL1-Fc, but not with L1-Fc. It was suggested that CHL1-Fc could mimic the CHL1-CHL1 homophilic interaction and mediates calcium release, resulting in a specific CHL1-synaptogyrin-3 interaction in the presence of calcium. To further demonstrate this idea, CHL1-Fc was used in calcium imaging of hippocampal neurons to investigate how CHL1-Fc influences the binding of CHL1 to synaptogyrin-3 as a synaptic vesicle protein. In

the present study, changes in intracellular  $\text{Ca}^{2+}$  levels in response to CHL1-Fc treatment have been observed. Indeed, an increase in the intracellular calcium concentration in hippocampal neurons loaded with the calcium probe Fura2-AM seems to promote the interaction of CHL1 with synaptogyrin-3. These conclusions are consistent with previous studies, which demonstrated that stimulation of neurons with synthetic peptides attached to the extracellular domain of NCAM could trigger calcium signaling (Ronn *et al.*, 2002, Kiryushko *et al.*, 2006, Sheng *et al.*, 2013). These results raise the question in which physiological processes CHL1 and synaptogyrin-3 could be involved.

Exocytosis is extensively studied in neurons. Here, the molecular mechanism and the key proteins involved in exocytosis are illustrated (Fig. 35). SNARE (soluble NSF attachment protein receptor) complex is reported to be the mediators of fusion process, while rapid influx of calcium also triggers membrane fusion.

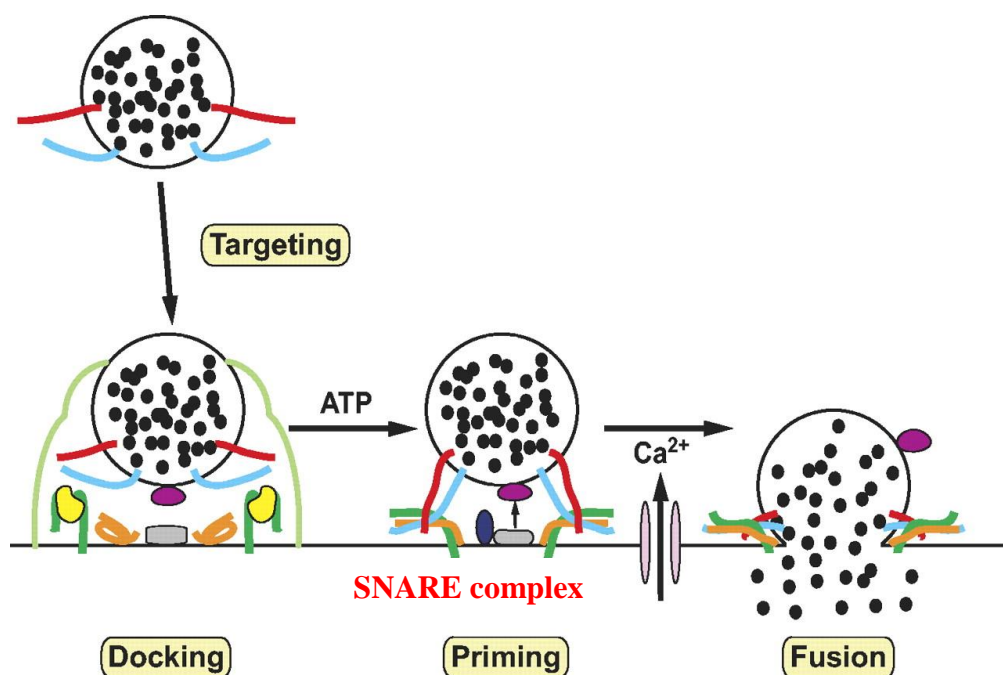


**Figure 35. Schematic model of exocytosis.**

Critical proteins are involved in docking, priming, and fusion steps. Synaptic vesicles contain neurotransmitters are targeted to active zones. Docking is an association between the vesicle and plasma membranes *via* protein-protein interactions. Next, An ATP-dependent priming stag occurs, followed by rapid  $\text{Ca}^{2+}$ -triggered membrane fusion.  $\text{Ca}^{2+}$  influx occurs through voltage-dependent  $\text{Ca}^{2+}$  channels (VDCCs). SNARE (soluble NSF attachment protein receptor) complex are reported to be the mediators of fusion process. The SNARE complex consists of three proteins: VAMP (light blue), syntaxin (green), SNAP-25 (orange). **Presentation was taken from (Seino and Shibasaki, 2005)**

Following action potential in neurons, influx of  $\text{Ca}^{2+}$  through VDCCs can trigger exocytosis. The fusion of synaptic vesicles to the plasma membrane is a critical step in exocytosis and neurotransmitter release. Although an increase in intracellular  $\text{Ca}^{2+}$  levels as a principle signal triggers fusion process, the formation of the SNARE complex is also suggested to mediate membrane fusion and to facilitate neurotransmission (Rothman and Warren, 1994).

In a previous study, the importance of the interactions between CHL1 and the SNARE complex as a part of the exocytotic machinery was reported (Andreyeva *et al.*, 2010). Since the SNARE complex proteins such as SNAP25, syntaxin1B and VAMP2 were immunoprecipitated with CHL1 (Andreyeva *et al.*, 2010), and since CHL1 interacts with the synaptic vesicle protein synaptogyrin-3 in the presence of calcium, it is admissible to assume that the association of CHL1 with synaptogyrin-3 occurs when synaptic vesicle fusion to the membrane is induced by calcium influx. Hence, CHL1-synaptogyrin-3 interaction may involve in neurotransmitter release through exocytosis. Interestingly, it has been reported that another synaptic vesicle protein, synaptophysin, does not interact with CHL1 (Andreyeva *et al.*, 2010). This provides noteworthy evidence regarding the ‘physiological significance’ of the binding of CHL1 to synaptogyrin-3.

Several behavior studies have shown that CHL1 play roles in synaptic plasticity, but the molecular mechanism underlying CHL1 functions in synaptic plasticity are not well understood. On the other hand, it is well known that the regulation of synaptic vesicle exocytosis and synaptic plasticity includes protein–protein interactions. Notably, strong immunoreactivity of synaptogyrin-3, but not synaptogyrin-1, was observed in the mossy fiber region of hippocampus, suggesting the special role of synaptogyrin-3 in mossy fiber long-term potentiation (LTP) (Belizaire *et al.*, 2004). In contrast to Schaffer collateral LTP, the induction of mossy fiber LTP is NMDA receptor-independent, based on an increase in presynaptic calcium levels followed by vesicular release in response to action potential (Mellor *et al.*, 2002). In this context, our results have shown that stimulation of hippocampal neurons with CHL1-Fc triggers calcium influx, resulting in a specific CHL1-synaptogyrin-3 interaction in the presence of calcium. Considering that hippocampal mossy fibers and their terminal organizations are altered in CHL1-deficient mice (Montag-Sallaz *et al.*, 2002), and regarding the multiple defects in neurotransmission, long-term potentiation and behavior in

CHL1 deficient mice, one could speculate that the interaction of CHL1 and synaptogyrin-3 in the presence of calcium may further correlate with neurotransmitter release and synaptic plasticity in mossy fibers of hippocampus. However, more detailed investigations are required to reveal the role of CHL1 in NMDAR-independent LTP mechanism in hippocampal mossy fibers.

#### **6.4. Investigation of the interaction of CHL1 and the dopamine transporter (DAT)**

Although synaptogyrin-3 is involved in neurotransmitter release, other studies have shown that synaptogyrin-3 interacts with the dopamine transporter (DAT) to positively regulate DAT activity (Egana *et al.*, 2009). DAT is a presynaptic plasma membrane protein, which regulates the re-uptake of dopamine back into nerve terminals and is thus essential for homeostasis of dopamine at the cleft. DAT function and dopamine signaling contribute to neurological and psychiatric diseases. Furthermore, DAT plays an important role in addiction and is the principle target for psychostimulants, such as cocaine and amphetamine (AMPH). Since synaptogyrin-3 interacts with both DAT and CHL1, I was interested to investigate whether CHL1 also interacts directly with DAT. This observation could help to further understand the functional interplay between CHL1 and DAT, with the objective of maintaining the dopaminergic tone at the synapse. Therefore, studying the interaction of CHL1 and DAT was a major focus of my study.

From the Duolink assay, a first impression regarding a potential interaction between CHL1 and DAT *in situ* could be obtained, indicating that CHL1 and DAT are in close proximity with less than 40 nm distance in the striatum tissue. Also, the physical interactions were confirmed by Co-IP from wild-type and CHL-deficient mice brain homogenates. Since synaptogyrin-3 and DAT precipitated with the CHL1 antibody, and since CHL1 was precipitated with the DAT antibody in an inverse fashion, this suggests that ‘CHL1-DAT-synaptogyrin-3’ could associate in a calcium dependent manner and form a complex *in vitro*. In this context, the co-localization of endogenous ‘CHL1-DAT-synaptogyrin-3’ complex proteins were also investigated in striatal tissue to further strengthen the hypothesis that these three proteins possess physiological interactions *in vivo*.

## 6.5. Functional interplay between CHL1 and DAT

In previous studies, several DAT interacting proteins have been identified (Torres, 2006), suggesting that trafficking and functional properties of DAT can be regulated *via* protein–protein interactions. In this regard, the interaction between CHL1 and DAT was verified by applying different methods. In addition, functional studies were performed to analyze the possible involvement of CHL1 in the regulation of DAT function and trafficking.

### 6.5.1. CHL1 internalizes with DAT after stimulation by PMA

It has been demonstrated that DAT is a dynamic molecule on the cell surface which cycles from the plasma membrane through endocytosis (internalization). DAT undergoes the constitutive or protein kinase C (PKC) stimulated internalization. Activation of PKC by phorbol esters, such as PMA is well established, which causes an acute internalization of the DAT in cell lines (Daniels and Amara, 1999; Melikian and Buckley, 1999; Blakely and Bauman, 2000; Granas et al., 2003; Miranda et al., 2007; (Eriksen *et al.*, 2009).

Since NCAM is known to be a modulator of the dopaminergic system and regulates D2 receptor trafficking (Xiao *et al.*, 2009), I was interested to study the involvement of CHL1 in DAT trafficking. In this context, DAT internalization was analyzed by using *in vivo* immunocytochemistry staining. These results revealed that CHL1 internalizes with DAT in response to PMA stimulation in live HEK 293 cells. Concerning these results, the next question raised is: Which possible internalization pathway may mediate the endocytosis of CHL1 and DAT?

The presence of cell adhesion molecules like L1, NCAM and CHL1 in lipid rafts have been reported (Olive *et al.*, 1995, Niethammer *et al.*, 2002, Tian *et al.*, 2012). It was described that the palmitoylation site within the intracellular domain of CHL1 induces its capacity to associate with lipid raft, mediating CHL1 internalization (Tian *et al.*, 2012). On the other hand, other studies have demonstrated that DAT internalization arises from lipid raft and non-lipid raft domains, but PKC-stimulated DAT endocytosis occurs specifically from lipid rafts. Since our results indicate the internalization of CHL1 with DAT after PKC stimulation,

followed by appearance of CHL1 and DAT in intracellular vesicular structures, it is conceivable that both CHL1 and DAT internalize through lipid raft micro domains. However, the results do not exclude the possibility that CHL1 might be also involved in constitutive internalization of DAT. So far, the specific molecular mechanism remains to be determined.

### **6.5.2. CHL1 role in maintenance and/or survival of dopaminergic neurons**

Considering that the CHL1 gene is involved in mental retardation and schizophrenia (Sakurai *et al.*, 2002, Angeloni *et al.*, 1999) (Frints *et al.*, 2003), and regarding the role of the dopaminergic system in the etiology of schizophrenia, the next question appeared whether the pattern of midbrain dopaminergic neurons in wild-type and CHL1-deficient mice are the same.

The tyrosine hydroxylase (TH) antibody has been reported as a gold-standard for identifying dopamine neurons in the midbrain region. In CHL1-deficient mice, immunohistochemical stains for TH revealed obvious loss of midbrain dopamine neurons based on the lower density of TH-positive cells in substantia nigra (SN) as compared to the wild-type tissue. This observation is in agreement with a previous stereological analysis in our lab, which indicated an ‘age-dependent’ loss of TH<sup>+</sup> neurons in CHL1-deficient mice. A predominant reduction of TH<sup>+</sup> neurons covering 25% was noted between the ages of two months and six months in CHL1-deficient mice (Thilo, B.E. 2005, PhD dissertation). Taken together, the strong evidence of TH<sup>+</sup> neurons loss in CHL1-deficient mice was gained, suggesting that CHL1 is implicated in maintenance and/or in the survival of the dopaminergic system, since it has been shown that the lack of L1 also resulted in a redistribution of dopaminergic neurons of the substantia nigra (Demyanenko *et al.*, 2001).

## Conclusion

In this thesis, novel potential interacting partners of CHL1-ICD were identified. After confirmation of the interactions by different approaches, functional analyses were performed. This study established a physical and functional interaction between CHL1 and ALG-2 (apoptosis-linked gene-2). Concerning the survival role of CHL1 against cell death induced by high levels of intracellular calcium, it is suggested that CHL1 may play role as a ‘neuroprotective’ molecule during calcium overload and excitotoxicity in parallel fibers in the cerebellum.

The present work demonstrates a novel binding of CHL1 to synaptogyrin-3 as a synaptic vesicle protein, which may further correlate with neurotransmitter release through exocytosis and synaptic plasticity. This can be assumed since impairments in neurotransmission, long-term potentiation and behavior in CHL1 deficient mice have been reported, respectively.

Finally, identification of CHL1-DAT interaction, as well as physiological significance of such interaction, resulted in a better understanding of the role of CHL1 in regulating dopamine homeostasis in the synaptic cleft along with dopamine neurons maintenance or survival in midbrain. This work opens a new series of questions regarding possible protein–protein interactions involved in the etiology of mental retardation and schizophrenia relevant to CHL1.

## VII. References

- Andreyeva, A., Leshchyn'ska, I., Knepper, M., Betzel, C., Redecke, L., Sytnyk, V. & Schachner, M. 2010. CHL1 is a selective organizer of the presynaptic machinery chaperoning the SNARE complex. *PLoS One*, 5, e12018.
- Angeloni, D., Lindor, N. M., Pack, S., Latif, F., Wei, M. H. & Lerman, M. I. 1999. CALL gene is haploinsufficient in a 3p- syndrome patient. *Am J Med Genet*, 86, 482-5.
- Ango, F., Wu, C., Van Der Want, J. J., Wu, P., Schachner, M. & Huang, Z. J. 2008. Bergmann glia and the recognition molecule CHL1 organize GABAergic axons and direct innervation of Purkinje cell dendrites. *PLoS Biol*, 6, e103.
- Appel, F., Holm, J., Conscience, J. F., Von Bohlen Und Halbach, F., Faissner, A., James, P. & Schachner, M. 1995. Identification of the border between fibronectin type III homologous repeats 2 and 3 of the neural cell adhesion molecule L1 as a neurite outgrowth promoting and signal transducing domain. *J Neurobiol*, 28, 297-312.
- Arribas, J. & Borroto, A. 2002. Protein ectodomain shedding. *Chem Rev*, 102, 4627-38.
- Aviel-Ronen, S., Coe, B. P., Lau, S. K., Da Cunha Santos, G., Zhu, C. Q., Strumpf, D., Jurisica, I., Lam, W. L. & Tsao, M. S. 2008. Genomic markers for malignant progression in pulmonary adenocarcinoma with bronchioloalveolar features. *Proc Natl Acad Sci U S A*, 105, 10155-60.
- Belizaire, R., Komanduri, C., Wooten, K., Chen, M., Thaller, C. & Janz, R. 2004. Characterization of synaptogyrin 3 as a new synaptic vesicle protein. *J Comp Neurol*, 470, 266-81.
- Bennett, V. & Baines, A. J. 2001. Spectrin and ankyrin-based pathways: metazoan inventions for integrating cells into tissues. *Physiol Rev*, 81, 1353-92.
- Brummendorf, T., Kenwrick, S. & Rathjen, F. G. 1998. Neural cell recognition molecule L1: from cell biology to human hereditary brain malformations. *Curr Opin Neurobiol*, 8, 87-97.
- Brummendorf, T. & Rathjen, F. G. 1996. Structure/function relationships of axon-associated adhesion receptors of the immunoglobulin superfamily. *Curr Opin Neurobiol*, 6, 584-93.
- Buhusi, M., Midkiff, B. R., Gates, A. M., Richter, M., Schachner, M. & Maness, P. F. 2003. Close homolog of L1 is an enhancer of integrin-mediated cell migration. *J Biol Chem*, 278, 25024-31.
- Burgoon, M. P., Grumet, M., Mauro, V., Edelman, G. M. & Cunningham, B. A. 1991. Structure of the chicken neuron-glia cell adhesion molecule, Ng-CAM: origin of the polypeptides and relation to the Ig superfamily. *J Cell Biol*, 112, 1017-29.
- Chaisuksunt, V., Campbell, G., Zhang, Y., Schachner, M., Lieberman, A. R. & Anderson, P. N. 2000a. The cell recognition molecule CHL1 is strongly upregulated by injured and regenerating thalamic neurons. *J Comp Neurol*, 425, 382-92.
- Chaisuksunt, V., Campbell, G., Zhang, Y., Schachner, M., Lieberman, A. R. & Anderson, P. N. 2003. Expression of regeneration-related molecules in injured and regenerating striatal and nigral neurons. *J Neurocytol*, 32, 161-83.
- Chaisuksunt, V., Zhang, Y., Anderson, P. N., Campbell, G., Vaudano, E., Schachner, M. & Lieberman, A. R. 2000b. Axonal regeneration from CNS neurons in the cerebellum and brainstem of adult rats: correlation with the patterns of expression and distribution of messenger RNAs for L1, CHL1, c-jun and growth-associated protein-43. *Neuroscience*, 100, 87-108.

- Chang, S., Rathjen, F. G. & Raper, J. A. 1987. Extension of neurites on axons is impaired by antibodies against specific neural cell surface glycoproteins. *J Cell Biol*, 104, 355-62.
- Chen, C. & Sytkowski, A. J. 2005. Apoptosis-linked gene-2 connects the Raf-1 and ASK1 signalings. *Biochem Biophys Res Commun*, 333, 51-7.
- Chen, N. & Reith, M. E. 2008. Substrates dissociate dopamine transporter oligomers. *J Neurochem*, 105, 910-20.
- Chen, Q. Y., Chen, Q., Feng, G. Y., Lindpaintner, K., Chen, Y., Sun, X., Chen, Z., Gao, Z., Tang, J. & He, L. 2005. Case-control association study of the close homologue of L1 (CHL1) gene and schizophrenia in the Chinese population. *Schizophr Res*, 73, 269-74.
- Chen, S., Mantei, N., Dong, L. & Schachner, M. 1999. Prevention of neuronal cell death by neural adhesion molecules L1 and CHL1. *J Neurobiol*, 38, 428-39.
- Chu, T. T. & Liu, Y. 2010. An integrated genomic analysis of gene-function correlation on schizophrenia susceptibility genes. *J Hum Genet*, 55, 285-92.
- Conacci-Sorrell, M., Kaplan, A., Raveh, S., Gavert, N., Sakurai, T. & Ben-Ze'ev, A. 2005. The shed ectodomain of Nr-CAM stimulates cell proliferation and motility, and confers cell transformation. *Cancer Res*, 65, 11605-12.
- Crossin, K. L. & Krushel, L. A. 2000. Cellular signaling by neural cell adhesion molecules of the immunoglobulin superfamily. *Dev Dyn*, 218, 260-79.
- Cuoco, C., Ronchetto, P., Gimelli, S., Bena, F., Divizia, M. T., Lerone, M., Mirabelli-Badenier, M., Mascaretti, M. & Gimelli, G. 2011. Microarray based analysis of an inherited terminal 3p26.3 deletion, containing only the CHL1 gene, from a normal father to his two affected children. *Orphanet J Rare Dis*, 6, 12.
- D'souza, S. E., Ginsberg, M. H. & Plow, E. F. 1991. Arginyl-glycyl-aspartic acid (RGD): a cell adhesion motif. *Trends Biochem Sci*, 16, 246-50.
- Debiec, H., Christensen, E. I. & Ronco, P. M. 1998. The cell adhesion molecule L1 is developmentally regulated in the renal epithelium and is involved in kidney branching morphogenesis. *J Cell Biol*, 143, 2067-79.
- Demyanenko, G. P., Schachner, M., Anton, E., Schmid, R., Feng, G., Sanes, J. & Maness, P. F. 2004. Close homolog of L1 modulates area-specific neuronal positioning and dendrite orientation in the cerebral cortex. *Neuron*, 44, 423-37.
- Demyanenko, G. P., Shibata, Y. & Maness, P. F. 2001. Altered distribution of dopaminergic neurons in the brain of L1 null mice. *Brain Res Dev Brain Res*, 126, 21-30.
- Demyanenko, G. P., Siesser, P. F., Wright, A. G., Brennaman, L. H., Bartsch, U., Schachner, M. & Maness, P. F. 2011. L1 and CHL1 Cooperate in Thalamocortical Axon Targeting. *Cereb Cortex*, 21, 401-12.
- Dong, L., Chen, S., Richter, M. & Schachner, M. 2002. Single-chain variable fragment antibodies against the neural adhesion molecule CHL1 (close homolog of L1) enhance neurite outgrowth. *J Neurosci Res*, 69, 437-47.
- Draeby, I., Woods, Y. L., La Cour, J. M., Mollerup, J., Bourdon, J. C. & Berchtold, M. W. 2007. The calcium binding protein ALG-2 binds and stabilizes Scotin, a p53-inducible gene product localized at the endoplasmic reticulum membrane. *Arch Biochem Biophys*, 467, 87-94.
- Egana, L. A., Cuevas, R. A., Baust, T. B., Parra, L. A., Leak, R. K., Hochendoner, S., Pena, K., Quiroz, M., Hong, W. C., Dorostkar, M. M., Janz, R., Sitte, H. H. & Torres, G. E. 2009. Physical and functional interaction between the dopamine transporter and the synaptic vesicle protein synaptogyrin-3. *J Neurosci*, 29, 4592-604.
- Eriksen, J., Rasmussen, S. G., Rasmussen, T. N., Vaegter, C. B., Cha, J. H., Zou, M. F., Newman, A. H. & Gether, U. 2009. Visualization of dopamine transporter trafficking in live neurons by use of fluorescent cocaine analogs. *J Neurosci*, 29, 6794-808.

- Fischer, G., Kunemund, V. & Schachner, M. 1986. Neurite outgrowth patterns in cerebellar microexplant cultures are affected by antibodies to the cell surface glycoprotein L1. *J Neurosci*, 6, 605-12.
- Freigang, J., Proba, K., Leder, L., Diederichs, K., Sonderegger, P. & Welte, W. 2000. The crystal structure of the ligand binding module of axonin-1/TAG-1 suggests a zipper mechanism for neural cell adhesion. *Cell*, 101, 425-33.
- Friedli, A., Fischer, E., Novak-Hofer, I., Cohrs, S., Ballmer-Hofer, K., Schubiger, P. A., Schibli, R. & Grunberg, J. 2009. The soluble form of the cancer-associated L1 cell adhesion molecule is a pro-angiogenic factor. *Int J Biochem Cell Biol*, 41, 1572-80.
- Frints, S. G., Marynen, P., Hartmann, D., Fryns, J. P., Steyaert, J., Schachner, M., Rolf, B., Craessaerts, K., Snellinx, A., Hollanders, K., D'hooge, R., De Deyn, P. P. & Froyen, G. 2003. CALL interrupted in a patient with non-specific mental retardation: gene dosage-dependent alteration of murine brain development and behavior. *Hum Mol Genet*, 12, 1463-74.
- Gabriel, L. R., Wu, S., Kearney, P., Bellve, K. D., Standley, C., Fogarty, K. E. & Melikian, H. E. 2013. Dopamine transporter endocytic trafficking in striatal dopaminergic neurons: differential dependence on dynamin and the actin cytoskeleton. *J Neurosci*, 33, 17836-46.
- Gall, D., Roussel, C., Nieuws, T., Cheron, G., Servais, L., D'angelo, E. & Schiffmann, S. N. 2005. Role of calcium binding proteins in the control of cerebellar granule cell neuronal excitability: experimental and modeling studies. *Prog Brain Res*, 148, 321-8.
- Grumet, M., Mauro, V., Burgoon, M. P., Edelman, G. M. & Cunningham, B. A. 1991. Structure of a new nervous system glycoprotein, Nr-CAM, and its relationship to subgroups of neural cell adhesion molecules. *J Cell Biol*, 113, 1399-412.
- Hall, H. & Hubbell, J. A. 2004. Matrix-bound sixth Ig-like domain of cell adhesion molecule L1 acts as an angiogenic factor by ligating  $\alpha$ v $\beta$ 3-integrin and activating VEGF-R2. *Microvasc Res*, 68, 169-78.
- Hassel, B., Rathjen, F. G. & Volkmer, H. 1997. Organization of the neurofascin gene and analysis of developmentally regulated alternative splicing. *J Biol Chem*, 272, 28742-9.
- Hemperly, J. J., Edelman, G. M. & Cunningham, B. A. 1986. cDNA clones of the neural cell adhesion molecule (N-CAM) lacking a membrane-spanning region consistent with evidence for membrane attachment via a phosphatidylinositol intermediate. *Proc Natl Acad Sci U S A*, 83, 9822-6.
- Herron, L. R., Hill, M., Davey, F. & Gunn-Moore, F. J. 2009. The intracellular interactions of the L1 family of cell adhesion molecules. *Biochem J*, 419, 519-31.
- Hillenbrand, R., Molthagen, M., Montag, D. & Schachner, M. 1999. The close homologue of the neural adhesion molecule L1 (CHL1): patterns of expression and promotion of neurite outgrowth by heterophilic interactions. *Eur J Neurosci*, 11, 813-26.
- Holm, J., Hillenbrand, R., Steuber, V., Bartsch, U., Moos, M., Lubbert, H., Montag, D. & Schachner, M. 1996. Structural features of a close homologue of L1 (CHL1) in the mouse: a new member of the L1 family of neural recognition molecules. *Eur J Neurosci*, 8, 1613-29.
- Hortsch, M. 1996. The L1 family of neural cell adhesion molecules: old proteins performing new tricks. *Neuron*, 17, 587-93.
- Hynes, R. O. 1992. Integrins: versatility, modulation, and signaling in cell adhesion. *Cell*, 69, 11-25.
- Irintchev, A., Koch, M., Needham, L. K., Maness, P. & Schachner, M. 2004. Impairment of sensorimotor gating in mice deficient in the cell adhesion molecule L1 or its close homologue, CHL1. *Brain Res*, 1029, 131-4.

- Itoh, K., Cheng, L., Kamei, Y., Fushiki, S., Kamiguchi, H., Gutwein, P., Stoeck, A., Arnold, B., Altevogt, P. & Lemmon, V. 2004. Brain development in mice lacking L1-L1 homophilic adhesion. *J Cell Biol*, 165, 145-54.
- Jakovcevski, I., Siering, J., Hargus, G., Karl, N., Hoelters, L., Djogo, N., Yin, S., Zecevic, N., Schachner, M. & Irintchev, A. 2009. Close homologue of adhesion molecule L1 promotes survival of Purkinje and granule cells and granule cell migration during murine cerebellar development. *J Comp Neurol*, 513, 496-510.
- Jakovcevski, I., Wu, J., Karl, N., Leshchyn'ska, I., Sytnyk, V., Chen, J., Irintchev, A. & Schachner, M. 2007. Glial scar expression of CHL1, the close homolog of the adhesion molecule L1, limits recovery after spinal cord injury. *J Neurosci*, 27, 7222-33.
- Jang, I. K., Hu, R., Lacana, E., D'adamio, L. & Gu, H. 2002. Apoptosis-linked gene 2-deficient mice exhibit normal T-cell development and function. *Mol Cell Biol*, 22, 4094-100.
- Janowicz, A., Michalak, M. & Krebs, J. 2011. Stress induced subcellular distribution of ALG-2, RBM22 and hSlu7. *Biochim Biophys Acta*, 1813, 1045-9.
- Jouet, M., Rosenthal, A. & Kenwrick, S. 1995. Exon 2 of the gene for neural cell adhesion molecule L1 is alternatively spliced in B cells. *Brain Res Mol Brain Res*, 30, 378-80.
- Kamiguchi, H., Hlavin, M. L., Yamasaki, M. & Lemmon, V. 1998. Adhesion molecules and inherited diseases of the human nervous system. *Annu Rev Neurosci*, 21, 97-125.
- Kamiguchi, H. & Lemmon, V. 1997. Neural cell adhesion molecule L1: signaling pathways and growth cone motility. *J Neurosci Res*, 49, 1-8.
- Katayama, M., Iwamatsu, A., Masutani, H., Furuke, K., Takeda, K., Wada, H., Masuda, T. & Ishii, K. 1997. Expression of neural cell adhesion molecule L1 in human lung cancer cell lines. *Cell Struct Funct*, 22, 511-6.
- Katic, J., Loers, G., Kleene, R., Karl, N., Schmidt, C., Buck, F., Zmijewski, J. W., Jakovcevski, I., Preissner, K. T. & Schachner, M. 2014. Interaction of the cell adhesion molecule CHL1 with vitronectin, integrins, and the plasminogen activator inhibitor-2 promotes CHL1-induced neurite outgrowth and neuronal migration. *J Neurosci*, 34, 14606-23.
- Katidou, M., Vidaki, M., Strigini, M. & Karagogeos, D. 2008. The immunoglobulin superfamily of neuronal cell adhesion molecules: lessons from animal models and correlation with human disease. *Biotechnol J*, 3, 1564-80.
- Katoh, K., Suzuki, H., Terasawa, Y., Mizuno, T., Yasuda, J., Shibata, H. & Maki, M. 2005. The penta-EF-hand protein ALG-2 interacts directly with the ESCRT-I component TSG101, and Ca<sup>2+</sup>-dependently co-localizes to aberrant endosomes with dominant-negative AAA ATPase SKD1/Vps4B. *Biochem J*, 391, 677-85.
- Keilhauer, G., Faissner, A. & Schachner, M. 1985. Differential inhibition of neurone-neurone, neurone-astrocyte and astrocyte-astrocyte adhesion by L1, L2 and N-CAM antibodies. *Nature*, 316, 728-30.
- Kemler, R. & Ozawa, M. 1989. Uvomorulin-catenin complex: cytoplasmic anchorage of a Ca<sup>2+</sup>-dependent cell adhesion molecule. *Bioessays*, 11, 88-91.
- Kiefel, H., Bondong, S., Hazin, J., Ridinger, J., Schirmer, U., Riedle, S. & Altevogt, P. 2012. L1CAM: a major driver for tumor cell invasion and motility. *Cell Adh Migr*, 6, 374-84.
- Kiryushko, D., Berezin, V. & Bock, E. 2004. Regulators of neurite outgrowth: role of cell adhesion molecules. *Ann N Y Acad Sci*, 1014, 140-54.

- Kiryushko, D., Korshunova, I., Berezin, V. & Bock, E. 2006. Neural cell adhesion molecule induces intracellular signaling via multiple mechanisms of Ca<sup>2+</sup> homeostasis. *Mol Biol Cell*, 17, 2278-86.
- Kleene, R., Chaudhary, H., Karl, N., Katic, J., Kotarska, A., Guitart, K., Loers, G. & Schachner, M. 2015. Interaction between CHL1 and serotonin receptor 2c regulates signal transduction and behavior in mice. *J Cell Sci*, 128, 4642-52.
- Kolata, S., Wu, J., Light, K., Schachner, M. & Matzel, L. D. 2008. Impaired working memory duration but normal learning abilities found in mice that are conditionally deficient in the close homolog of L1. *J Neurosci*, 28, 13505-10.
- Koticha, D., Babiarez, J., Kane-Goldsmith, N., Jacob, J., Raju, K. & Grumet, M. 2005. Cell adhesion and neurite outgrowth are promoted by neurofascin NF155 and inhibited by NF186. *Mol Cell Neurosci*, 30, 137-48.
- Krog, L. & Bock, E. 1992. Glycosylation of neural cell adhesion molecules of the immunoglobulin superfamily. *APMIS Suppl*, 27, 53-70.
- Kurumaji, A., Nomoto, H., Okano, T. & Toru, M. 2001. An association study between polymorphism of L1CAM gene and schizophrenia in a Japanese sample. *Am J Med Genet*, 105, 99-104.
- La Cour, J. M., Hoj, B. R., Mollerup, J., Simon, R., Sauter, G. & Berchtold, M. W. 2008. The apoptosis linked gene ALG-2 is dysregulated in tumors of various origin and contributes to cancer cell viability. *Mol Oncol*, 1, 431-9.
- La Cour, J. M., Mollerup, J., Winding, P., Tarabykina, S., Sehested, M. & Berchtold, M. W. 2003. Up-regulation of ALG-2 in hepatomas and lung cancer tissue. *Am J Pathol*, 163, 81-9.
- Lander, E. S., Linton, L. M., Birren, B., Nusbaum, C., Zody, M. C., Baldwin, J., Devon, K., Dewar, K., Doyle, M., Fitzhugh, W., Funke, R., Gage, D., Harris, K., Heaford, A., Howland, J., Kann, L., Lehoczky, J., Levine, R., Mcewan, P., Mckernan, K., Meldrim, J., Mesirov, J. P., Miranda, C., Morris, W., Naylor, J., Raymond, C., Rosetti, M., Santos, R., Sheridan, A., Sougnez, C., Stange-Thomann, Y., Stojanovic, N., Subramanian, A., Wyman, D., Rogers, J., Sulston, J., Ainscough, R., Beck, S., Bentley, D., Burton, J., Clee, C., Carter, N., Coulson, A., Deadman, R., Deloukas, P., Dunham, A., Dunham, I., Durbin, R., French, L., Grafham, D., Gregory, S., Hubbard, T., Humphray, S., Hunt, A., Jones, M., Lloyd, C., McMurray, A., Matthews, L., Mercer, S., Milne, S., Mullikin, J. C., Mungall, A., Plumb, R., Ross, M., Shownkeen, R., Sims, S., Waterston, R. H., Wilson, R. K., Hillier, L. W., Mcpherson, J. D., Marra, M. A., Mardis, E. R., Fulton, L. A., Chinwalla, A. T., Pepin, K. H., Gish, W. R., Chissoe, S. L., Wendl, M. C., Delehaunty, K. D., Miner, T. L., Delehaunty, A., Kramer, J. B., Cook, L. L., Fulton, R. S., Johnson, D. L., Minx, P. J., Clifton, S. W., Hawkins, T., Branscomb, E., Predki, P., Richardson, P., Wenning, S., Slezak, T., Doggett, N., Cheng, J. F., Olsen, A., Lucas, S., Elkin, C., Uberbacher, E., Frazier, M., et al. 2001. Initial sequencing and analysis of the human genome. *Nature*, 409, 860-921.
- Lane, R. P., Chen, X. N., Yamakawa, K., Vielmetter, J., Korenberg, J. R. & Dreyer, W. J. 1996. Characterization of a highly conserved human homolog to the chicken neural cell surface protein Bravo/Nr-CAM that maps to chromosome band 7q31. *Genomics*, 35, 456-65.
- Law, J. W., Lee, A. Y., Sun, M., Nikonenko, A. G., Chung, S. K., Dityatev, A., Schachner, M. & Morellini, F. 2003. Decreased anxiety, altered place learning, and increased CA1 basal excitatory synaptic transmission in mice with conditional ablation of the neural cell adhesion molecule L1. *J Neurosci*, 23, 10419-32.

- Lee, J. H., Rho, S. B. & Chun, T. 2005. Programmed cell death 6 (PDCD6) protein interacts with death-associated protein kinase 1 (DAPk1): additive effect on apoptosis via caspase-3 dependent pathway. *Biotechnol Lett*, 27, 1011-5.
- Lee, T. W., Tsang, V. W. & Birch, N. P. 2008. Synaptic plasticity-associated proteases and protease inhibitors in the brain linked to the processing of extracellular matrix and cell adhesion molecules. *Neuron Glia Biol*, 4, 223-34.
- Leshchyn'ska, I. & Sytnyk, V. 2016. Reciprocal Interactions between Cell Adhesion Molecules of the Immunoglobulin Superfamily and the Cytoskeleton in Neurons. *Front Cell Dev Biol*, 4, 9.
- Leshchyn'ska, I., Sytnyk, V., Richter, M., Andreyeva, A., Puchkov, D. & Schachner, M. 2006. The adhesion molecule CHL1 regulates uncoating of clathrin-coated synaptic vesicles. *Neuron*, 52, 1011-25.
- Lindner, J., Rathjen, F. G. & Schachner, M. 1983. L1 mono- and polyclonal antibodies modify cell migration in early postnatal mouse cerebellum. *Nature*, 305, 427-30.
- Linnemann, D., Raz, A. & Bock, E. 1989. Differential expression of cell adhesion molecules in variants of K1735 melanoma cells differing in metastatic capacity. *Int J Cancer*, 43, 709-12.
- Liu, Q., Dwyer, N. D. & O'leary, D. D. 2000. Differential expression of COUP-TFI, CHL1, and two novel genes in developing neocortex identified by differential display PCR. *J Neurosci*, 20, 7682-90.
- Loers, G., Makhina, T., Bork, U., Dorner, A., Schachner, M. & Kleene, R. 2012. The interaction between cell adhesion molecule L1, matrix metalloproteinase 14, and adenine nucleotide translocator at the plasma membrane regulates L1-mediated neurite outgrowth of murine cerebellar neurons. *J Neurosci*, 32, 3917-30.
- Loers, G. & Schachner, M. 2007. Recognition molecules and neural repair. *J Neurochem*, 101, 865-82.
- Lutz, D., Wolters-Eisfeld, G., Joshi, G., Djogo, N., Jakovcevski, I., Schachner, M. & Kleene, R. 2012. Generation and nuclear translocation of sumoylated transmembrane fragment of cell adhesion molecule L1. *J Biol Chem*, 287, 17161-75.
- Maki, M., Suzuki, H. & Shibata, H. 2011. Structure and function of ALG-2, a penta-EF-hand calcium-dependent adaptor protein. *Sci China Life Sci*, 54, 770-9.
- Maness, P. F. & Schachner, M. 2007. Neural recognition molecules of the immunoglobulin superfamily: signaling transducers of axon guidance and neuronal migration. *Nat Neurosci*, 10, 19-26.
- Martini, R. & Schachner, M. 1986. Immunoelectron microscopic localization of neural cell adhesion molecules (L1, N-CAM, and MAG) and their shared carbohydrate epitope and myelin basic protein in developing sciatic nerve. *J Cell Biol*, 103, 2439-48.
- Mason, M. R., Lieberman, A. R. & Anderson, P. N. 2003. Corticospinal neurons up-regulate a range of growth-associated genes following intracortical, but not spinal, axotomy. *Eur J Neurosci*, 18, 789-802.
- Mccrea, P. D., Gu, D. & Balda, M. S. 2009. Junctional music that the nucleus hears: cell-cell contact signaling and the modulation of gene activity. *Cold Spring Harb Perspect Biol*, 1, a002923.
- Mechtersheimer, S., Gutwein, P., Agmon-Levin, N., Stoeck, A., Oleszewski, M., Riedle, S., Postina, R., Fahrenholz, F., Fogel, M., Lemmon, V. & Altevogt, P. 2001. Ectodomain shedding of L1 adhesion molecule promotes cell migration by autocrine binding to integrins. *J Cell Biol*, 155, 661-73.

- Meijers, R., Puettmann-Holgado, R., Skiniotis, G., Liu, J. H., Walz, T., Wang, J. H. & Schmucker, D. 2007. Structural basis of Dscam isoform specificity. *Nature*, 449, 487-91.
- Mellor, J., Nicoll, R. A. & Schmitz, D. 2002. Mediation of hippocampal mossy fiber long-term potentiation by presynaptic Ih channels. *Science*, 295, 143-7.
- Miura, M., Asou, H., Kobayashi, M. & Uyemura, K. 1992. Functional expression of a full-length cDNA coding for rat neural cell adhesion molecule L1 mediates homophilic intercellular adhesion and migration of cerebellar neurons. *J Biol Chem*, 267, 10752-8.
- Montag-Sallaz, M., Schachner, M. & Montag, D. 2002. Misguided axonal projections, neural cell adhesion molecule 180 mRNA upregulation, and altered behavior in mice deficient for the close homolog of L1. *Mol Cell Biol*, 22, 7967-81.
- Montaville, P., Dai, Y., Cheung, C. Y., Giller, K., Becker, S., Michalak, M., Webb, S. E., Miller, A. L. & Krebs, J. 2006. Nuclear translocation of the calcium-binding protein ALG-2 induced by the RNA-binding protein RBM22. *Biochim Biophys Acta*, 1763, 1335-43.
- Moos, M., Tacke, R., Scherer, H., Teplow, D., Fruh, K. & Schachner, M. 1988. Neural adhesion molecule L1 as a member of the immunoglobulin superfamily with binding domains similar to fibronectin. *Nature*, 334, 701-3.
- Morellini, F., Lepsveridze, E., Kahler, B., Dityatev, A. & Schachner, M. 2007. Reduced reactivity to novelty, impaired social behavior, and enhanced basal synaptic excitatory activity in perforant path projections to the dentate gyrus in young adult mice deficient in the neural cell adhesion molecule CHL1. *Mol Cell Neurosci*, 34, 121-36.
- Mortl, M., Sonderegger, P., Diederichs, K. & Welte, W. 2007. The crystal structure of the ligand-binding module of human TAG-1 suggests a new mode of homophilic interaction. *Protein Sci*, 16, 2174-83.
- Naus, S., Richter, M., Wildeboer, D., Moss, M., Schachner, M. & Bartsch, J. W. 2004. Ectodomain shedding of the neural recognition molecule CHL1 by the metalloprotease-disintegrin ADAM8 promotes neurite outgrowth and suppresses neuronal cell death. *J Biol Chem*, 279, 16083-90.
- Niethammer, P., Dellinger, M., Sytnyk, V., Dityatev, A., Fukami, K. & Schachner, M. 2002. Cosignaling of NCAM via lipid rafts and the FGF receptor is required for neurogenesis. *J Cell Biol*, 157, 521-32.
- Nikonenko, A. G., Sun, M., Lepsveridze, E., Apostolova, I., Petrova, I., Irintchev, A., Dityatev, A. & Schachner, M. 2006. Enhanced perisomatic inhibition and impaired long-term potentiation in the CA1 region of juvenile CHL1-deficient mice. *Eur J Neurosci*, 23, 1839-52.
- Nishimune, H., Bernreuther, C., Carroll, P., Chen, S., Schachner, M. & Henderson, C. E. 2005. Neural adhesion molecules L1 and CHL1 are survival factors for motoneurons. *J Neurosci Res*, 80, 593-9.
- Okumura, M., Ichioka, F., Kobayashi, R., Suzuki, H., Yoshida, H., Shibata, H. & Maki, M. 2009. Penta-EF-hand protein ALG-2 functions as a Ca<sup>2+</sup>-dependent adaptor that bridges Alix and TSG101. *Biochem Biophys Res Commun*, 386, 237-41.
- Olive, S., Dubois, C., Schachner, M. & Rougon, G. 1995. The F3 neuronal glycosylphosphatidylinositol-linked molecule is localized to glycolipid-enriched membrane subdomains and interacts with L1 and fyn kinase in cerebellum. *J Neurochem*, 65, 2307-17.
- Panicker, A. K., Buhusi, M., Thelen, K. & Maness, P. F. 2003. Cellular signalling mechanisms of neural cell adhesion molecules. *Front Biosci*, 8, d900-11.

- Patel, K., Kiely, F., Phimister, E., Melino, G., Rathjen, F. & Kemshead, J. T. 1991. The 200/220 kDa antigen recognized by monoclonal antibody (MAb) UJ127.11 on neural tissues and tumors is the human L1 adhesion molecule. *Hybridoma*, 10, 481-91.
- Pratte, M. & Jamon, M. 2009. Impairment of novelty detection in mice targeted for the Chl1 gene. *Physiol Behav*, 97, 394-400.
- Pratte, M., Rougon, G., Schachner, M. & Jamon, M. 2003. Mice deficient for the close homologue of the neural adhesion cell L1 (CHL1) display alterations in emotional reactivity and motor coordination. *Behav Brain Res*, 147, 31-9.
- Rathjen, F. G. & Schachner, M. 1984. Immunocytological and biochemical characterization of a new neuronal cell surface component (L1 antigen) which is involved in cell adhesion. *Embo j*, 3, 1-10.
- Reichardt, L. F. & Tomaselli, K. J. 1991. Extracellular matrix molecules and their receptors: functions in neural development. *Annu Rev Neurosci*, 14, 531-70.
- Reid, R. A. & Hemperly, J. J. 1992. Variants of human L1 cell adhesion molecule arise through alternate splicing of RNA. *J Mol Neurosci*, 3, 127-35.
- Richter, M. 2002. PhD dissertation, Identification and characterization of intracellular binding partners of the CHL1 (Close Homologue of L1) neural cell recognition molecule, Supervisor: Professor Melitta Schachner, ZMNH, Hamburg
- Ronn, L. C., Dissing, S., Holm, A., Berezin, V. & Bock, E. 2002. Increased intracellular calcium is required for neurite outgrowth induced by a synthetic peptide ligand of NCAM. *FEBS Lett*, 518, 60-6.
- Rothman, J. E. & Warren, G. 1994. Implications of the SNARE hypothesis for intracellular membrane topology and dynamics. *Curr Biol*, 4, 220-33.
- Sadoul, K., Sadoul, R., Faissner, A. & Schachner, M. 1988. Biochemical characterization of different molecular forms of the neural cell adhesion molecule L1. *J Neurochem*, 50, 510-21.
- Sakurai, K., Migita, O., Toru, M. & Arinami, T. 2002. An association between a missense polymorphism in the close homologue of L1 (CHL1, CALL) gene and schizophrenia. *Mol Psychiatry*, 7, 412-5.
- Salyakina, D., Cukier, H. N., Lee, J. M., Sacharow, S., Nations, L. D., Ma, D., Jaworski, J. M., Konidari, I., Whitehead, P. L., Wright, H. H., Abramson, R. K., Williams, S. M., Menon, R., Haines, J. L., Gilbert, J. R., Cuccaro, M. L. & Pericak-Vance, M. A. 2011. Copy number variants in extended autism spectrum disorder families reveal candidates potentially involved in autism risk. *PLoS One*, 6, e26049.
- Sasaki-Osugi, K., Imoto, C., Takahara, T., Shibata, H. & Maki, M. 2013. Nuclear ALG-2 protein interacts with Ca<sup>2+</sup> homeostasis endoplasmic reticulum protein (CHERP) Ca<sup>2+</sup>-dependently and participates in regulation of alternative splicing of inositol trisphosphate receptor type 1 (IP3R1) pre-mRNA. *J Biol Chem*, 288, 33361-75.
- Satoh, H., Nakano, Y., Shibata, H. & Maki, M. 2002. The penta-EF-hand domain of ALG-2 interacts with amino-terminal domains of both annexin VII and annexin XI in a Ca<sup>2+</sup>-dependent manner. *Biochim Biophys Acta*, 1600, 61-7.
- Sawaya, M. R., Wojtowicz, W. M., Andre, I., Qian, B., Wu, W., Baker, D., Eisenberg, D. & Zipursky, S. L. 2008. A double S shape provides the structural basis for the extraordinary binding specificity of Dscam isoforms. *Cell*, 134, 1007-18.
- Schachner, M. 1997. Neural recognition molecules and synaptic plasticity. *Curr Opin Cell Biol*, 9, 627-34.
- Schachner, M. & Martini, R. 1995. Glycans and the modulation of neural-recognition molecule function. *Trends Neurosci*, 18, 183-91.

- Schafer, M. K. & Altevogt, P. 2010. L1CAM malfunction in the nervous system and human carcinomas. *Cell Mol Life Sci*, 67, 2425-37.
- Schafer, M. K., Schmitz, B. & Diestel, S. 2010. L1CAM ubiquitination facilitates its lysosomal degradation. *FEBS Lett*, 584, 4475-80.
- Sebens Muerkoster, S., Werbing, V., Sipos, B., Debus, M. A., Witt, M., Grossmann, M., Leisner, D., Kotteritzsch, J., Kappes, H., Kloppel, G., Altevogt, P., Folsch, U. R. & Schafer, H. 2007. Drug-induced expression of the cellular adhesion molecule L1CAM confers anti-apoptotic protection and chemoresistance in pancreatic ductal adenocarcinoma cells. *Oncogene*, 26, 2759-68.
- Seino, S. & Shibasaki, T. 2005. PKA-dependent and PKA-independent pathways for cAMP-regulated exocytosis. *Physiol Rev*, 85, 1303-42.
- Sheng, L., Leshchyn'ska, I. & Sytnyk, V. 2013. Cell adhesion and intracellular calcium signaling in neurons. *Cell Commun Signal*, 11, 94.
- Shibata, H., Suzuki, H., Kakiuchi, T., Inuzuka, T., Yoshida, H., Mizuno, T. & Maki, M. 2008. Identification of Alix-type and Non-Alix-type ALG-2-binding sites in human phospholipid scramblase 3: differential binding to an alternatively spliced isoform and amino acid-substituted mutants. *J Biol Chem*, 283, 9623-32.
- Shibata, H., Suzuki, H., Yoshida, H. & Maki, M. 2007. ALG-2 directly binds Sec31A and localizes at endoplasmic reticulum exit sites in a Ca<sup>2+</sup>-dependent manner. *Biochem Biophys Res Commun*, 353, 756-63.
- Shoukier, M., Fuchs, S., Schwaibold, E., Lingen, M., Gartner, J., Brockmann, K. & Zirn, B. 2013. Microduplication of 3p26.3 in nonsyndromic intellectual disability indicates an important role of CHL1 for normal cognitive function. *Neuropediatrics*, 44, 268-71.
- Stoeck, A., Gast, D., Sanderson, M. P., Issa, Y., Gutwein, P. & Altevogt, P. 2007. L1-CAM in a membrane-bound or soluble form augments protection from apoptosis in ovarian carcinoma cells. *Gynecol Oncol*, 104, 461-9.
- Su, X. D., Gastinel, L. N., Vaughn, D. E., Faye, I., Poon, P. & Bjorkman, P. J. 1998. Crystal structure of hemolin: a horseshoe shape with implications for homophilic adhesion. *Science*, 281, 991-5.
- Takeichi, M. 1991. Cadherin cell adhesion receptors as a morphogenetic regulator. *Science*, 251, 1451-5.
- Tam, G. W., Van De Lagemaat, L. N., Redon, R., Strathdee, K. E., Croning, M. D., Malloy, M. P., Muir, W. J., Pickard, B. S., Deary, I. J., Blackwood, D. H., Carter, N. P. & Grant, S. G. 2010. Confirmed rare copy number variants implicate novel genes in schizophrenia. *Biochem Soc Trans*, 38, 445-51.
- Thelen, K., Kedar, V., Panicker, A. K., Schmid, R. S., Midkiff, B. R. & Maness, P. F. 2002. The neural cell adhesion molecule L1 potentiates integrin-dependent cell migration to extracellular matrix proteins. *J Neurosci*, 22, 4918-31.
- Tian, N., Leshchyn'ska, I., Welch, J. H., Diakowski, W., Yang, H., Schachner, M. & Sytnyk, V. 2012. Lipid raft-dependent endocytosis of close homolog of adhesion molecule L1 (CHL1) promotes neuritogenesis. *J Biol Chem*, 287, 44447-63.
- Thilo, B.E. 2005. PhD dissertation, Age dependent and region-specific alterations in the brain of CHL1 deficient mice: an emerging animal-based model of schizophrenia, Supervisor: Professor Melitta Schachner, ZMNH, Hamburg
- Torres, G. E. 2006. The dopamine transporter proteome. *J Neurochem*, 97 Suppl 1, 3-10.
- Torres, G. E., Carneiro, A., Seamans, K., Fiorentini, C., Sweeney, A., Yao, W. D. & Caron, M. G. 2003a. Oligomerization and trafficking of the human dopamine transporter.

- Mutational analysis identifies critical domains important for the functional expression of the transporter. *J Biol Chem*, 278, 2731-9.
- Torres, G. E., Gainetdinov, R. R. & Caron, M. G. 2003b. Plasma membrane monoamine transporters: structure, regulation and function. *Nat Rev Neurosci*, 4, 13-25.
- Vaughan, R. A. & Foster, J. D. 2013. Mechanisms of dopamine transporter regulation in normal and disease states. *Trends Pharmacol Sci*, 34, 489-96.
- Vergarajauregui, S., Martina, J. A. & Puertollano, R. 2009. Identification of the penta-EF-hand protein ALG-2 as a Ca<sup>2+</sup>-dependent interactor of mucolipin-1. *J Biol Chem*, 284, 36357-66.
- Volkmer, H., Hassel, B., Wolff, J. M., Frank, R. & Rathjen, F. G. 1992. Structure of the axonal surface recognition molecule neurofascin and its relationship to a neural subgroup of the immunoglobulin superfamily. *J Cell Biol*, 118, 149-61.
- Von Bohlen Und Halbach, F., Taylor, J. & Schachner, M. 1992. Cell Type-specific Effects of the Neural Adhesion Molecules L1 and N-CAM on Diverse Second Messenger Systems. *Eur J Neurosci*, 4, 896-909.
- Voura, E. B., Ramjeesingh, R. A., Montgomery, A. M. & Siu, C. H. 2001. Involvement of integrin alpha(v)beta(3) and cell adhesion molecule L1 in transendothelial migration of melanoma cells. *Mol Biol Cell*, 12, 2699-710.
- Walsh, F. S. & Doherty, P. 1997. Neural cell adhesion molecules of the immunoglobulin superfamily: role in axon growth and guidance. *Annu Rev Cell Dev Biol*, 13, 425-56.
- Wei, C. H. & Ryu, S. E. 2012. Homophilic interaction of the L1 family of cell adhesion molecules. *Exp Mol Med*, 44, 413-23.
- Westphal, D., Sytnyk, V., Schachner, M. & Leshchyn'ska, I. 2010. Clustering of the neural cell adhesion molecule (NCAM) at the neuronal cell surface induces caspase-8- and -3-dependent changes of the spectrin meshwork required for NCAM-mediated neurite outgrowth. *J Biol Chem*, 285, 42046-57.
- Westphal, N., Kleene, R., Lutz, D., Theis, T. & Schachner, M. 2016. Polysialic acid enters the cell nucleus attached to a fragment of the neural cell adhesion molecule NCAM to regulate the circadian rhythm in mouse brain. *Mol Cell Neurosci*, 74, 114-27.
- Williams, A. F. & Barclay, A. N. 1988. The immunoglobulin superfamily--domains for cell surface recognition. *Annu Rev Immunol*, 6, 381-405.
- Williams, E. J., Doherty, P., Turner, G., Reid, R. A., Hemperly, J. J. & Walsh, F. S. 1992. Calcium influx into neurons can solely account for cell contact-dependent neurite outgrowth stimulated by transfected L1. *J Cell Biol*, 119, 883-92.
- Wood, P. M., Schachner, M. & Bunge, R. P. 1990. Inhibition of Schwann cell myelination in vitro by antibody to the L1 adhesion molecule. *J Neurosci*, 10, 3635-45.
- Wright, A. G., Demyanenko, G. P., Powell, A., Schachner, M., Enriquez-Barreto, L., Tran, T. S., Polleux, F. & Maness, P. F. 2007. Close homolog of L1 and neuropilin 1 mediate guidance of thalamocortical axons at the ventral telencephalon. *J Neurosci*, 27, 13667-79.
- Xiao, M. F., Xu, J. C., Tereshchenko, Y., Novak, D., Schachner, M. & Kleene, R. 2009. Neural cell adhesion molecule modulates dopaminergic signaling and behavior by regulating dopamine D2 receptor internalization. *J Neurosci*, 29, 14752-63.
- Yang, M., Adla, S., Temburni, M. K., Patel, V. P., Lagow, E. L., Brady, O. A., Tian, J., Boulos, M. I. & Galileo, D. S. 2009. Stimulation of glioma cell motility by expression, proteolysis, and release of the L1 neural cell recognition molecule. *Cancer Cell Int*, 9, 27.
- Ye, H., Tan, Y. L., Ponniah, S., Takeda, Y., Wang, S. Q., Schachner, M., Watanabe, K., Pallen, C. J. & Xiao, Z. C. 2008. Neural recognition molecules CHL1 and NB-3

- regulate apical dendrite orientation in the neocortex via PTP alpha. *Embo j*, 27, 188-200.
- Zakharenko, S. S., Zablow, L. & Siegelbaum, S. A. 2001. Visualization of changes in presynaptic function during long-term synaptic plasticity. *Nat Neurosci*, 4, 711-7.
- Zhang, Y., Roslan, R., Lang, D., Schachner, M., Lieberman, A. R. & Anderson, P. N. 2000. Expression of CHL1 and L1 by neurons and glia following sciatic nerve and dorsal root injury. *Mol Cell Neurosci*, 16, 71-86.

## VIII. List of abbreviations

ADAM	A disintegrin and metalloproteinase
ADHD	Attention deficit hyperactivity disorder
AMPH	Amphetamine
ALG-2	Apoptosis-linked gene-2
BCA	Bicinchoninic acid
CAM	Cell adhesion molecule
CFP	Cyan fluorescence protein
CHERP	Calcium- homeostasis endoplasmic reticulum protein
CHL1	Close homologue of L1
CN-Br	Cyanogen bromide
CNS	Central nervous system
DAB	Diaminobenzidine
DAPK1	Death-associated protein kinase 1
DA	Dopamine
DAT	Dopamine transporter
DCX	Doublecortin
ECM	Extracellular matrix
EGTA	Ethylene glycol-bis (2-aminoethylether)-tetraacetic acid
ER	Endoplasmic reticulum
ERM	Ezrin-radixin-moesin
Fc	Fragment, crystallizable
FNIII	Fibronectin-type III
FRET	Fluorescence resonance energy transfer
GFP	Green fluorescence protein
GPI	Glycosyl phosphatidyl inositol
HEK293	Human embryonic kidney 293
His	Histidine
HNK-1	Human killer cell glycan
HRP	Horseradish peroxidase
Hsc70	Heat shock cognate protein 70

5-HT2C	Serotonin 2c receptor
ICD	Intracellular domain
IF	Immunofluorescence
Ig	Immunoglobulin
IgSF	Immunoglobulin superfamily
IP	Immunoprecipitation
IPTG	Isopropyl-D-thiogalactopyranoside
IRES	Internal ribosome entry site
L1	Cell adhesion molecule L1
MAG	Myelin-associated glycoprotein
MASA syndrome	Mental retardation, aphasia, shuffling gait, and adducted thumbs
NCAM180	Neural cell adhesion molecule isoform 180
NgCAM	Neuron-glia cell adhesion molecule
NrCAM	NgCAM-related cell adhesion molecule
OD	Optical density
PDCD6	Programmed cell death protein 6
PEF-1	Peflin1
PICK1	Protein interacting with C kinase-1
PKC	Protein kinase C
PLL	Poly-L-lysine
PLSCR3	Phospholipid scramblase 3
PMA	Phorbol 12-myristate13-acetate
PP2A	Protein phosphatase 2A
PSA	Polysialic acid
PTEN	Phosphatase and tensin homolog
RACK1	Receptor for activated C kinase-1
RBM22	RNA binding motif protein 22
RIPA	Radio immunoprecipitation assay
SDS-PAGE	Sodium dodecyl sulfate-polyacrylamide gel electrophoresis
SLC6	Solute carrier family 6
SN	Substantia nigra
SNAP25	Synaptosomal-associated protein-25
SNARE	N-ethylmaleimide-sensitive factor attachment protein receptor

Syg-3	Synaptogyrin-3
TAG-1	Transient axonal glycoprotein-1
TG	Thapsigargin
TH	Tyrosine hydroxylase
TSG101	Tumor susceptibility gene 101
Vamp2	Vesicle-associated membrane protein 2
VDCC	Voltage-dependent calcium channel
VMAT2	Vesicular monoamine transporter 2
VTA	Ventral tegmental area
WB	Western blot

## ACKNOWLEDGEMENTS

I owe gratitude to many people for the completion of this dissertation. First of all, I would like to express sincere appreciation to my supervisor Prof. Dr. Melitta Schachner for the great opportunity to work in her group on such an interesting research topic. I am deeply honored to work for a great pioneer, who established the first professorship of molecular neuroscience in Germany. Her fruitful and inspiring discussions, support and guidance throughout these years have helped me to develop my skills and broaden my knowledge in the field of molecular neurobiology.

I would like to thank for the support given by Prof. Thorsten Burmester that I could finish and publish my work.

Special thanks go to Dr. Sabine Hoffmeister-Ulleric at the service facility Bioanalytics at the ZMNH for her spontaneous helps.

I am grateful to Prof. Michael Frotscher, Ms. Katja Husen and Dr. Sabine Fleischer from the ZMNH Ph.D program for their support.

I would like to thank to my lab mates dear Kawish, Thomas, Harshita, Hardeep and Vedangana for their friendship and help during my thesis work.

Finally, I wish to convey my heartiest gratitude to my wonderful parents. I could not have done it without their prayers and support. I want to thank my husband for his unyielding support and love every step of the way.